THESIS

HYALURONIC ACID ENHANCEMENT OF EXPANDED

POLYTETRAFLUOROETHYLENE FOR SMALL DIAMETER VASCULAR GRAFTS

Submitted by

Nicole R. Lewis

Graduate Degree Program in Bioengineering

In partial fulfillment of the requirements

For the Degree of Master of Science

Colorado State University

Fort Collins, Colorado

Summer 2014

Master's Committee:

    Advisor: Susan P. James

    Ketul C. Popat
    Travis Bailey

ABSTRACT

HYALURONIC ACID ENHANCEMENT OF EXPANDED

POLYTETRAFLUOROETHYLENE FOR SMALL DIAMETER VASCULAR GRAFTS

Cardiovascular disease is the leading cause of mortality and morbidity in the United States and other developed countries. In the United States alone, 8 million people are diagnosed with peripheral arterial disease per year and over 250,000 patients have coronary bypass surgery each year. Autologous blood vessels are the standard graft used in small diameter (<6mm) arterial bypass procedures. Synthetic small diameter grafts have had limited success.   While polyethylene (Dacron) and expanded polytetrafluoroethylene (ePTFE) are the most commonly used small diameter synthetic vascular graft materials, there are significant limitations that make these materials unfavorable for use in the low blood flow conditions of the small diameter arteries. Specifically, Dacron and ePTFE grafts display failure due to early thrombosis or late intimal hyperplasia. With the shortage of tissue donors and the limited supply of autologous blood vessels available, there is a need for a small diameter synthetic vascular graft alternative. The aim of this research is to create and characterize ePTFE grafts prepared with hyaluronic acid (HA), evaluate thrombogenic potential of ePTFE-HA grafts, and evaluate graft mechanical properties and coating durability. The results in this work indicate the successful production of ePTFE-HA materials using a solvent infiltration technique. Surface interactions with blood show increased platelet adhesion on HA-modified surfaces, though evidence may suggest less platelet activation and erythrocyte lysis. Significant changes in mechanical properties of HA-modified ePTFE materials were observed. Further investigation into solvent selection,

uniformity of HA, endothelialization, and dynamic flow testing would be beneficial in the evaluation of these materials for use in small diameter vascular graft bypass procedures.

ACKNOWLEDGEMENTS

from the Colorado Office of Economic Development and International Trade - Bioscience

Discovery Evaluation Grant Program.

TABLE OF CONTENTS

CHAPTER 1: INTRODUCTION AND OVERVIEW

1.1 Motivation for Research

Cardiovascular disease is the leading cause of mortality and morbidity in the United States and other developed countries. [1] In the United States alone, 8 million people are diagnosed with peripheral arterial disease per year and over 250,000 patients have coronary bypass surgery each year. [2], [3] More than 86 million people in the United States have cardiovascular disease, and 16 million have coronary heart disease. In 2007, there were over 406,000 deaths and 408,000 coronary revascularization procedures performed. [4] Almost half of all deaths in Europe are attributed to atherosclerosis. [5] Patients diagnosed with cardiovascular disease often require revascularization surgery through bypass grafting to restore blood flow to tissue. [1], [6] The gold standard bypass graft is an autologous vein or artery. However, autologous vessels are only available in a third of cases. Synthetic grafts have high patency in large diameter arteries (>8mm), where graft thrombogenicity can be overcome by high blood flow volume. For example, synthetic aorto-iliac grafts have a five year patency rate of 90%. Medium size arteries (6-8mm diameter), such as the carotid and common femoral arteries, show little difference in patency between prosthetic and autologous implants. However, small diameter arteries with a diameter less than 6mm, such as the coronary and peripheral arteries below the knee, are common sites of atherosclerosis and exhibit low patency rates. [6]–[8] The antithrombogenic properties of synthetic grafts are not as effective as autologous grafts and have a higher complication rate due to thrombosis and the formation of intimal hyperplasia. There is an urgent need for safer synthetic grafts with higher patency rates. [1], [5], [9]

1.2 Cardiovascular Disease: Anatomy, Causes, Symptoms, and Risk Factors

The most common cause of cardiovascular disease is atherosclerosis. Atherosclerosis occurs when plaque, composed of fat, cholesterol, calcium, fibrous tissue, and other substances in the blood, accumulates on the inside surface of an artery or vein. With time, plaque can harden. As more plaque collects, it occludes the artery or vein, limiting perfusion of blood, and therefore limiting oxygen and nutrient delivery throughout the body. [10], [11] As shown in Figure 1.1, plaque has accumulated in an artery of the leg, partially occluding the artery, and decreasing blood flow to the leg and foot compared to a reference artery without occlusion. [10]
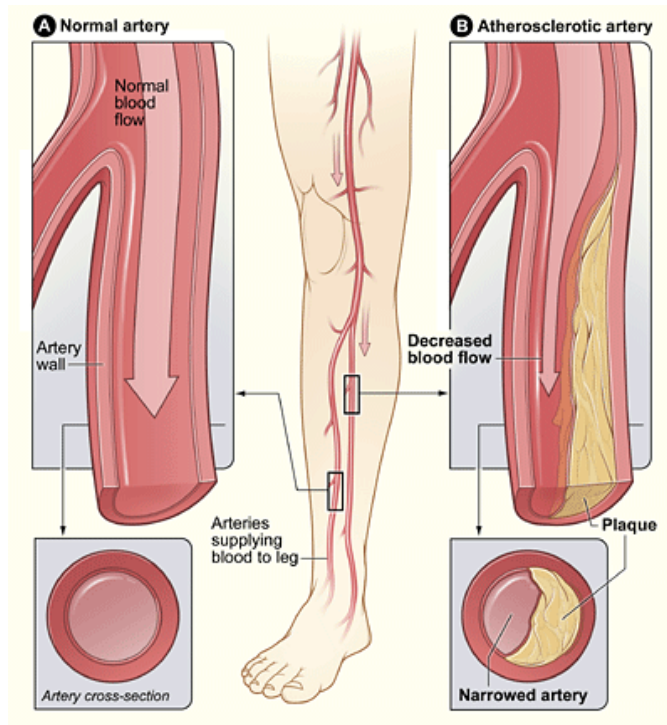
Figure 1.1: Accumulated plaque partially occludes an artery, decreasing blood flow to the leg and foot. [10]

1.2.1 Anatomy of Small Diameter Arteries

Blood vessels have three layers of tissue: the intima, media, and adventitia, as seen in Figure 1.2. Arteries deliver oxygenated blood to tissue, and veins circulate deoxygenated blood

back to the heart. Veins have thinner walls and deform more easily than arteries. Veins also lack the distinct molecular and tissue organization of arteries. [12]

The intima is composed of endothelial cells that form epithelium tissue on a basement membrane made of connective tissue and matrix molecules. This layer is in contact with blood and important for preventing thrombosis. Endothelial cells produce elastin molecules that contribute some elasticity to the vessel. Endothelial cells also produce laminin that functions in structural and organizational stability. The extracellular matrix of the intima consists of fibrillin microfibrils and collagen fibers. The intima is separated from the media by the internal elastic lamina. [8], [12]–[15]

The media is the middle layer and contains a dense population of smooth muscle cells organized concentrically with bands of elastic tissue. It contains most elastin within the vessel and is rich in proteoglycans. The media maintains the structure of blood vessels, confers mechanical properties to blood vessels, including high elasticity and strength, and functions in the tolerance and regulation of blood pressure. These mechanical properties are important for overall function of a vascular graft. The media is separated from the adventitia by the external elastic lamina. [8], [12]–[14]

The adventitia is composed of multiple types of connective tissue. It contains a highly collagenous extracellular matrix that helps prevent vessel rupture at high pressure, fibroblasts, blood vessels, and nerves. Small blood vessels called the vaso vasorum provide nourishment and oxygen to cells within the vessel wall. The adventitia also contributes rigidity and form to the blood vessel. In the event of serious arterial damage, mechanisms within the adventitia should cause coagulation. The collagen confers thrombogenic properties, leading to platelet adhesion and thrombus formation. Fibronectin, laminin, and thrombospondin can also promote platelet

adhesion. The expression of antithrombin III is reduced when the subendothelium is exposed to blood components. [8], [12]–[14]

Hyaluronic acid (HA) is present in the intima and adventitia of all blood vessels, and it can be found in the media with less homogeneous distribution. The amount of HA present in blood vessels depends on the age and type of vessel, ranging from 40% to 4% of the total glycosaminoglycan (GAG) content in the fetal umbilical artery compared to the adult aorta, respectively. The higher HA content in younger vessels results in a loose, hydrated, and flexible extracellular matrix. [16], [17]
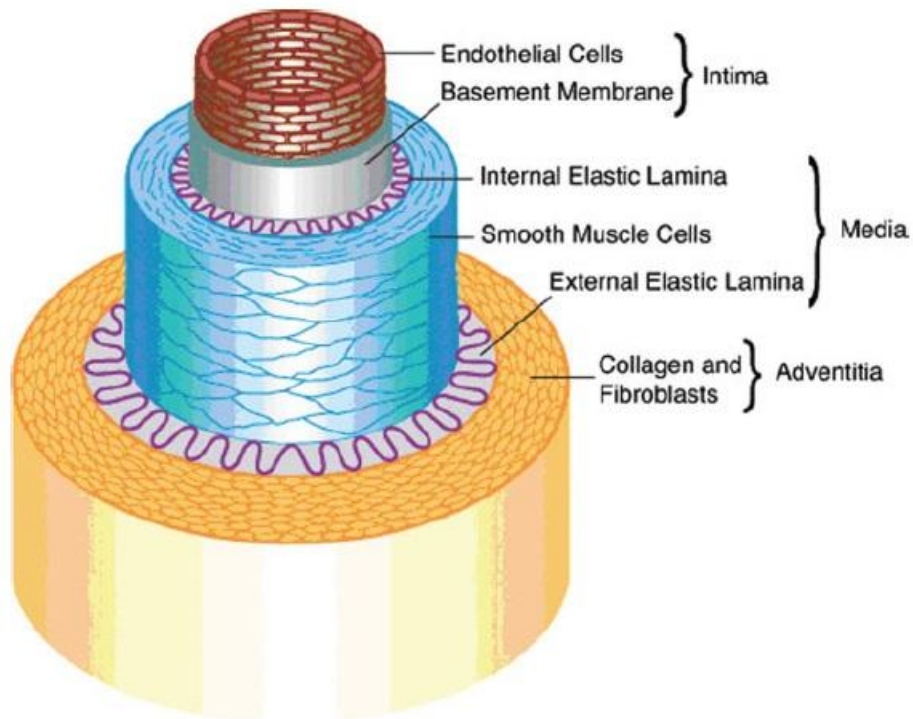
Figure 1.2: Multilayer anatomy of an arterial wall with tunica intima, media, and adventitial separated by the internal and external elastic lamina. [13]

1.2.2 Peripheral arteries

The peripheral arteries deliver blood to the limbs, head, and other organs. Peripheral arterial disease (PAD) is most commonly associated with the arteries of the lower legs below the

knees but also occurs in arteries which transport blood in the arms, head, and other organs. It is estimated that 5% of adults over the age of 50 in the United States have PAD, and 12-20% of adults over the age of 65 have PAD. [18]

The peripheral arteries of the legs receive blood from the aorta as shown in Figure 1.3. The aorta then splits into the left and right iliac arteries around the navel area. When the iliac arteries reach the pelvis, the iliac arteries are renamed the femoral arteries. The femoral arteries pass through the back of the knees and are then renamed the popliteal arteries. In the lower legs, the popliteal arteries split into three branches, the posterior tibial, anterior tibial, and peroneal arteries. [19]
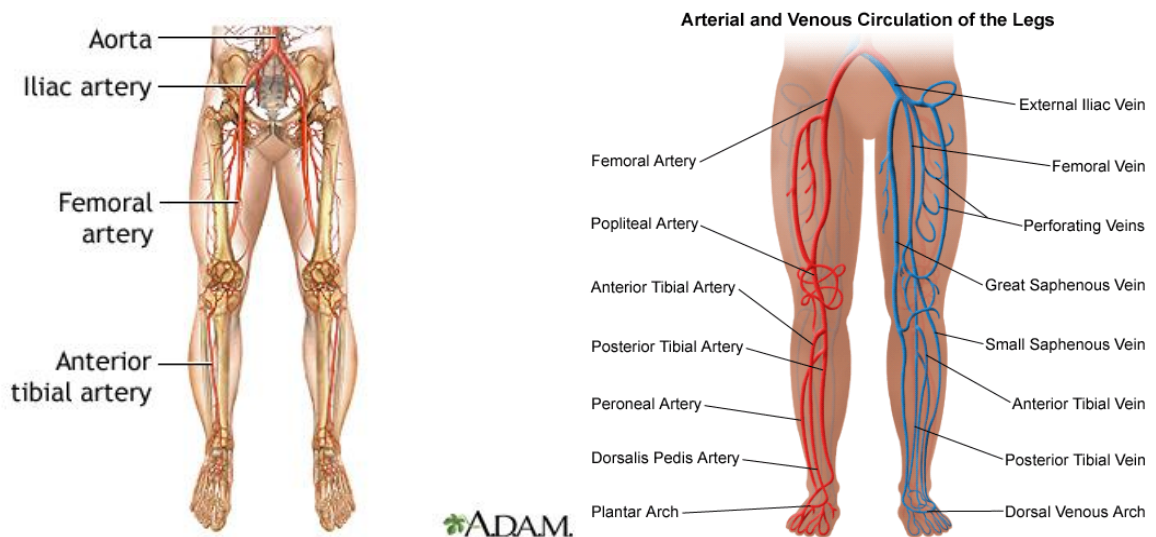
Figure 1.3: Blood flow from the aorta to the peripheral arteries of the legs. [19], [11], [20]

1.2.3 Coronary Arteries

Coronary heart disease (CHD) is the leading cause of death in both men and women. Over 400,000 men and women die every year from CHD in the United States. [21] According to the American Heart Association, there were 13.2 million cases of coronary artery disease in 2003 worldwide. [22]

The coronary arteries supply blood to the heart muscle as shown in Figure 1.4. There are four main coronary arteries. Near where the aorta and left ventricle connect, two main coronary arteries (the right and left coronary arteries) branch off from the aorta. The right coronary artery supplies blood to the right atrium and right ventricle and subsequently to the lungs. It further branches into the posterior descending artery and supplies blood to the bottom of the ventricles and back of the septum. The left main coronary artery divides into two branches, the Circumflex artery and the Left Anterior Descending artery (LAD). These two branches supply blood to the left atrium and back side of the left ventricle, and to the front and bottom of the left ventricle and front of the septum, respectively. [23]
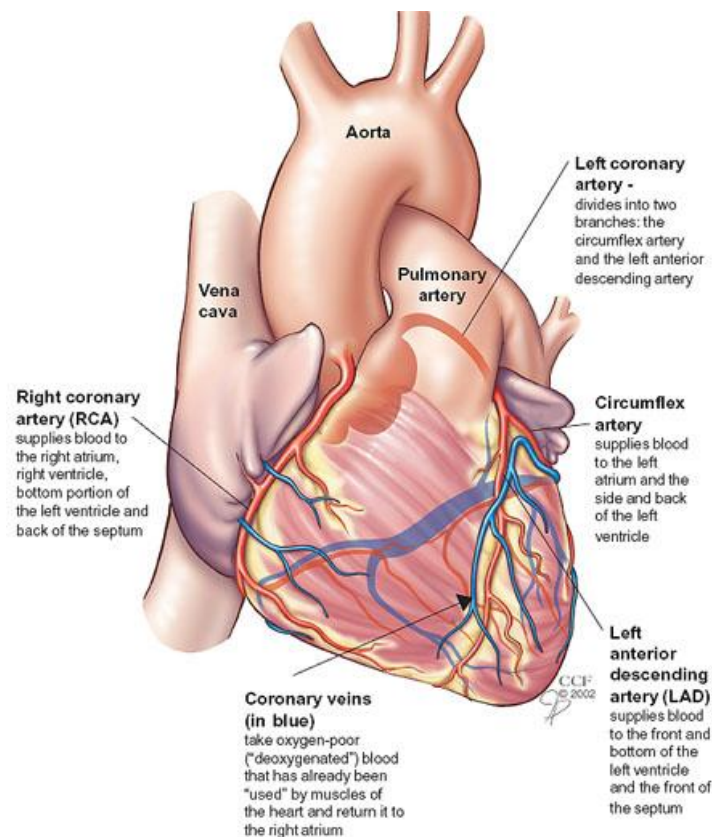
Figure 1.4: The four coronary arteries supply blood to the heart muscle. [23]

1.3 Symptoms

Symptoms of cardiovascular disease can greatly impact quality of life. Symptoms vary in severity from silent to a heart attack. Symptoms also vary depending on the location of the occluded artery. [21]

Occlusion of peripheral arteries in the legs decreases circulation, causing pain, fatigue, burning or discomfort in muscles of the feet, calves, or thighs, cold feet, numbness, open sores, and gangrene. [19], [20] Pain when walking that is relieved upon rest is called intermittent claudation. [18] Critical limb ischemia occurs when there is pain in the legs at rest. [11]

Reducing blood flow to the heart muscle can cause angina (chest pain or discomfort) or a heart attack when blood flow is further blocked. Shortness of breath, trouble breathing, fatigue, and swelling of the ankles, feet, legs, stomach, and veins in the neck can be symptoms of heart failure. Occluded coronary arteries can also weaken heart muscle and lead to heart failure or arrhythmias. [21]

1.4 Risk Factors

Elevated blood pressure, obesity, diabetes mellitus, and high blood lipid count increase the likelihood of developing peripheral arterial disease. [6] Smoking, age, and a history of stroke also increases the risk of peripheral arterial disease. Smoking, high levels of certain fats, cholesterol, or sugar in the blood, insulin resistance, diabetes, high blood pressure, obesity, physical activity, diet, age, family history, and blood vessel formation are risk factors for coronary arterial disease. [21] To reduce the risk of coronary arterial disease or peripheral arterial disease, lifestyle changes can be made. These include smoking cessation, lowering cholesterol, controlling blood pressure and blood sugar, and physical activity. [10], [20]

1.5 Current Treatments for Vascular Disease of Small Diameter Arteries

There are multiple nonsurgical and surgical methods to treat cardiovascular disease. Some nonsurgical treatments for cardiovascular disease include diet, exercise, maintaining a healthy weight, smoking cessation, managing stress, and medication. [10], [20], [21] Medicine can be prescribed to lower cholesterol, lower high blood pressure, prevent blood clots, and to relieve leg pain. [10], [18] For coronary arterial disease, anticoagulants, ACE inhibitors, beta blockers, calcium channel blockers, or other medicines may be prescribed. [21] However, these minimally invasive treatment techniques are often not adequate depending on the stage and prognosis of the atherosclerosis. When minimally invasive treatment is inadequate, surgical treatment may be necessary.

1.5.1 Angioplasty

Angioplasty is an endovascular procedure that opens arteries and may be performed when arteries are less than 70% occluded. [7], [10] During angioplasty, a catheter is inserted into a blood vessel and used to place a balloon at the site of occlusion. The balloon is then inflated to compress the plaque towards the arterial wall. The balloon is then deflated and removed. Compressing plaque buildup increases blood flow and delivery of oxygen and nutrients throughout the body. A stent can also be placed inside the artery to maintain the opening. [10], [10], [21]

1.5.2 Atherectomy

In addition to angioplasty, another endovascular procedure is atherectomy. In an atherectomy, catheter-based devices are used to remove plaque from an artery. [3], [10] Atherectomy can be advantageous because it removes obstructing atherosclerotic or intimal

hyperplastic lesions without the placement of a stent. Reintervention at the same site is also a low risk to the patient. [24]

1.5.3 Bypass Surgery

When an artery is more than 70% occluded, lifestyle changes, angioplasty, and atherectomy are insufficient at treating atherosclerosis. In these cases, arterial bypass grafting surgery may be recommended. [21] Arterial bypass grafting is a surgical procedure in which a bypass, or alternate pathway, around a narrowed or blocked portion of an artery is created. A graft is attached above and below the narrowed area, allowing blood to flow through an alternate conduit, or graft. [21]

Grafts can be autologous, meaning veins or arteries from another location within the body, or synthetic. Autologous veins are considered the gold standard because of accessibility, ease of use, higher patency rates, and lower rates of infection compared to currently available synthetic grafts. [1], [6], [25], [26] Autologous vessels are generally harvested from the saphenous vein, internal mammary artery, and radial artery. [6] When autologous vessels are not available, synthetic grafts are needed for use as bypass grafts. [6], [27]

1.6 Limitations of Current Treatments for Vascular Disease of Small Diameter Arteries

Balloon angioplasty compresses the plaque and stretches the artery wall, causing the plaque to crack and fracture. This process injures the artery and leads to acute vessel closure or restenosis. Acute vessel closure occurred in 3-5% of procedures within 24 hours of operation. Restenosis is characterized by a 50% occlusion of the artery due to a vessel injury response including vessel recoil and intimal hyperplasia. It occurs in 25-50% of balloon angioplasty procedures, with a majority of patients requiring additional intervention within six months.

Stenting, including drug eluting stents, has improved these patient outcomes. However, balloon angioplasty and stenting are still not viable options when vessels are occluded more than 70%. [28]

When vessels are more than 70% occluded, lifestyle changes, angioplasty, atherectomy, and stenting are not adequate treatments. In these cases, bypass surgery is performed. Autologous veins or arteries are the gold standard as a bypass conduit, but they are not suitable in a third of cases due to previous harvest, anatomical limitations, or donor site morbidity. For the coronary arteries, an internal mammary artery or radial artery graft typically shows better results than a greater sapheous vein graft. In peripheral arterial bypass, the greater saphenous vein is typically used. Allografts are not routinely used as bypass conduits. Due to the shortage of tissue donors and the limited supply of autologous blood vessels, there is a need for a synthetic vascular graft alternative to autologous vessels. While synthetic vascular grafts have been successful for large diameter vessels, they have not been as successful for small diameter vessels where the inner diameter is less than 6mm. Small diameter grafts have lower blood flow than larger diameter grafts. [4], [5], [7], [8], [22], [26] Viscoelastic properties of graft materials are more important at low flow rates. [29] The major causes of small diameter synthetic vascular graft failure are under dispute, but there is generally agreement that graft failure can be characterized by early thrombosis and late intimal hyperplasia. [6], [7], [30]

1.6.1 Early Thrombosis

A blood clot that forms within an artery or vein is called a thrombus. It is composed of platelets, fibrin, and other blood components. A thrombus that breaks loose and travels to another location in the body is called an embolus. Several factors can contribute to graft thrombosis, including graft surface properties (chemistry, morphology, etc.), graft

10

hemodynamics, surgical technique, patient thrombotic profile, and the degree of neointimal formation and endothelialization. [7] Decreasing surface thrombogenicity could improve short term and long term vascular graft patency.

1.6.1.1 Coagulation Cascade

When a material is implanted in the body and exposed to blood, protein adsorption occurs within seconds to minutes. [31], [32] Adsorbed proteins then undergo conformational changes and direct subsequent adhesion and activation of platelets. Platelets function in formation of the fibrin clot and release biochemical cues that recruit leukocytes (monocytes and neutrophils) to the site of injury. [13], [31]–[34] Inflammatory cells then lead to acute and chronic inflammation and the differentiation of monocytes into macrophages, apoptosis, and intercellular communication through cytokines and chemokines. Further cellular infiltration and activation by lymphocytes and fibroblasts occurs, initiating granulocyte recruitment. Foreign body giant cells can then encapsulate the implant. This response limits the integration of the implant with natural tissue. [31] Eventually, smooth muscle cell migration from the media to the intima can occur. [5]

Thrombin is the key enzyme in the coagulation system. It plays a role in platelet activation, conversion of fibrinogen to a fibrin network, and feedback amplification of coagulation. An ordered series of reactions at the site of vascular injury leads to the generation and activation of thrombin and is known as blood coagulation. A fibrin clot is formed when fibrin assembles into fibrils. [32], [34]

The coagulation cascade can be activated through two interconnected pathways. The extrinsic pathway of the coagulation system is initiated by the exposure of blood to extravascular tissue that occurs when the endothelium is ruptured. The second mechanism, the intrinsic

pathway, activates the coagulation system through changes in conformation of the coagulation factor XII, high molecular weight kininogen, preakallikrein, and factor XI. The intrinsic pathway results in the activation of factor XI. [32], [34]–[36] Implantation of a small diameter vascular graft damages epithelial tissue and initiates the extrinsic pathway.

1.6.1.2 Protein Adsorption

Upon implantation of a synthetic vascular graft, proteins from blood plasma adsorb to the wall of the graft immediately. Plasma proteins include albumin, γ-globulin, fibrinogen, and pro-thrombin. These proteins have binding sites for integrin receptors of platelets and other types of cells. When platelets bind to the integrin receptors or to the graft wall, they can become activated. [13], [36] Platelets can then initiate an inflammatory immune response and series of events that ultimately leads to thrombosis and fibrous growth around the implant. [13], [35], [36]

Surface hydrophobicity, roughness, and electrostatic interactions affect the quantity and type of proteins adsorbed [5], [7]. In general, small and abundant plasma proteins adsorb fast and are then displaced by larger proteins. This temporal displacement process is called the Vroman effect. [7] The composition of the adsorbed protein layer differs from the protein composition in blood. Proteins also change conformation upon binding and can change their function or immunological properties. [32]

Hydrophobic surfaces generally adsorb more proteins and cause more changes in protein conformation than hydrophilic surfaces with a neutral charge. Conformation changes can lead to the expression of neoepitopes, which promote inflammatory reactions, cell adhesion, and platelet adhesion. It has also been generalized that hydrophillic materials increase platelet adhesion rates, and hydrophobic materials increase platelet activation rates. An exception to this generalization is that hydrophilic polyethylene with plasma oxidation had more protein

adsorption but less platelet adhesion. Another exception is ePTFE, which has high hydrophobicity but is relatively hemocompatible. [32]

Another factor that affects protein adsorption is surface roughness. Smooth surfaces generally have less protein adhesion than rough surfaces. Roughness and turbulent blood flow highly activate platelets. Without flow, rough surfaces can reduce shear forces and increase endothelialization. [32]

There are disadvantages to both negative and positive surface charges in regards to surface hemocompatibility. Negatively charged surfaces can activate the plasmatic coagulation system. Positively charged surfaces can cause platelet adhesion and activation. Heparin is an exception that is a highly negative molecule yet has been shown to reverse these events. [32]

Trends in platelet adhesion with surface hydrophobicity, roughness, and charge are difficult to generalize. As platelet adhesion is widely related to adsorbed fibrinogen, Latour et al have investigated whether platelet adhesion to fibrinogen is the result of the amount of adsorbed protein or the conformation of the protein. Their work concludes that platelet adhesion is determined by the conformation of fibrinogen, where adsorption-induced unfolding of the protein exposes two types of platelet binding sites. One binding site was shown to induce platelet adhesion, while the other binding site was shown to induce both platelet adhesion and activation. [37] Further, Latour et al found evidence that increasing surface hydrophobicity increases the amount of fibrinogen and albumin adsorbed and also increases the degree of conformation change. [38]

While fluoropolymers are often regarded as chemically inert, they are not inert regarding protein adsorption and blood clotting *in vivo* or *in vitro*. In particular, albumin binds tightly with fluropolymers, and albumin, fibrinogen, and fibronectin bind in high amounts on PTFE surfaces.

Solid fluoropolymers have been found to have high protein adsorption for most blood serum proteins. Porous fluropolymers with pore size 60-80μm, can lead to rapid blood clotting and bacterial growth due to blood protein adsorption, cell and bacterial adhesion, and integration into the material pores. Additionally, fluorinated surfaces have different interactions with different types of media, (for example, whole blood or blood plasma). [39]

Protein adsorption on fluorinated polymers has also been shown to have a passivating effect that hinders endothelial cell growth. In particular, high amounts of adsorbed albumin can create a biofouling surface which prevents biological interaction. Lack of endothelial cell growth has been attributed to excessive albumin binding compared to cell binding proteins, such as fibronectin and collagen. Attempts have been made to attach adhesive cell proteins to surfaces in attempt to increase endothelial cell growth on fluoropolymers. [39]

1.6.1.3 Shear Stress

Thrombus formation is also been related to shear stress on the graft lumen. A higher shear stress is correlated with a decrease in thrombus formation. A small diameter graft has a lower shear stress than a large diameter graft and is more likely to develop a blood clot. This follows Pouiselles law that flow rate through a narrow tube is low. [7]

1.6.1.4 Endothelialization

Endothelial cells have anti-thrombogenic functions, and a lining of endothelial cells on the lumen of a graft can decrease thrombosis. Conversely, a lack of functional endothelial cell coverage on the lumen surface can lead to thrombosis and subsequent occlusion. [22] A layer of endothelial cells on the graft lumen could increase the patency of synthetic vascular grafts.

Endothelial cells produce anticoagulants, including heparans, thrombomodulin, and coagulation inhibiting proteins. The endothelium is also a protective physical barrier between

14

circulating blood proteins and the subendothelium, where molecules that cause platelet adhesion can be found. These molecules include collagen, fibronectin, and thrombospondin.

Endothelial cell coverage can also limit inflammation. Anti-coagulant phenotype endothelial cells produce vasoprotective factors and inhibit the production of factors that cause inflammation. One such factor, inducible nitric oxide, forms nitric oxide and decreases the adhesion of platelets. Another factor, tissue factor, is a procoagulant protein which, in combination with fVIIa, activates FX and leads to the production of thrombin. Tissue plasminogen activator plays a role in plasminogen activation, fibrinolysis, and fibrin clot degradation. Vascular cell adhesion molecule 1 supports white blood cell adhesion, including monocytes and lymphocytes. [4]

Natural endothelialization occurs by three mechanisms within the body: direct migration from the anastomotic edge, transmural migration, and cell transformation from progenitor cells. The blood is not an efficient source for endothelial cells. The formation of capillaries within the pores of a graft is also important for endothelialization. ePTFE typically has poor capillary formation due to a small pore size of 30μm. Knitted Dacron is more porous and can form a patchy endothelial layer on the graft. Further modifications to increase endothelialization, such as microporosity and extracellular matrix deposition are also being pursued. Endothelial cells can also be seeded into a synthetic graft. [13]

In practice, endothelialization has had mixed results. Endothelial cells have poor retention on graft surfaces when exposed to dynamic blood flow. One study reports that endothelialization of ePTFE grafts has shown only moderate improvement over nonendothelialized ePTFE grafts. Another study using Dacron grafts seeded with endothelial cells implanted in a canine model demonstrated a 76% patency rate compared to unseeded grafts

15

with a 22% patency rate at four weeks. Extracellular matrix proteins such as collagen, laminin, and fibronectin can be used to coat materials to increase retention of endothelial cells. [4] A surface that increases endothelial cell growth and proliferation on a surface could decrease thrombus formation.

1.6.2 Late Intimal Hyperplasia

Intimal hyperplasia (IH) is characterized by a migration of vascular smooth muscle cells from the media to the intima. After migration, smooth muscle cells synthesize matrix proteins and other extracellular material that can cause blood vessels to become stenosed. While much research has been done regarding the development of IH, its causes are not fully understood. IH formation within 2-24 months of implantation has been attributed to a difference in mechanical compliance between the relatively stiff synthetic graft and more elastic artery, mismatch in diameter between the graft and artery, lack of endothelialization, trauma from surgery, and changes in blood flow [5], [29].

1.6.2.1 Mechanical Compliance

Graft compliance is quantified by the changes in graft diameter with changes in pressure. The mismatch between compliance of relatively rigid synthetic and more compliant natural vessels can contribute to IH formation at the downstream anastomosis by altering hemodynamics. Specifically, a compliance mismatch at the anastomosis can increase shear stress, reducing perfusion, and causing injury to the vessel wall. [29], [40] Disturbances in flow patterns are caused by divergent and convergent flow geometries. A divergent geometry can decrease mean wall shear stress, causing flow separation. A convergent geometry can increase wall shear stress, causing injury of the endothelium and platelet activation. [41] A change in blood flow velocity can cause stagnant flow regions. It can also cause a pulsatile stress on the

arterial wall at both anastomosis sites, leading to local arterial hypertrophy. Previous studies by Roeder et al indicate that high pulsatile stress in stiffer grafts led to arterial hypertrophy and earlier graft failure compared to less stiff grafts. [42]

A stiffer tube reduces the pulsatile component of diastolic recoil by up to 40% of the pulsatile energy. This leads to vibratory weakening of the natural artery, thereby injuring endothelial cells and causing anastomotic aneurysm. [41]

Convergent and divergent geometries also alter the wall shear rate distribution. The distal anastomosis has a lower mean shear stress and higher degree of oscillation compared to the proximal anastomosis, which has a higher mean shear stress and lower degree of oscillation. When there is an increase in graft-artery compliance mismatch, the mean shear stress decreases and the oscillatory shear increases at the distal anastomosis through three mechanisms. (1) The distal anastomosis then has increased shear stress, which can cause vessel injury, which can lead to intimal hyperplasia. (2) Cyclic stretching can cause smooth muscle cell replication and subsequent production of extracellular matrix. (3) A discontinuity in compliance causes flow changes associated with prolonged particle residence time, flow separation, and stasis, leading to lower shear stress. Intimal thickening occurs in regions with low shear stress. [41]

It has become widely accepted that Dacron® and ePTFE are less compliant (more stiff) than natural arteries. [29] Dacron® and ePTFE are relatively rigid and are less compliant than natural vessels, as shown in Table 1.1. Synthetic grafts become less compliant upon implantation. Post-implantation stiffening must be considered when matching graft-artery compliance. [29], [43]

17

Table 1.1: Mechanical compliance and graft patency for various graft materials. [41]

Graft	Compliance (%mmHg x 10^2)	Graft Patency (%)
Natural artery	5.9 ± 0.5	N/A
Saphenous vein	4.4 ± 0.8	75
Umbilical vein	3.7 ± 0.5	60
Bovine heterograft	2.6 ± 0.3	59
Dacron®	1.9 ± 0.3	50
PTFE	1.6 ± 0.2	40

1.7 Material Selection

The two synthetic graft materials most commonly used for small diameter arterial bypass procedures are polyethylene terepthalate (Dacron ®) and expanded polytetrafluoroethylene (ePTFE). Much research on polyurethanes (PUs) as another material option has been done due to their mechanical property matching to natural vessels. [7]

While Dacron and ePTFE are the most commonly used synthetic vascular graft materials, there are significant limitations that make them unfavorable for use. Specifically, Dacron and ePTFE grafts display failure due to early thrombosis or late intimal hyperplasia. [7], [44] ePTFE grafts are generally preferred for peripheral artery bypass in the UK, but most studies have not shown a difference in long-term patency between ePTFE and Dacron grafts. [5], [29]

Dacron® is a brand name for polyethylene terephthalate (PET) materials. It is a hydrophobic thermoplastic polymer resin made of fibers that are either woven or knitted. Porosity is defined by water permeability. Crimping can be used to increase distensibility and kink resistance. [25], [44] It has a mechanical compliance, elastic modulus, and ultimate tensile strength of 1.9 MPa, 14,000 MPa, and 170-180 MPa, respectively. [41] Dacron is successfully used to treat large diameter vascular grafts but has low patency as a small diameter vascular graft, particularly for lower limb bypass procedures. Dacron grafts do not develop an endothelial

cell layer on the lumen when implanted, leading to platelet adhesion, fibrin layer formation, and thrombosis. [44]

PTFE is an inert fluoropolymer consisting of carbon-fluorine bonds. Extrusion, stretching, and sintering processing techniques can make PTFE more porous, forming expanded PTFE (ePTFE). The result is a nontextile porous tube with irregular shaped fibrous channels and peaks, called nodes. ePTFE is not biodegradable and is electronegative. It has a mechanical compliance, elastic modulus, and ultimate tensile strength of 1.6 MPa, 14 MPa, and 500 MPa, respectively. [41] It is a thermoplastic with melting temperature around 327°C. The coefficient of dynamic friction is as low as 0.05, and ePTFE has self lubricating properties. [45] Porosity is described as the intermodal distance (IND), which is typically 30-90μm, where the space available for actual cellular ingrowth is smaller than the IND. An IND of 60μm was suggested as the optimum size for tissue ingrowth and endothelialization, although in practice, tissue ingrowth did not fully extend into pores and did not produce an endothelial lining. [5], [7] The patency of ePTFE as a femoropopliteal graft was determined to be 39% and 45%, whereas the patency of autologous vein grafts was 74% and 77%, as reported by Tatterton et al and Wang et al. [7], [44] ePTFE grafts do not develop an endothelial cell layer, leading to a platelet rich fibrin layer, thrombus, and encapsulation. [5], [7]

PUs are a large group of elastic polymers that contain a urethane group. In general, PUs are copolymers with crystalline (hard) and amorphous (soft) segments that can be altered during manufacturing. PUs are gaining interest for use in small diameter vascular grafts because mechanical properties can be tailored to match those of native blood vessels. Particularly, polyurethane is more compliant than ePTFE. These materials can have a fibrillar or foamy microstructure, where both structures lack space for capillary ingrowth. Fibrillar PUs become

19

covered by a fibrin layer thinner than that of Dacron, and the outer surface becomes encapsulated

by foreign body giant cells. Foamy PUs can have increased capillary ingrowth with pore sizes

up to 157μm and a diminished foreign body giant cell response. However, polyurethane

materials have been susceptible to hydrolytic degradation *in vivo* and require further

investigation before commercial clinical use. Advances have been made to produce PUs

resistant to hydrolytic degradation that promoted faster endothelialization and less IH compared

to ePTFE in rats. [5], [29]

A totally engineered blood vessel that can remodel, grow, self-repair, and respond to the

environment could be highly advantageous. Such a graft could have a functional endothelial cell

lining with antithrombogenic properties that completely integrates into host tissue. If the graft

had mechanical properties matching those of natural blood vessels it could temporarily provide

support to function as a blood vessel while gradually degrading as natural tissue grows over the

graft. Both biological and synthetic materials have been used for this application. Biological

materials are often decellularized. Synthetic polymers include poly(ester urethane) urea (PEUU)

polyethylene glycol acid (PGA), polylactic acid (PLA), and polyglycolic acid (PLLA).

Biodegradable scaffolds have potential limitations, including: off-the-shelf availability,

insufficient mechanical matching to native tissue (low mechanical strength could lead to rupture

or aneurysm and compliance mismatch could cause obstruction of the graft), acidic degradation

products that could cause inflammation, thrombogenicity, complex processing, and high prices.

However, the fabrication of such a graft is a long-term and complex goal. [5], [12], [22], [46]

1.8 Material Surface Modifications

Various modifications to materials in attempt to create a more inherently antithrombogenic

graft material have been attempted. Modifications include physical, chemical, and bioactive

surface structuring (including surface roughening, plasma etching, and peptide motif modifications). [30] Chemical modifications include attachment of functional polypeptide groups (including cell adhesive ligands), antithrombogenic proteins (heparin), or cell monolayers (endothelial cells). [46] Various suturing techniques have also been tested for decreased IH formation. [5]

Biomimetic microarchitectures and nanoarchitectures modeled after the three-dimensional morphology of natural extracellular matrix have been used in attempt to decrease surface thrombogenicity. [30] Plasma surface modification (PSM) can be used to modify surfaces through physiochemical techniques including etching, chemical reactivity, sterilization, and ion irradiation. It can also be used to create thin film coatings, macromolecule grafts, and immobilize specified proteins. PSM can be used to modify graft-blood surfaces while maintaining the mechanical properties of the bulk material. [25]

Electrospinning is one method to fabricate nanostructured grafts with a desired shape and porosity. Electrospinning can be an advantageous technique for fabricating vascular grafts because materials and constructs can be tailored to match the biomechanical and structural properties of natural blood vessels. This can promote cell attachment, proliferation, and differentiation. Smooth muscle cells and endothelial cells have been shown to maintain phenotype and form three-dimensional cell networks on electrospun scaffolds *in vitro*. However, *in vivo* studies with electrospun materials are limited. [30]

Surface modifications could be a useful technique to improve surface function for contact with blood. [25] Surface modification through coatings to attenuate the coagulation cascade have been attempted. Heparin, covalently bonded dipyridamole, adenosine diphosphatase, Hirudin, nitric oxide, and zwitterionic monomers have been used with limited success due to lack

of immobilization, degradation, long-term durability, and limited testing. [13], [36] Surface

treatments have been performed in an effort to improve endothelial cell retention and to reduce

protein adsorption and platelet adhesion to the graft wall. [13] Such modifications include

attachment of RGD peptides, matrix proteins (fibronectin), growth factors (fibroblast growth

factor or endothelial cell growth factor), or a combination of coatings. [4], [44]

Several surface modifications specifically on ePTFE surfaces have been attempted.

Carbon coating on the graft lumen is resistant to platelet adhesion and fibrin deposition and has

been commercialized by Bard. However, coating the lumen of ePTFE grafts with carbon did not

show an increase in graft patency. [4], [47] Polyethylene glycol (PEG) is a molecule used for

surface modifications that passively adsorbs on glass surfaces, decreasing protein and platelet

adsorption and subsequent thrombosis. The decrease in protein adsorption is thought to be the

result of the highly hydrophilic CH_2-CH_2-O repeat units that form a "liquid-like" surface with

mobile molecular chains. In contrast to other water-solvated coatings, PEG has small

hydrophobic groups and no prominent surface charge. A PEG coating on ePTFE in a porcine

model was shown to reduce thrombus formation and IH, resulting in higher patency. One

disadvantage of PEG coatings is limited durability, where the surfaces quickly loose stability and

resistance to protein adsorption. A second disadvantage is oxidation of the hydroxyl group on

PEG, forming an aldehyde group, which can interact with proteins. Similarly,

phosphatydilcholine (PC) binds strongly with water, forming a hydrated surface layer that resists

protein adsorption. PC is a phospholipid in animal cell membranes that limits protein, platelet,

and cellular adhesion due to zwitterionic properties of the molecule containing both positive and

negative charges but having a net neutral charge. A 4mm diameter ePTFE graft with PC

decreased platelet adhesion in a baboon model. A polyester elastomer, poly(diol citrate) (PDC)

22

is another hydrophilic molecule used in medical applications that has been proven to reduce

blood clotting with a limited inflammatory response while improving endothelial cell retention.

Albumin has been used to passivate surfaces to prevent binding of thrombogenic proteins, such

as fibrinogen and fibronectin. While hydrophobic, albumin is thought to reduce protein, platelet,

and cellular adhesion due to a lack of cellular binding sites with peptide groups. However, there

is a lack of evidence for improved patency with albumin coatings, and albumin coatings are

susceptible to displacement by other proteins, limiting the long-term antithrombogenic

properties. Elastin, an extracellular matrix protein that functions in vessel elasticity, has also

been found to produce minimal platelet adhesion and aggregation. It also inhibits monocytes,

leukocytes, and smooth muscle cells, thereby inhibiting both thrombosis and IH. Preliminary

results of ePTFE-elastin grafts in baboons showed minimal thrombogenicity. [47] Heparin-

coated ePTFE grafts have also been shown to reduce platelet adhesion and inhibit whole blood

clotting kinetics. Heparin is used in anticoagulation and has a high negative charge density. [1],

[48]

1.9 Hyaluronan and its Biomedical Applications

1.9.1 Hyaluronan: An Overview

Hyaluronan (HA) was first isolated from the vitreous humor of bovine as an acid in 1934

by Karl Meyer and John Palmer from Columbia University. At that time, the molecule was

named hyaluronic acid in reference to its acidic form. Endre Balazs later developed the term

"hyaluronan" in 1986 to be more inclusive of the different forms the molecule can take, such as

an acid or a salt. [49]

HA is nontoxic, biodegradable, biocompatible, and nonimmunogenic. The enzymatic

degradation products are oligomeric sugars that are also considered nontoxic and are actually

mitogenic for endothelial cells *in vitro*. They are also correlated with blood vessel growth *in vitro* and *in vivo*. HA has therefore been used in wound healing, ophthalmic surgery, and other applications. HA immobilization on PU surfaces has been shown to increase hydophilicity and prolong the coagulation time, resulting in improved biocompatibility compared to PU without HA. [50]

HA is a nonsulfated glycosaminoglycan (GAG) component of the extracellular matrix. [51] It occurs naturally in vertebrate tissue and body fluids. It is found in relatively high concentrations in the vitreous humor of the eye, umbilical cord, synovial joint fluid, and rooster combs. [52] HA is a large and unbranched molecule and has repeating disaccharide structure of N-acetylglucosamine and glucuronic acid. [49]

As a polysaccharide, HA has a unique combination of properties. HA is viscoelastic, where HA solutions are primarily viscous at a low shear rate and elastic at a high shear rate. This is thought to be associated with the single carboxyl group (-COOH) per disaccharide unit of HA. The carboxyl group dissociates at a physiological pH, producing polyanionic properties. The negatively charged chains can expand and entangle at low concentrations, which can contribute to viscoelastic properties. The viscoelastic properties of HA make it an effective lubricant. [49]

HA is also hydrophilic and retains water. When hydrated, HA can swell to 1,000 times the size of the dry molecule. The large molecular volume can cause HA molecular domains to overlap, entangle, and thus enabling the molecule to hold up to 1,000 times its weight in water. Other glycosaminoglycans are not known to retain water the same way. [49]

HA is present in the intima and adventitia of all blood vessels, and it can be found in the media with less homogeneous distribution. The amount of HA present in blood vessels depends

on the age and type of vessel, ranging from 40% to 4% of the total glycosaminoglycan content in the fetal umbilical artery compared to the adult aorta, respectively. The higher HA content in younger vessels results in a loose, hydrated, and flexible extracellular matrix. Multiple studies have reported that HA plays a role in endothelial cell proliferation, migration, and retention. It has also been shown that HA functions in the formation of new blood vessels. A hyaluronan-based biodegradable polymer, Hyaff-11, has been shown to promote endothelialization. [16], [17], [51], [53]–[55] HA is present in the endothelial cell glycocalax, but it is unknown how HA is attached or whether it is bound to assembly proteins or forms a HA-HA complex. As HA can form highly viscous films, it may be unbound. [56] However, the role of HA in atherogenesis is complex and somewhat conflicting. In addition to interaction with endothelial cells, HA has also been shown to interact with smooth muscle cells, platelets, and leukocytes. [52]

HA has also been used in nanoparticles for drug delivery [57], synovial fluid in arthritic patients, cosmetic surgery, cosmetic and soft tissue surgery, and abdominal procedures. It is also used as a diagnostic marker for cancer, rheumatoid arthritis, liver disease, and organ transplantation rejection. [58] Medical devices, including catheters, guidewires, and sensors use HA to increase lubricity and decrease biofouling. Additional applications of HA include viscosupplementation, viscoseparation, viscosurgery, viscoaugmentation, drug delivery, wound repair, medical devices, and other applications of tissue engineering [49].

1.9.2 HA and Hemocompatibility

Much research has been directed towards finding materials that are inert and have minimal interaction with blood. [59] Due to the hydrophilic, electronegative, and polyanionic properties of hyaluronic acid, it is thought to have potential to reduce thrombogenicity when incorporated with ePTFE. HA has been shown to reduce platelet adhesion and aggregation and

25

to prolong bleeding time. [51] As part of the extracellular matrix, HA functions both as a structural and cell-signaling component of a vessel wall. It can be non-cytotoxic, non-thrombogenic, non-immunogenic, and does not cause chronic inflammation. It plays a role in regulating angiogenesis, morphogenesis, wound healing, tissue organization, embryonic development, and cell adhesion, migration, and differentiation. [52], [60]

Previous studies indicate that these qualities of HA depend on the molecular weight of the HA monomers. High molecular weight HA (1500 kDa) is naturally anti-inflammatory and immunosuppressive, thereby inhibiting migration of free-radical producing microbes into other tissues. On the other hand, low molecular weight HA (0.75 – 10 kDa) interacts with cell receptors to induce multiple signaling cascades. An HA oligomer mixture of 6 and 12 mers was previously produced and enhanced endothelial cell proliferation and angiogenesis but stimulated an inflammatory response. High molecular weight HA (1500 kDa) inhibited platelet adherence to endothelial cells and had less of inflammatory effect. [60]

1.10 Chemical Modification of Hyaluronan

While HA has biomedical applications, it is soluble in water and is unstable in the body in its native form, where it is subject to enzymatic degradation. It can be necessary to modify HA to create a more stable molecule, such as through chemical crosslinking or coupling reactions. [49]

Chemical crosslinking of the hydroxyl, carboxyl, and both the hydroxyl and carboxyl groups of HA has been performed. The extent of crosslinking, the type of covalent bond, and the binding group involved affect the viscoelasticity and type of material formed. Zhang et al. selected hexamethylene diisocyanate (HMDI) as a chemical crosslinker because of the location of crosslinking within the HA molecule. HMDI crosslinks the hydroxyl groups of HA. It was

important to maintain lubricious properties conferred by the carboxyl groups for application to focal cartilage defect repair in knees. [49]

1.11 Prior Work Combining HA and Synthetic Plastics for Medical Applications

Previous work by Zhang and James et al. led to a microcomposite composed of ultra high molecular weight polyethylene (UHMWPE) and HA used for articular cartilage repair of focal defects. Porous preforms of UHMWPE were prepared for HA modification because a porous material was needed for HA infiltration. The preforms were compression molded to a desired density after modification with HA. Zhang et al used HA with a molecular weight of 1.36×10^6 Da. [49], [61]

The HA molecules are first modified to be more hydrophobic to match the chemical properties of UHMWPE. HA is processed to form silylated HA-CTA to make it hydrophobic and soluble in organic solvents. This makes it possible to dissolve into a solution and wick into a hydrophobic material. However, HA cannot be silylated directly; a complex of sodium HA and cetyltrimethylammonium bromide (CTAB), HA-CTA, is first formed as shown in Figure 1.5. HA-CTA is an ion-paired complex formed when bromide and sodium ions separate and subsequently bind in solution. The HA-CTA is then silylated as shown in Figure 1.6. With a high enough degree of silylation, silyl HA-CTA will dissolve in xylenes. With a lower degree of silylation, it will dissolve in acetone, THF, or 1,2-dichloroethane. Xylenes were selected based on the similarity of the Hildebrand Solubility factor to the host material. Once silylated and dissolved into xylenes, silyl HA-CTA diffuses into pores of the UHMWPE. The silyl HA-CTA is then cross-linked with hexamethyl diisocyanate (HMDI) through the hydroxyl groups on HA. Due to the hydrophilicity of HA, it does not chemically bind with UHMWPE. A hydrolysis

procedure then changes silylated HA-CTA back to HA as shown in Figure 1.7. The UHMWPE-

HA microcomposites were then compression molded to a desired density. [49], [61]–[63]
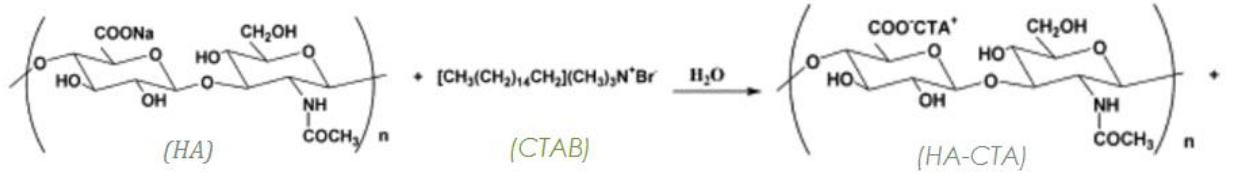
Figure 1.5: Complexation of HA-CTA from HA and CTAB
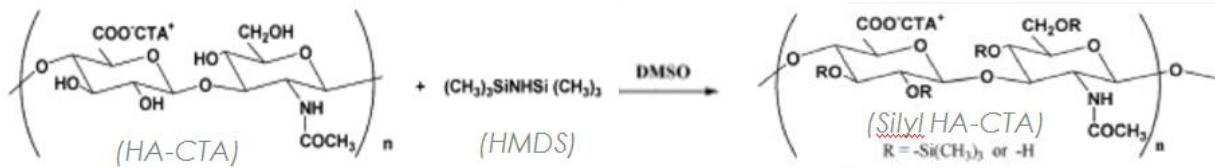
Figure 1.6: Silylation of HA-CTA using HMDS and DMSO
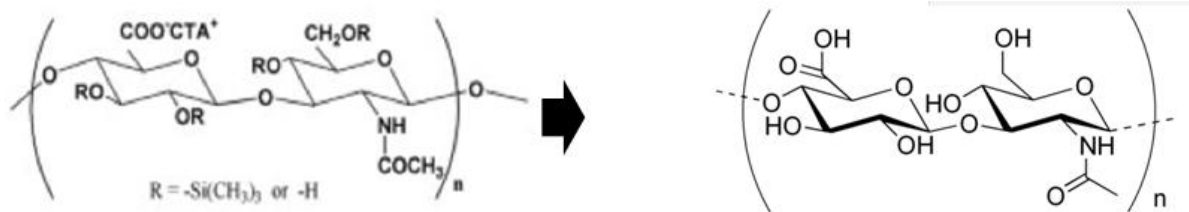
Figure 1.7: Hydrolysis of silyl HA-CTA into HA

Modifying polyethylene materials with HA for use as prosthetic heart valve replacements

was pursued by Dean et al. Linear low density polyethylene (LLDPE) was selected as one such

material based on mechanical property matching to natural heart valve leaflets. Polyethylene

terephthalate (PET) was selected as a second material based on previous success in

cardiovascular applications. Swelling times and temperatures were selected for successful

creation of interpenetrating networks of HA within the two base materials. Mechanical

properties were measured, and the HA treatment was also shown to decrease blood clotting at 30

and 60 mins, as measured by the absorbance of free hemoglobin. [62], [63]

1.12 Thesis Overview and Specific Aims

There is a major need to develop a small diameter vascular graft with higher patency rates, less thrombogenicity, and less IH. ePTFE is well established for use in blood-contacting applications despite propensity for thrombosis and IH formation. Hydrophilic groups such as PEG can be covalently attached to the material surface and are proven to reduce thrombosis through the formation of a water-solvated surface. However, attachment of chemical groups to ePTFE with long-term stability has been a challenge. [13] HA is highly hydrophillic and has been shown to reduce thrombosis, forms a lubricious coating, and encourages endothelial cell migration and proliferation. An ePTFE-HA material with durable HA coating has potential as a less thrombogenic small diameter vascular graft. The goal of the present work is to make ePTFE less thrombogenic by enhancement with HA. Specifically, a synthetic small diameter vascular graft microcomposite of ePTFE and HA is proposed. While this work is focused on the application of HA-modified ePTFE for use in small diameter vascular grafts, such a material could be useful for other applications, such as blood filtration systems or catheters. The potential of ePTFE materials prepared using HA as a small diameter vascular graft was evaluated by characterizing materials, evaluating graft thrombogenicity, and assessing mechanical properties. Specific aims and hypotheses are listed below.

1. Specific Aim: Characterize HA-modified ePTFE materials through FTIR, XPS, SEM, TGA, contact angle, and SWLI.

    a. Hypothesis: More HA will be observed on samples prepared with swelling solutions with a higher concentration of HA with potential for diffusion limitations at the highest concentration.

2. <u>Specific Aim</u>: Evaluate the efficacy of HA-modified ePTFE materials at reducing thrombogenicity in synthetic vascular grafts under static conditions through protein adsorption, platelet and leukocyte adhesion and activation, cell viability assay, and assessment of free hemoglobin.

   a. <u>Hypothesis</u>: HA will reduce surface thrombogenicity of ePTFE-HA materials compared to ePTFE only.

3. <u>Specific Aim</u>: Characterize mechanical properties of HA-modified ePTFE materials. Specifically, assess radial and longitudinal tensile properties and water entry pressures. Assess durability of the crosslinked HA against enzymatic degradation by hyaluronidase.

   a. <u>Hypothesis</u>: HA will increase the ultimate tensile strength and stiffness of ePTFE but will resist enzymatic degradation when crosslinked. Lubricious properties of HA may lower the water entry pressure of HA-modified ePTFE.

REFERENCES

[1] Hoshi, R.A.; Van Lith, R.; Jen, M.C.; Allen, J.B.; Lapidos, K.A.; Ameer, G. The blood and vascular cell compatibility of heparin-modified ePTFE vascular grafts. *Biomaterials* **2013,** 34, 30–41.

[2] Peck, M.; Gebhart, D.; Dusserre, N.; McAllister, T.N.; L'Heureux, N. The Evolution of Vascular Tissue Engineering and Current State of the Art. *Cells Tissues Organs* **2012,** 195, 144–158.

[3] Goodney, P.P.; Beck, A.W.; Nagle, J.; Welch, H.G.; Zwolak, R.M. National trends in lower extremity bypass surgery, endovascular interventions, and major amputations. *J. Vasc. Surg.* **2009,** 50, 54–60.

[4] Dudash, L.A.; Kligman, F.; Sarett, F.M.; Kottke-Marchant, K.; Marchant, R.E. Endothelial cell attachment and shear response on biomimetic polymer-coated vascular grafts. *J. Biomed. Mater. Res. A* **2012,** 100, 2204–2210.

[5] Chlupác, J.; Filová, E.; Bacáková, L. Blood vessel replacement: 50 years of development and tissue engineering paradigms in vascular surgery. *Physiol. Res. Acad. Sci. Bohemoslov.* **2009,** 58, S119–139.

[6] Baguneid, M.; de Mel, A.; Yildirimer, L.; Fuller, B.J.; Hamilton, G.; Seifalian, A.M. In vivo study of a model tissue-engineered small-diameter vascular bypass graft. *Biotechnol. Appl. Biochem.* **2011,** 58, 14–24.

[7] Tatterton, M.; Wilshaw, S.P.; Ingham, E.; Homer-Vanniasinkam, S. The use of antithrombotic therapies in reducing synthetic small-diameter vascular graft thrombosis. *Vasc. Endovascular. Surg.* **2012,** 46, 212–222.

[8] Mun, C.H.; Jung, Y.; Kim, S.H.; Lee, S.H.; Kim, H.C.; Kwon, I.K.; Kim, S.H. Three-Dimensional Electrospun Poly(Lactide-Co-ε-Caprolactone) for Small-Diameter Vascular Grafts. *Tissue Eng. Part A* **2012,** 18, 1608–1616.

[9] Zhu, A.P.; Ming, Z.; Jian, S. Blood compatibility of chitosan/heparin complex surface modified ePTFE vascular graft. *Appl. Surf. Sci.* **2005,** 241, 485–492.

[10] National Institutes of Health. What is Peripheral Arterial Disease?. http://www.nhlbi.nih.gov/health/health-topics/topics/pad (accessed 2011).

[11] Robert Wood Johnson University Hospital. Peripheral Arterial Disease Treatment, PAD Treatment. http://www.rwjuh.edu/medical_services/peripheral-arterial-disease.html (accessed Jan 9, 2013).

[12] Ratcliffe, A. Tissue engineering of vascular grafts. *Matrix Biol.* **2000,** (19), 353–357.

[13] Sarkar, S.; Sales, K.M.; Hamilton, G.; Seifalian, A.M. Addressing thrombogenicity in vascular graft construction. *J. Biomed. Mater. Res. B Appl. Biomater.* **2007,** 82B, 100–108.

[14] Wagenseil, J.E.; Mecham, R.P. Vascular Extracellular Matrix and Arterial Mechanics. *Physiol. Rev.* **2009,** 89, 957–989.

[15] Davis, G.E.; Senger, G.R. Endothelial Extracellular Matrix Biosynthesis, Remodeling, and Functions During Vascular Morphogenesis and Neovessel Stabilization. *Circ. Res.* **2005,** 97, 1093–1107.

[16] Lepidi, S.; Grego, F.; Vindigni, V.; Zavan, B.; Tonello, C.; Deriu, G.P.; Abatangelo, G.; Cortivo, R. Hyaluronan Biodegradable Scaffold for Small-caliber Artery Grafting: Preliminary Results in an Animal Model. *Eur. J. Vasc. Endovasc. Surg.* **2006,** 32, 411–417.

[17] Turner, N.J.; Kielty, C.M.; Walker, M.G.; Canfield, A.E. A novel hyaluronan-based biomaterial (Hyaff-11®) as a scaffold for endothelial cells in tissue engineered vascular grafts. *Biomaterials* **2004,** 25, 5955–5964.

[18] CardioSmart: Peripheral Arterial Disease (PAD). http://cardiosmart.org/HeartDisease/CTT.aspx?id=134 (accessed Jan 10, 2013).

[19] Artery Bypass Procedures. http://catalog.nucleusinc.com/displaymonograph.php?MID=216 (accessed Jan 9, 2013).

[20] Peripheral artery disease - legs: MedlinePlus Medical Encyclopedia. http://www.nlm.nih.gov/medlineplus/ency/article/000170.htm (accessed Jan 9, 2013).

[21] National Institutes of Health. What Is Coronary Heart Disease?. http://www.nhlbi.nih.gov/health/health-topics/topics/cad/ (accessed Jan 9, 2013).

[22] Kong, X.; Han, B.; Li, H.; Liang, Y.; Shao, K.; Liu, W. New biodegradable small-diameter artificial vascular prosthesis: A feasibility study. *J. Biomed. Mater. Res. Part A* **2012,** 100A, 1494–1504.

[23] Cleveland Clinic. The Coronary Arteries. http://my.clevelandclinic.org/heart/heartworks/coronaryartery.aspx (accessed Jan 10, 2013).

[24] Shrikhande, G.V.; McKinsey, J.F. Use and abuse of atherectomy: where should it be used?. *Semin. Vasc. Surg.* **2008,** 21, 204–209.

[25] Solouk, A.; Cousins, B.G.; Mirzadeh, H.; Seifalian, A.M. Application of plasma surface modification techniques to improve hemocompatibility of vascular grafts: A review. *Biotechnol. Appl. Biochem.* **2011,** 58, 311–327.

[26] Konig, G.; McAllister, T.N.; Dusserre, N.; Garrido, S.A.; Iyican, C,; Marini, A.; Fiorillo, A.; Avila, H.; Wystrychowski, W.; Zagalski, K.; Maruszewski, M.; Jones, A.L.; Cierpka, L.; de la Fuente, L.M.; L'Heureux, N. Mechanical properties of completely autologous human tissue engineered blood vessels compared to human saphenous vein and mammary artery. *Biomaterials* **2009,** 30, 1542–1550.

[27] Zhao, J.; Liu, L.; Wei, J.; Ma, D.; Geng, W.; Yan, X.; Zhu, J.; Du, H.; Liu,Y.; Li,L.; Chen, F. A novel strategy to engineer small-diameter vascular grafts from marrow-derived mesenchymal stem cells. *Artif. Organs* **2012,** 36, 93–101.

[28] Hamid, H.; Coltart, J. Miracle stents' - a future without restenosis. *McGill J. Med. MJM* **2007,** 10, 105–111.

[29] Tiwari, A.; Salacinski, H.; Seifalian, A.M.; Hamilton, G. New prostheses for use in bypass grafts with special emphasis on polyurethanes. *Cardiovasc. Surg.* **2002,** 10, 191–197.

[30] Bergmeister, H.; Grasl, C.; Walter, I.; Plasenzotti, R.; Stoiber, M.; Schreiber, C.; Losert, U.; Weigel, G.; Schima, H. Electrospun small-diameter polyurethane vascular grafts: ingrowth and differentiation of vascular-specific host cells. *Artif. Organs* **2012,** 36, 54–61.

[31] Smith, B. Titania Nanotube Arrays: Interfaces for Implantable Devices. Ph.D. Dissertation, Colorado State University, Fort Collins, CO, 2012.

[32] Werner, C.; Maitz, M.F.; Sperling, C. Current strategies towards hemocompatible coatings. *J. Mater. Chem.* **2007,** 17, 3376.

[33] Heemskerk, J.W.M.; Bevers, E.M.; Lindhout, T. Platelet activation and blood coagulation. *Thromb. Haemost.* **2002,** 88, 186–193.

[34] Dahlbäck, B. Blood coagulation. *The Lancet* **2000,** 355, 1627–1632.

[35] Smith, B.S.; Popat, K.C. Titania nanotube arrays as interfaces for blood-contacting implantable devices: a study evaluating the nanotopography-associated activation and expression of blood plasma components. *J. Biomed. Nanotechnol.* **2012,** 8, 642–658.

[36] Mao, C.; Qiu, Y.; Sang, H.; Mei, H.; Zhu, A.; Shen, J.; Lin, S. Various approaches to modify biomaterial surfaces for improving hemocompatibility. *Adv. Colloid Interface Sci.* **2004,** 110, 5–17.

[37] Sivaraman, B.; Latour, R.A. The relationship between platelet adhesion on surfaces and the structure versus the amount of adsorbed fibrinogen. *Biomaterials* **2010,** 31, 832–839.

[38] Sivaraman, B.; Fears, K.P.; Latour, R.A. Investigation of the Effects of Surface Chemistry and Solution Concentration on the Conformation of Adsorbed Proteins Using an Improved Circular Dichroism Method. *Langmuir* **2009,** 25, 3050–3056.

[39] Ratner, B.D.; Hoffman, A.S.; Schoen, F.J.; Lemons, J.E. Biomaterials Science: An Introduction to Materials in Medicine. *Academic Press* **2012**.

[40] Kidson, I.G. The effect of wall mechanical properties on patency of arterial grafts. *Ann. R. Coll. Surg. Engl.* **1983,** 65, 24–29.

[41] Salacinski, H.J.; Goldner, S.; Giudiceandrea, A.; Hamilton, G.; Seifalian, A.M.; Edwards, A.; Carson, R.J. The Mechanical Behavior of Vascular Grafts: A Review. *J. Biomater. Appl* **2001,** 15, 241–278.

[42] Roeder, R.A.; Lantz, G.C.; Geddes, L.A. Mechanical remodeling of small-intestine submucosa small-diameter vascular grafts: A preliminary report. *Biomed. Instrum. Technol.*, 35, 110–120.

[43] Chandran, K.B.; Gao, D.; Han, G.; Baraniewski, H.; Corson, J.D. Finite-element analysis of arterial anastomoses with vein, Dacron and PTFE grafts. *Med. Biol. Eng. Comput.* **1992,** 30, 413–418.

[44] Wang, X.; Lin, P.; Yao, Q.; Chen, C. Development of Small-Diameter Vascular Grafts. *World J. Surg.* **2007,** 31, 682–689.

[45] Dupont. Fluoroplastic Comparison - Typical Properties. http://www2.dupont.com/Teflon_Industrial/en_US/tech_info/techinfo_compare.html (accessed 2014).

[46] Soletti, L.; Nieponice, A.; Hong, Y.; Ye, S.H.; Stankus, J.J.; Wagner, W.R.; Vorp, D.A. In vivo performance of a phospholipid-coated bioerodable elastomeric graft for small-diameter vascular applications. *J. Biomed. Mater. Res. A* **2011,** 96A, 436–448.

[47] Pallua, N.; Suschek, C.V. Tissue Engineering: From Lab to Clinic. *Springer* **2010**.

[48] Lehninger, A.L.; Nelson, D.L.; Cox, M.M. Lehninger Principles of Biochemistry. *Macmillan* **2005**.

[49] Zhang, M. Surface Modification of Ultra High Molecular Weight Polyethylene With Hyaluronan For Total Joint Replacement Application. Ph.D. Dissertation, Colorado State University, Fort Collins, CO, 2005.

[50] Gong, F.; Lu, Y.; Guo, H.; Cheng, S.; Gao, Y. Hyaluronan Immobilized Polyurethane as a Blood Contacting Material. *Int. J. Polym. Sci.* **2010**.

[51] Verheye, S.; Markou, C.P.; Salame, M.Y.; Wan, B.; King, S.B.; Robinson, K.A.; Chronos, N.A.F.; Hanson, S.R. Reduced Thrombus Formation by Hyaluronic Acid Coating of Endovascular Devices. *Arterioscler. Thromb. Vasc. Biol.* **2000,** 20, 1168–1172.

[52] Sadowitz, B.; Seymour, K.; Gahtan, V.; Maier, K.G. The Role of Hyaluronic Acid in Atherosclerosis and Intimal Hyperplasia. *J. Surg. Res.* **2012,** 173, e63–e72.

[53] Genasetti, A.; Vigetti, D.; Viola, M.; Karousou, E.; Moretto, P.; Rizzi, M.; Bartolini, B.; Clerici, M.; Pallotti, F.; De Luca, G.; Passi, A. Hyaluronan and human endothelial cell behavior. *Connect. Tissue Res.* **2008,** 49, 120–123.

[54] Takahashi, Y.; Li, L.; Kamiryo, M.; Asteriou, T.; Moustakas, A.; Yamashita, H.; Heldin, P. Hyaluronan fragments induce endothelial cell differentiation in a CD44- and CXCL1/GRO1-dependent manner. *J. Biol. Chem.* **2005,** 280, 24195–24204.

[55] Tang, Z.C.W.; Liao, W.Y.; Tang, A.C.L.; Tsai, S.J.; Hsieh, P.C.H. The enhancement of endothelial cell therapy for angiogenesis in hindlimb ischemia using hyaluronan. *Biomaterials* **2011,** 32, 75–86.

[56] Reitsma, S.; Slaaf, D.W.; Vink, H.; J. van Zandvoort, M.A.M.; A. oude Egbrink, M.G. The endothelial glycocalyx: composition, functions, and visualization. *Pflugers Arch.***2007,** 454, 345–359.

[57] Gaffney, J.; Matou-Nasri, S.; Grau-Olivares, M.; Slevin, M. Therapeutic applications of hyaluronan. *Mol. Biosyst.* **2010,** 6, 437–443.

[58] Volpi, N.; Schiller, J.; Stern, R.; Soltés, L. Role, metabolism, chemical modifications and applications of hyaluronan. *Curr. Med. Chem.***2009,** 16, 1718–1745.

[59] Xue, L.; Greisler, H.P. Biomaterials in the development and future of vascular grafts. *J. Vasc. Surg.* **2003,** 37, 472–480.

[60] Ibrahim, S; Ramamurthi, A. Hyaluronic acid cues for functional endothelialization of vascular constructs. *J. Tissue Eng. Regen. Med.* **2008,** 2, 22–32.

[61] Zhang, M.; James, S.P. Silylation of hyaluronan to improve hydrophobicity and reactivity for improved processing and derivatization. *Polymer* **2005,** 46, 3639–3648.

[62] Dean IV, H. Development of BioPoly(R) Materials for use in Prosthetic Heart Valve Replacements. M.S. Thesis, Colorado State University, Fort Collins, CO, 2012.

[63] Prawel, D.A.; Dean, H,; Forleo, M.; Lewis, N.; Gangwish, J.; Popat, K.C.; Dasi, L.P.; James, S.P. Hemocompatibility and Hemodynamics of Novel Hyaluronan-Polyethylene Materials for Flexible Heart Valve Leaflets. *Cardiovasc. Eng. Technol.* **2014,** 5, 70–81.

CHAPTER 2: PREPARATION AND CHARACTERIZATION OF HA-ePTFE MATERIALS

2.1 Introduction

As ePTFE (i.e., Teflon®) is hydrophobic and hyaluronan is hydrophilic, hyaluronan treatment of expanded polytetrafluoroethylene (ePTFE) was performed using a silylation and wicking procedure. Hyaluronan can be complexed with a cationic salt and then silylated, forming a hydrophobic substance that can be dissolved in xylenes, as previously documented. [1]–[5] The hydrophobic ePTFE can then be soaked in a xylenes solution containing the silylated form of hyaluronan to form a microcomposite.

ePTFE materials were exposed to swelling solutions of 1.5%, 2.5%, and 3.5% (w/v). Some samples prepared with 2.5% and 3.5% swelling solutions received an additional surface dip in an aqueous 1% hyaluronan solution. Characterization tests were performed on ePTFE materials to visualize morphology, identify whether hyaluronan is present, quantify the amount of hyaluronan within samples, and assess the changes in surface hydrophobicity and roughness.

2.2 Materials and Methods

2.2.1 Expanded Polytetrafluoroethylene

Tubes of ePTFE (part number 70S10, Bard Peripheral Vascular OEM) straight-walled vascular grafts were received as 70cm lengths with an internal diameter of 9.5-10.5mm and a wall thickness of 0.70-0.80mm. Porosity as measured by intermodal distance of as received tubes was 10-40μm. To create ePTFE from PTFE, the PTFE was expanded by the manufacturer through stretching. The tubes are composed of 100% ePTFE and were not coated by the manufacturer. When received, tubes had been sterilized by Bard using ethylene oxide. In the

clinic, preclotting of these grafts is not necessary due to the hydrophobic nature of the ePTFE material.

2.2.2 Solvent

Xylenes were successfully used in the swelling of ultra high molecular weight polyethylene (UHMWPE) [5] and with LLDPE and Daron [4]. Xylenes were initially selected for use with UHMWPE due to the similarity in the Hildebrand solubility parameter between xylenes and UHMWPE. [4], [5] The Hildebrand solubility parameter of xylenes is 8.85 in standard units [6], [7]. The Hildebrand solubility parameter of PTFE is 6.2 [8]. Due to the high hydrophobicity of ePTFE, a solvent with a low Hildebrand solubility parameter was desirable. Therefore, xylenes were selected for use as the swelling solvent for ePTFE.

2.2.3 Synthesis of HA-CTA and Silyl HA-CTA

Refer to Appendix 1 for the protocols HA-CTA Complexation and HA-CTA Silylation. Methods to produce HA-CTA and silyl HA-CTA have previously been published. [1] In brief, 1.5 g of sodium hyaluronan (NaHA, intrinsic viscosity molecular weight 700kDa, Lifecore Biomedical, LLC) was dissolved in 500 ml of room temperature deionized water (DI H_2O) for 15-24 hours. The sodium ions dissociate from the NaHA in water. Next, 1.69 g of the cationic salt cetyltrimethylamonium bromide (CTAB, Fisher Scientific) was dissolved in 169 ml of DI H_2O at 40°C for 15-30 minutes or until clear. In water, bromine dissociates from CTAB, forming a precipitate of cetyltrimethyammonium (CTA). The CTA precipitate in water was then added to the hyaluronan solution to form a precipitate of HA-CTA. The HA-CTA was washed five times using a Buckner funnel to remove excess CTAB and then vacuum dried at 50°C for three days at -25 inHg. [1], [2], [4]

37

After drying, HA-CTA was placed in a 500 ml round bottom flask with a stir bar, and the flask was sealed using a rubber septum and copper wire. The round bottom flask was suspended in an oil bath on a hot plate and clamped in place using a ring stand. Next, 50 ml of dimethyl sulfoxide (DMSO, anhydrous ≥99.9%, Sigma Aldrich) was added to the HA-CTA under dry nitrogen flow. The solution was stirred until gel-like, and the HA-CTA was partially dissolved (4-12 hours). The solution was then heated at 50°C for an additional 4-24 hours, until the HA-CTA fully dissolved. Hexamethyldisilazane (HMDS, reagent grade, ≥99.9%, Sigma Aldrich) was then added under dry nitrogen flow, and the solution was stirred at 75°C for 48 hours. DMSO and HMDS are immiscible, so vigorous stirring was important for the transfer of trimethylsilyl groups from the HMDS to the DMSO at the liquid interface, and subsequently to the HA-CTA. The two phase solution was then separated, saving the upper layer containing DMSO and silyl HA-CTA. The silyl HA-CTA was washed with 25 ml of xylenes five times using a rotavap (Buchi) at 60-70°C and 60 rpm while connected to a cold trap containing ice. The precipitate was dried in a vacuum oven equipped with a vapor trap at 50°C and -25 inHg for 24 hours or until no change in weight was observed. Once dry, silyl HA-CTA was stored in a vacuum dessicator. Only silyl HA-CTA with a degree of silylation greater than or equal to 3.0 as determined by attenuated total reflectance Fourier transform infrared spectroscopy (ATR-FTIR) was used in this work. [1], [2], [4]

Glassware used with HMDS or silyl HA-CTA was dried in an oven at 125°C overnight prior to use. Glassware was silylated by adding hexamethyldisilazane (HMDS, ≥ 97%, Sigma Aldrich), swirling the HMDS to contact inside surfaces, and soaking for five minutes. This binds silyl groups to the glassware to prevent binding during silylation, which would reduce the number of silyl groups available for reaction with HA-CTA. Glassware was then rinsed with

acetone (certified ACS, Fisher Scientific) and dried in an oven at 125°C for 10 minutes. Glassware was then removed from the oven and cooled to room temperature before use.

2.2.4 Sample preparation of ePTFE with silyl HA-CTA

The 70cm ePTFE tubes were cut to 13 cm length segments for treatment with silyl HA-CTA. Tubes were weighed and then cleaned by soaking in xylenes (certified ACS, Fisher Scientific) for 12-24 hours in a covered Erlenmeyer flask. Tubes were then dried in a vacuum oven equipped with a vapor trap for 12-24 hours at room temperature and -25 inHg. Sample weight was measured and recorded.

Prior to use, silyl HA-CTA was vacuum dried in a vacuum oven without heat for a minimum of 24 hours. Solutions of silyl HA-CTA in xylenes were then prepared at desired concentrations of 1.5% HA, 2.5% HA, and 3.5% HA (w/v). Solutions were stirred in covered Erlenmeyer flasks for 12-24 hours at room temperature to fully dissolve the silyl HA-CTA. At this time, there were no visible pieces of silyl HA-CTA in solution, and the solution had a yellow color that increased in hue as concentration increased. These solutions will be referred to as swelling solutions. Note that they are written as a concentration of HA, where the solution actually contains silyl HA-CTA. For example, a 1.5% HA swelling solution is made with 1.5g of silyl HA-CTA and 100ml of xylenes. [1], [2], [4]

Once samples were dry and the silyl HA-CTA was fully dissolved in xylenes, the silyl HA-CTA solutions of desired concentrations were transferred to separate ceramic dishes (Coors Tek) 14x2.5x1.5cm. Samples were soaked in the silyl HA-CTA solutions, fully submersed, for 15 minutes at room temperature. Samples were then dried in a vacuum oven equipped with a vapor trap at -25 inHg at 50°C for three hours. Once dry, sample weights were recorded and compared to weight prior to treatment. Ceramic dishes were used because there was minimal

39

adhesion between the ePTFE tubes and the ceramic material. [1], [2], [4] Refer to Appendix 1 for the Sample Swelling protocol.

2.2.5 Chemical Crosslinking

A 2.0% v/v chemical crosslinking solution with hexamethylene diisocyanate (HMDI, viscosity 1300-2200 cP, Sigma Aldrich) in xylenes was prepared in a round bottom flask with a stir bar. The round bottom flask was connected to a cold water condenser with the round bottom flask suspended in an oil bath at 50°C. The solution stirred for 12-24 hours to fully dissolve the HMDI in xylenes. [1], [2], [4]

After samples were soaked in silyl HA-CTA and xylenes solutions of desired concentrations and vacuum dried for three hours, sample weight was recorded. The crosslinking solution was removed from heat and allowed to cool to room temperature. Crosslinking solution (50ml) was then placed in crystallizing dishes, and samples were placed into the crosslinking solution, fully submersed, for 15 minutes at room temperature. Samples were then dried in a vacuum oven equipped with a vapor trap at -25 in Hg at 50°C for three hours. Heat during this drying process is important for curing the crosslinker. [1], [2], [4]

After crosslinking, samples were rinsed with acetone for 30 seconds using a Vortex Mixer (Fisher Scientific) to remove excess HMDI. Samples were then dried in a vacuum oven equipped with a vapor trap at -25 in Hg at room temperature until no change in weight was observed. Sample weights were recorded. [1], [2], [4] The changes in sample weights with treatment and subsequent hydrolysis are used to verify the thermogravimetric analysis (TGA) findings for the amount of HA incorporated into the samples. Refer to Appendix 1 for the Sample Swelling protocol.

2.2.6 Hydrolysis

A hydrolysis procedure was used to return silyl HA-CTA back to HA by removing silyl and –CTA groups from the silyl HA-CTA. The hydrolysis procedure involves soaking samples in a series of ionic salt solutions containing combinations of DI H_2O, ethyl alcohol (absolute, anhydrous ACS/USP grade, Pharmco-Aaper), and sodium chloride (NaCl, Fisher Scientific). An initial hydrolysis attempt did not successfully recover HA from silyl HA-CTA, as CTA and silyl groups were still evident in the ATR-FTIR spectra. A revised hydrolysis protocol with added soaking steps was therefore used and provided in Appendix 1.

Initially, samples were placed in a 0.2M NaCl solution in 1:1 DI H_2O: 100% ethyl alcohol (v/v) for one hour in a 2210 Ultrasonic Cleaner Water Bath (Branson). After one hour, the solution was replaced with a fresh 0.2M NaCl solution. Samples were placed in the ultrasonic bath a second time for one hour. A third time, samples were placed in a fresh 0.2M NaCl solution in an ultrasonic cleaner for one hour. Next, samples were placed in a 0.2M NaCl aqueous solution without alcohol in an ultrasonic bath for one hour. Samples were then transferred to a 3:2 DI H_2O: 100% ethyl alcohol (v/v) solution to soak for two hours without sonication. Samples were then sonicated in 100% DI H_2O for 30 minutes. Next, samples were partially dehydrated by soaking in acetone for one hour. Finally, samples were dried in a vacuum oven equipped with a solvent trap at -25 inHg until no change in weight was observed.

After performing this initial hydrolysis, it was determined through ATR-FTIR that HA-CTA and silyl HA-CTA were still present on the surface of the ePTFE. The hydrolysis protocol was then modified to add soaking time in three of the solutions. The modified hydrolysis protocol is provided in Table 2.1 and began with sonicating samples for one hour in a 0.2M NaCl solution in DI H_2O: 100% ethyl alcohol (1:1). The solution was then replaced with a fresh 0.2M

NaCl solution in DI H_2O: 100% ethyl alcohol (1:1), and samples soaked at room temperature without sonication for 11 hours. Samples were then sonicated in a 0.2M NaCl aqueous solution without alcohol for one hour, followed by an 11 hour soak in a fresh 0.2M NaCl aqueous solution. Subsequently, samples were soaked for 12 hours in a 3:2 DI H_2O: 100% ethyl alcohol (v/v) solution. This was followed by sonication for 30mins in DI H_2O and soaking in acetone for one hour at room temperature to partially dehydrate samples. Lastly, samples were fully dried in a vacuum oven equipped with a solvent trap at -25 in Hg at room temperature until no change in weight was observed. Refer to Appendix 1 for the initial and revised hydrolysis protocols.

Table 2.1: Summary of revised hydrolysis procedure

Step	Solution	Time
1	0.2M NaCl in 1:1 DI H_2O: 100% Ethanol	Sonicate 1 hour
2	0.2M NaCl in 1:1 DI H_2O: 100% Ethanol	Soak 11 hours
3	0.2M NaCl in DI H_2O	Sonicate 1 hour
4	0.2M NaCl in DI H_2O	Soak 11 hours
5	3:2 DI H_2O: 100% Ethanol	Soak 12 hours
6	DI H_2O	Sonicate 0.5 hours
7	Acetone	Soak 1 hour

2.2.7 Aqueous HA Surface Dip

Following hydrolysis, some 2.5% HA and 3.5% HA samples received an additional aqueous surface dip (SD) in a 1.0% (w/v) aqueous HA solution. Samples were submerged for 15 minutes to create a film of HA on the surface. Dip coated samples were then vacuum dried at 50°C (until no change in weight was observed). Next, samples were submerged in a 2% (v/v) HMDI in xylenes solution for 15 minutes, vacuum dried for 3 hours at 50°C, washed in acetone for 30 seconds using a Vortexer Mixer, and vacuum dried at room temperature in a ceramic dish until no change in weight was observed. [3], [4] Samples receiving the surface dip are designated by the percent HA swelling solution with a plus sign and SD. For example, a 2.5% HA sample that

received a surface dip is designated "2.5% HA + SD." Refer to Appendix 1 for the Aqueous Surface Dip protocol.

2.2.8 Selection of Swelling Solution Concentration

Three swelling solution concentrations were used to treat ePTFE material. The resulting percent composition of HA in the different treatment groups was quantified using thermogravimetric analysis (TGA). Based on previous results, more HA does not necessarily increase hemocompatibility [4]. To determine the swelling solution concentration to be selected for further hemocompatibility and mechanical property testing, the effect of the amount of HA in the ePTFE on thrombogenicity was explored.

Samples from each swelling solution concentration and surface dipped samples were used in blood plasma studies to assess hemocompatibility based on calcein-AM (Invitrogen) fluorescence staining and scanning electron microscopy (SEM). The swelling solution used to treat the samples with the lowest thrombonenicity as determined by calcein-AM and SEM was used for additional hemocompatibility testing, as well as mechanical testing. Methods, results, and conclusions are included in Chapter 3.

2.2.9 Sham control

A sham control was included in material characterization testing and hemocompatibility screening. The sham control is ePTFE with the same dimensions (13cm length, 10mm internal diameter) as other samples. The sham control underwent the same sample swelling, crosslinking, and hydrolysis procedures as the 1.5% HA, 2.5% HA, and 3.5% HA samples but was not exposed to silyl HA-CTA or HMDI. The sham was soaked in xylenes solutions that did not contain silyl HA-CTA or HMDS for the swelling and crosslinking portions of the procedures.

2.3 Characterization of ePTFE-HA Materials

Multiple analytical techniques were used to characterize ePTFE-HA materials. ATR-FTIR was used to assess the quality of silyl HA-CTA and assess whether hydrolysis removed CTA and silyl groups, rendering HA. X-ray photoelectron spectroscopy (XPS) was used to analyze the changes in elements present at sample surfaces and changes in types of chemical bonds between treatment groups. Static contact angle goniometry was used to measure changes in the wettability of the various surfaces. Scanning white light interferometry (SWLI) was used to analyze changes in surface roughness between treatment groups.

2.3.1 Scanning Electron Microscopy

Scanning electron microscopy (SEM) was used to visualize the structure of ePTFE materials. Punches (8mm diameter) were obtained using sterile biopsy punches (Acuderm Inc.) of both ePTFE and the sham control. Prior to imaging, samples were coated with a 10nm layer of gold. A scanning electron microscope model JEOL JSM-6500F (Thermo Electron) with 5.0kV and working distance 10.6mm was used to obtain one image of each sample at 500x, five images at 2,000x, and one image at 5,000x magnification.

2.3.2 Attenuated Total Reflectance Fourier Transform Interferometry (ATR-FTIR)

The quality of the silyl HA-CTA was determined by the degree of silylation (DS). The DS is a measure of how many silyl groups per HA monomer are present, with a maximum of four. The DS affects the solubility of the silyl HA-CTA. Silyl HA-CTA with a DS higher than 3.0 dissolves in xylenes. Silyl HA-CTA used for this work had a minimum DS of 3.0.

ATR-FTIR was performed using a Nicolet SX-60 FTIR spectrometer (Thermo Scientific) was used to collect IR spectra for each batch of HA-CTA and silyl HA-CTA. HA-CTA and silyl HA-CTA were separately placed on the diamond crystal stage. Absorption

spectra over the range 600-4000 cm^{-1} were collected at a resolution of 8 with 128 scans. Atmospheric background was subtracted from sample infrared spectra. For each spectra, the area of the hydroxyl peak (wavenumber 3500 cm^{-1}) and the 1046-1150 cm^{-1} peak was determined using OMNIC software (Thermo Scientific). The peak area values were then used to calculate the DS using Equation 2.1 below. Silyl HA-CTA with a DS greater than or equal to 3.0 dissolves in xylenes and was used for this work.

$$DS = 4 * \frac{\left(\frac{A_{HA-CTA,3500}}{A_{HA-CTA,1046-1150}}\right) - \left(\frac{A_{silyl\ HA-CTA,3500}}{A_{silyl\ HA-CTA,1046-1150}}\right)}{A_{HA-CTA,3500} \ / \ A_{HA-CTA,1046-1150}} \qquad (2.1)$$

ATR-FTIR spectra were also obtained for ePTFE, the sham control, 1.5% HA, 2.5% HA, and 3.5% HA samples to evaluate whether HA, HA-CTA, or silyl HA-CTA were present on sample surfaces. Samples were tested before and after hydrolysis to analyze the effectiveness of hydrolysis at removing trimethyl silyl and -CTA groups. One 6mm punch was obtained from an ePTFE tube from each treatment group before and after hydrolysis. Samples were placed directly onto the ATR-FTIR stage for data acquisition such that the inside surface of the tube was scanned. Two spectra per sample were collected at a resolution of 8 with 128 scans. Atmospheric background was subtracted from sample infrared spectra.

2.3.3 Thermogravimetric Analysis (TGA)

The degradation temperature of ePTFE and the HA composition ePTFE, the sham control, 1.5% HA, 2.5% HA, 3.5% HA, 2.5% HA + SD, and 3.5% HA + SD samples was determined using thermogravimetric analysis (TGA). Samples were obtained using a 4 mm sterile biopsy punch (Miltex). Three samples at each swelling solution concentration were tested. The ePTFE tube was dissected longitudinally, and one sample was collected from each

45

end and the middle of each tube (3 samples per tube). Initial sample weights ranged from 5-15mg. Samples were placed on a clean platinum pan for analysis. A TA Instruments Thermogravimetric Analyzer 2950 V5.4A (Thermo Scientific) heated samples from ambient temperature to 550°C at a heating ramp rate of 10°C/min under nitrogen gas. Untreated ePTFE samples were tested to determine the degradation temperature and select a maximum temperature for calculating the percent composition of HA. TA Instruments Universal Analysis Software V4.3 was used for data analysis. Percent HA compositions based on decrease in percent weight of individual samples was determined between 150°C-450°C. Refer to Appendix 1 for the Thermogravimetric Analysis protocol.

2.3.4 X-Ray photoelectron spectrometry (XPS)

X-ray photoelectron spectrometry (XPS) was used to determine the surface elemental composition and binding energies on ePTFE, the sham control, 1.5% HA, 2.5% HA, 3.5% HA, 2.5% HA + SD, and 3.5% HA + SD samples. Samples were obtained using a sterile 4mm biopsy punch and dried in a vacuum dessicator before mounting for XPS testing. Samples were mounted such that the inside surface of the tube was analyzed using a 5800 ESCA/AES system with the monochromatic Al Kα X-ray source (1486.6 eV, Physical Electronics PHI). An electron gun (350 W) was used for charge neutralization. The photoelectron takeoff angle was 45° from the normal surface. Survey scans were collected with a pass energy of 187.85 eV, and high-resolution spectra were acquired with a pass energy of 23.50 eV. A survey and high resolution spectra were collected from one sample per group. Data analysis was performed using Multipak (Physical Electronics) software. All spectra were SG5 smoothed and shifted such that the C1s hydrocarbon peak was centered at 284.8 eV or the C1s carbon-fluorine bond peak was centered at 292 eV to account for charging of the sample surface. Surface elemental compositions of

carbon, fluorine, nitrogen, and oxygen were determined from peak gating of high resolution scans. Changes in binding energy peaks were observed.

2.3.5 Contact Angle Goniometry

Measurements of static surface contact angle between the HA-ePTFE materials and DI H_2O were collected using the sessile drop technique and a standard goniometer model 260-F4 (Ramé-Hart Instrument Co.). Tubes were dissected longitudinally, and rectangular sections (6.2cm x 1cm) were obtained. Rectangular specimens were taped to the goniometer stage using double sided carbon conductive tape (Ted Pella) such that the inside surface of the tube was exposed for contact angle measurements. At room temperature, a DI H_2O droplet was dispensed from a syringe ($\approx$ 5-10μl) onto the material surface, and a timer was started. Contact angle measurements for both the left and right side of the DI H_2O droplet were recorded after 30 seconds. Three locations were tested for the ePTFE, sham, 1.5% HA, 2.5% HA, 3.5% HA, 2.5% HA + SD, and 3.5% HA + SD samples. Contact angle measurements were recorded when samples were dry as well as after hydrating in 300 ml of DI H_2O for at least 12 hours. Hydrated samples were tested because HA can swell to 1,000 times its dry size when hydrated [2]. To measure the contact angle of hydrated samples, samples were removed from DI H_2O and immediately taped to the goniometer stage. No water was visible on the sample surfaces at the time a water droplet was placed on samples using the syringe.

The difference between the left and right contact angle values was within three degrees. The mean of the left and right contact angle values was determined and averaged across the three locations per sample. Treatment groups with a standard deviation greater than five degrees were additionally tested to obtain a higher sample size, but this did not reduce the standard deviation. The high standard deviation is likely a factor of inhomogeneity of HA on sample surfaces.

2.3.6 Scanning White Light Interferometry (SWLI)

Scanning white light interferometry (SWLI) uses broad band white light to measure three dimensional properties of a surface. Interference intensity data between the white light and the vertical axis of sample surfaces are processed using Fourier analysis. A noncontact SWLI model NewView 7300 (Zygo Corporation) with roughness and form measurement and less than one angstrom resolution was used to characterize surface roughness of ePTFE, the sham control, 1.5% HA, 2.5% HA, 3.5% HA, 2.5% HA + SD, and 3.5% HA + SD samples and is shown in Figure 2.1. Three locations per sample were tested in both dry and hydrated states at 100x magnification. Hydrated samples were soaked in DI H_2O for at least 12 hours prior to testing. Samples were placed on the SWLI platform such that the inside surface of the ePTFE tubes were examined.

The roughness measurements SR_z, SR_a, SP_k, SP_{vk}, and SP_{pk} were obtained for all treatment groups. A fitted fourth order polynomial was used to level data. A 0.008mm λ_a noise rejection filter was used. SR_z, SR_a, SP_k, SP_{vk}, and SP_{pk} parameters are used as comparators between surfaces. A 50x Mirau objective at 1x zoom with camera resolution of 0.219μm was used.

The ePTFE, sham, and 3.5% SD samples were additionally tested in both dry and hydrated states at 50x magnification to measure the roughness of the top of the ridge surfaces. The profile data was leveled by a least squares line removal to level the data and establish a reference line for roughness calculations. A high pass 0.001mm λ_c Gaussian Spline filter was used to obtain R_a, R_q, R_z, R_t, and Sa values for ridge surfaces and remove waviness from data. A 100x Mirau objective at 2x zoom with camera resolution of 0.051μm was used.

SR_z is the base roughness profile depth and is the average base roughness depth (height of the third highest peak from the third lowest valley) of five sampling segments. R_k is the core roughness depth measured when the major peaks and valleys are removed. R_{pk} is the reduced peak height, or the peak height above the core roughness. R_{vk} is the reduced valley depth, or a measure of the valley depths below the core roughness. [9], [10]

The R_a is the mean deviation of all points from a plane fit to the sample surface. The R_q is the root mean square roughness parameter corresponding to R_a, or the average of the measured height deviations over sampling segments. The R_t is the mean peak-to-valley roughness determined by the difference between the highest peak and the lowest valley for five sampling lengths. The R_z is the average peak-to-valley separation. The S_m is the average spacing between peaks at a line of mean depth. [9]

Figure 2.1: The Zygo New View Scanning White Light Interferometer used for data acquisition and processing.

2.4 Statistical Analysis

Each experiment was performed on at least three samples per treatment group. Quantitative results were analyzed using Minitab software with a one-way analysis of variance (ANOVA) with a statistical significance level of $p<0.05$.

2.5 Results and Discussion

2.5.1 Scanning Electron Microscopy

Representative SEM images are shown in Figure 2.2 at 500x, 2,000x, and 5,000x magnification of ePTFE anf the sham control to visualize material morphology and assess material changes caused by the xylenes. The ePTFE material has fibrous channels between relatively smooth peaks. The surfaces of the ridges are comparatively flat but appear to have surface texture. The channels contain fibers that extend across the width of the channels and connect to the sides of the ridges. The sham control does appear to have larger pores within the channels than the ePTFE. However, it is difficult to observe distinct differences. The 10nm gold coat layer may obscure features on the nanometer scale. Samples prepared with a 1.0% swelling solution are compared to ePTFE without HA and shown in Figure 2.2. There appear to be fragments in these samples that are not present in the ePTFE and sham samples that are likely HA. Note that the longitudinal direction of the ePTFE whole tube is perpendicular to the ridges and channels, or parallel to the channel fibers.
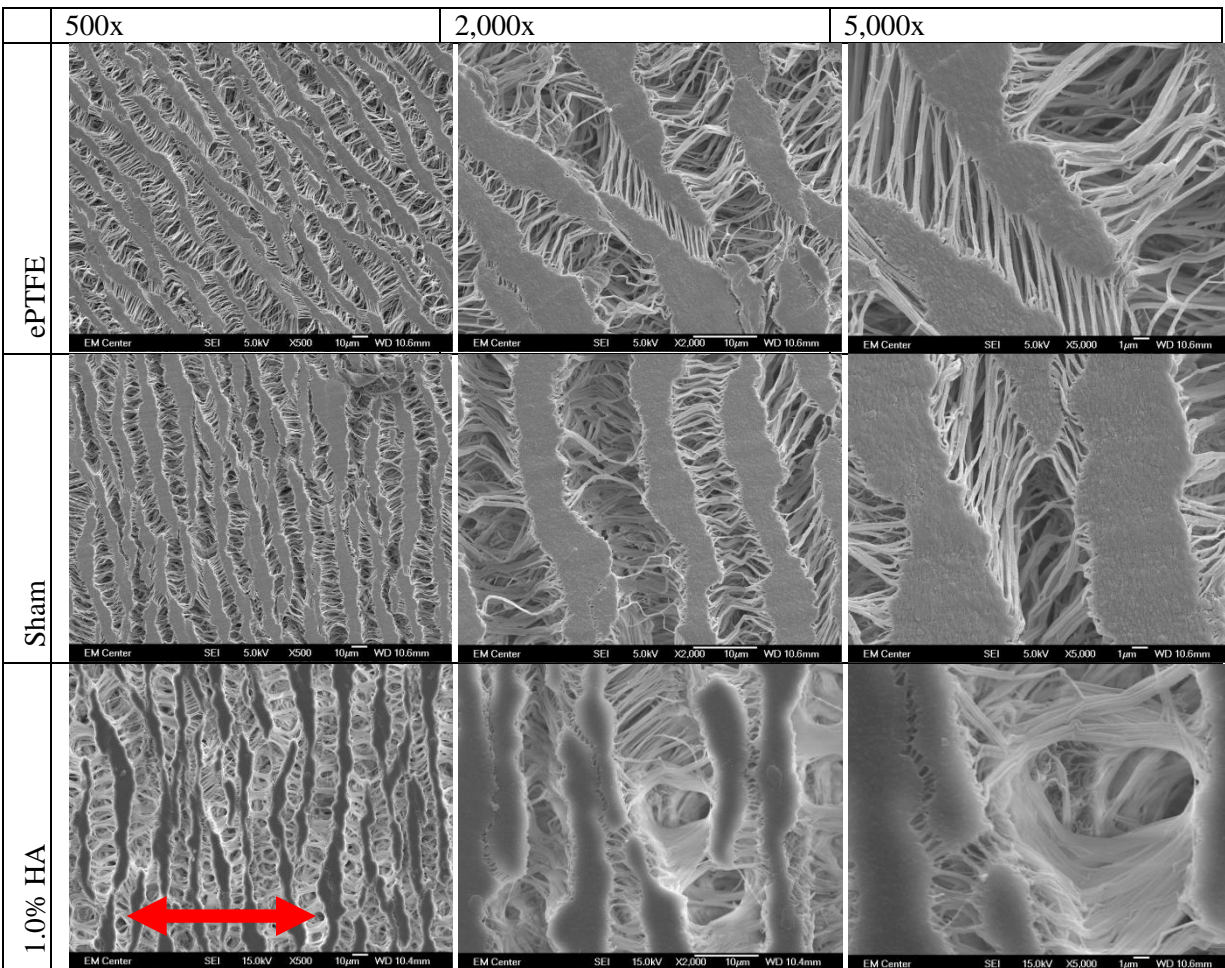
Figure 2.2: SEM images at 500x, 2,000x, and 5,000x magnification of ePTFE, the sham control, and samples prepared with 1.0% HA to visualize material morphology and assess material changes caused by xylenes. The nominal longitudinal direction of the graft tube is indicated by the arrow on the left (500x) 1.0% HA image.

2.5.2 Attenuated Total Reflectance Fourier Transform Interferometry (ATR-FTIR)

The degree of silylation (DS) was successfully calculated in accordance with Equation 2.1 for each batch of silyl HA-CTA synthesized and used in sample preparation. Only batches with a DS greater than or equal to three were used. No baseline corrections were performed on ATR-FTIR spectra. Figure 2.3: An example of ATR-FTIR peak gating in OMNIC software for HA-CTA and silyl HA-CTA 3500cm-1 and 1046-1150cm-1 peaks for calculation of silyl HA-CTA DS. Figure 2.3 shows how peak gates were set for the 3500cm^{-1} and 1046-1150cm^{-1} peaks for HA-CTA and silyl HA-CTA. Peak area values were calculated using OMNIC software. The

batch shown in the example had a DS= 3.74. When samples were prepared, silyl HA-CTA from at least three different batches was mixed.
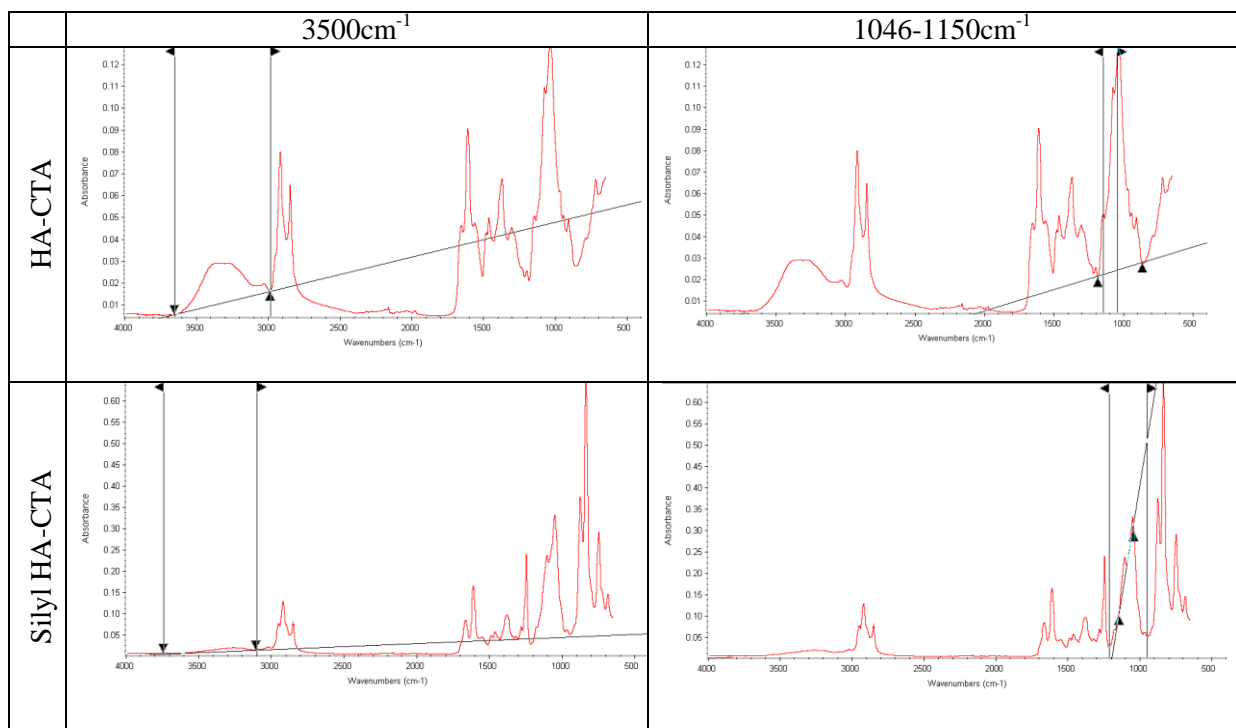
Figure 2.3: An example of ATR-FTIR peak gating in OMNIC software for HA-CTA and silyl HA-CTA 3500cm⁻¹ and 1046-1150cm⁻¹ peaks for calculation of silyl HA-CTA DS.

Samples (sham control, 1.5% HA, 2.5% HA, and 3.5% HA) were analyzed using ATR-FTIR after crosslinking and the acetone rinse both before and after the revised hydrolysis procedure. Resulting spectra from each treatment group both before and after hydrolysis are similar, as shown in Figure 2.4. There is a prominent carbon-fluorine stretching peak between 1100-1300 cm⁻¹, consistent with an expected infrared spectra for Teflon. The double peak in this range indicates a symmetric mode and an asymmetric mode due to multiple fluorine atoms present. [11] Before hydrolysis, ATR-FTIR was not sensitive enough to consistently detect silyl HA-CTA on the sample surfaces. These results are therefore inconclusive regarding the presence of silyl HA-CTA on the sample surface, as well as the effectiveness of hydrolysis at converting silylated HA-CTA back into HA. While ATR-FTIR had previously detected silyl

HA-CTA on ePTFE surfaces after the initial hydrolysis procedure as shown in Figure 2.5, a more

sensitive surface analysis technique, XPS, was performed to obtain more robust data.

	Hydrolyzed	Not hydrolyzed
1.5% HA		
2.5%HA		
3.5% HA		
Sham		
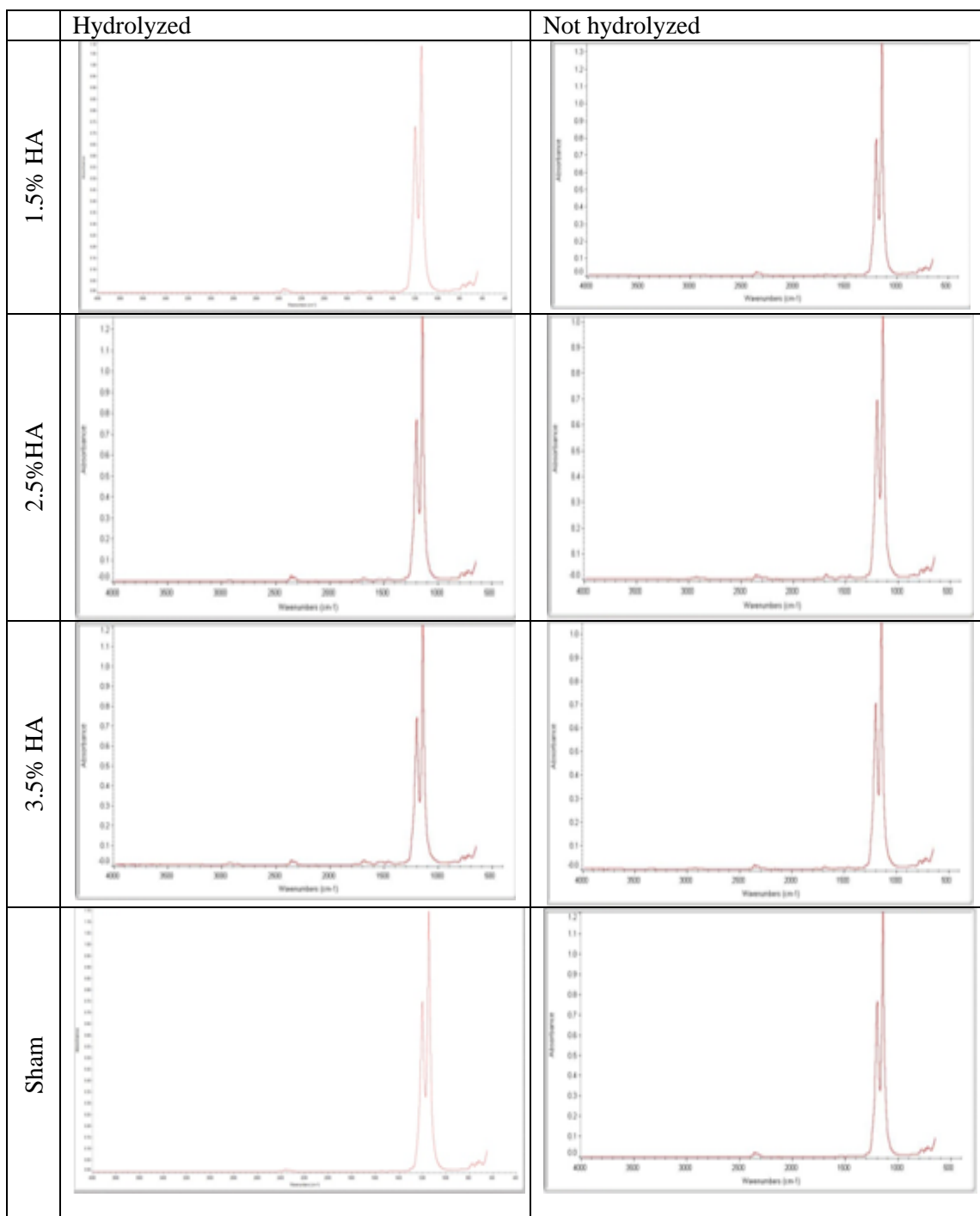
Figure 2.4: ATR-FTIR spectra for the sham control, 1.5% HA, 2.5% HA, and 3.5%HA after crosslinking and the acetone rinse, both before and after the revised hydrolysis procedure.

Figure 2.5: An example ATR-FTIR absorbance spectra of an ePTFE sample prepared with HA after the initial hydrolysis procedure. Silyl and CTA groups are still present.
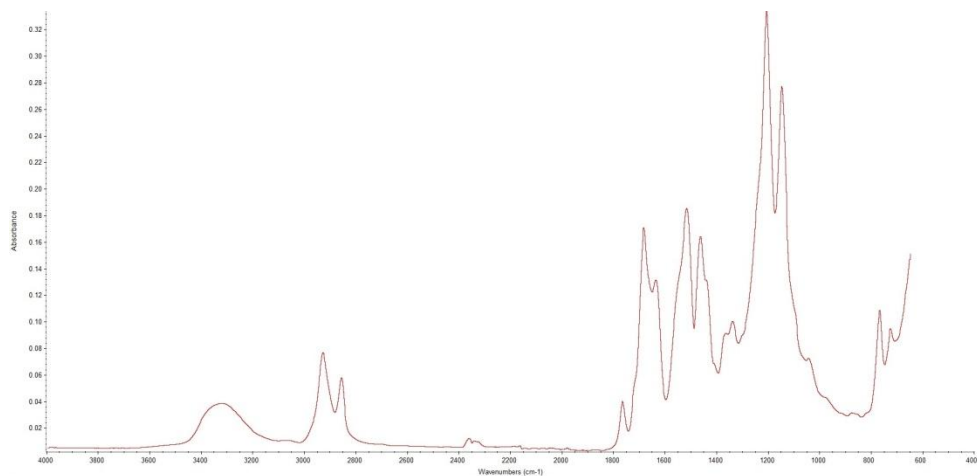
2.5.3 Thermogravimetric Analysis (TGA)

Tube sample weights were recorded during the treatment process with HA. In general, sample weight decreased after soaking in xylenes, increased after swelling in a silyl HA-CTA in xylenes solution, increased further after crosslinking, and after rinsing with acetone decreased slightly to an amount still greater than the sample weight after swelling. These results are as expected, as HA and HMDI will both increase sample weight and acetone removes excess HMDI. The decrease in sample weight after the xylenes soak is likely due to chemical etching of the ePTFE and explained further below [12].

TGA was performed on ePTFE, the sham control, 1.5% HA, 2.5% HA, 3.5% HA, 2.5% HA + SD, and 3.5% HA + SD samples after hydrolysis and drying. The percent decrease in weight from 150°C to 450°C was determined and recorded. Results for samples used with platelet population I are shown numerically in Table 2.2 and graphically in Figure 2.6. Results for samples used with platelet population I are shown numerically in Table 2.3 and graphically in Figure 2.7. There was minimal decrease in weight below 150°C, indicating that samples were dry at the time of testing. The base ePTFE material began to degrade after 450°C, so this temperature was selected as the upper boundary. The ePTFE and sham have minimal decrease in

weight within this temperature range that is likely attributed to moisture retention by samples. The difference in the percent decrease in weight between the 1.5% HA, 2.5% HA, 3.5% HA, 2.5% HA + SD, and 3.5% HA + SD samples compared to the sham is assumed to be HA. However, moisture retention would be higher in samples containing HA than in samples without HA. HA begins to degrade around 60-90°C. [13], [14]

TGA results from both platelet population I and platelet population II sample sets follow the same trends. On average, the higher the swelling solution concentration used, the higher the HA composition. The exception is that the 2.5% HA sample from platelet population I has a lower HA content than the 1.5% HA sample, on average. When receiving an additional SD, the percent HA composition increases above that of the corresponding samples without a SD. In both platelet population sample sets, there is a statistically significant difference between ePTFE and sham samples compared to the other treatment groups. Additionally, in platelet population I there is a statistically significant difference between the 3.5% HA treatment group compared to the 1.5% HA, 2.5% HA, and 2.5% HA + SD treatment groups. No statistically significant differences between samples prepared with HA are observed in platelet population II.

Observe that the average trend of increasing HA composition with an increasing swelling solution concentration exists, but there is variation across the longitudinal length of the tubes, as shown in Table 2.2 and Table 2.3. For example, the platelet population II 1.5% HA treatment group has a similar composition HA at end one as the average HA composition of the 2.5% HA treatment group. It is important to correlate future results with the actual HA composition of samples used.

Table 2.2: Sample percent HA composition at three locations per ePTFE tube with platelet population I

	Percent decrease in weight between 150-450°C (%)				
	End 1	Middle	End 2	Average	Standard Deviation
ePTFE	0.193	0.250	0.243	0.229	0.031
Sham	0.151	0.169	0.166	0.162	0.010
1.5% HA	0.938	0.806	0.844	0.862	0.068
2.5% HA	1.000	0.630	0.679	0.770	0.201
3.5% HA	0.762	1.916	1.286	1.321	0.578
2.5% HA + SD	1.000	0.924	0.937	0.954	0.040

Table 2.3: Sample percent HA composition at three locations per ePTFE tube used with platelet population II

	Percent decrease in weight between 150-450°C (%)				
	End 1	Middle	End 2	Average	Standard Deviation
ePTFE	0.193	0.250	0.243	0.229	0.031
Sham	0.164	0.205	0.126	0.165	0.039
1.5% HA	1.723	1.374	1.546	1.548	0.175
2.5% HA	1.658	1.719	1.736	1.704	0.041
3.5% HA	1.736	1.342	2.626	1.901	0.658
2.5% HA + SD	1.945	2.767	1.908	2.207	0.486
3.5% HA + SD	1.654	1.957	2.381	1.997	0.365
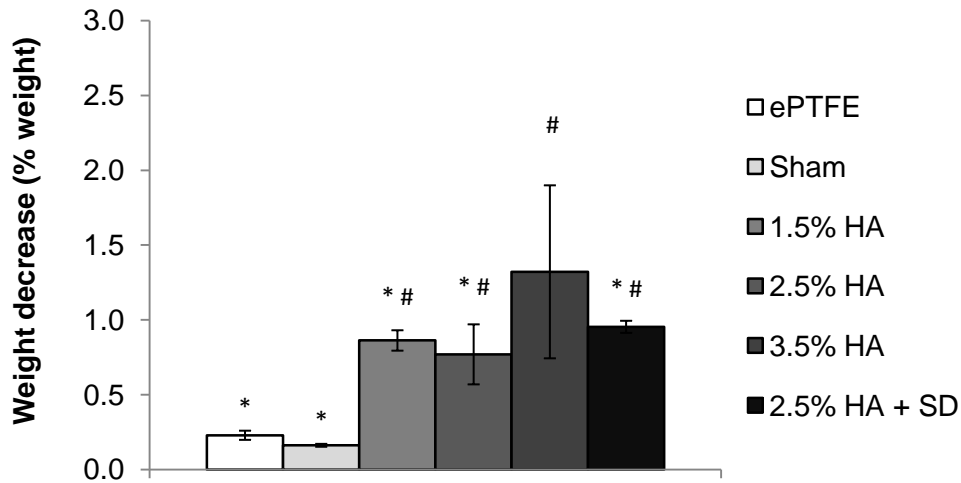
Figure 2.6: Percent decrease in weight between 150-450°C as determined by TGA for samples used in testing with platelet population I. Groups that do not share a symbol are significantly different. Error bars represent standard deviation.
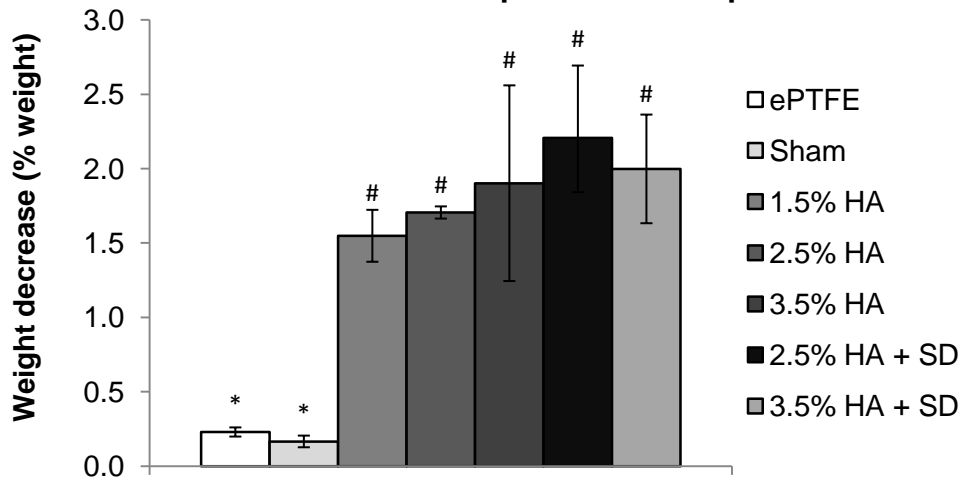
Figure 2.7: Percent decrease in weight between 150-450°C as determined by TGA for samples used in testing with platelet population II. Groups that do not share a symbol are significantly different. Error bars represent standard deviation.

2.5.4 X-Ray Photoelectron Spectrometry (XPS)

An ePTFE control, a sham control, a sample from each swelling concentration treatment group (1.5% HA, 2.5% HA, and 3.5% HA), and surface dipped samples (2.5% HA + SD and 3.5% HA + SD) were analyzed using X-Ray Photoelectron Spectrometry (XPS). Survey scans were collected to identify the elements carbon, fluorine, oxygen, and nitrogen. High resolution scans were then performed for these elements. Data analysis was performed using Multipak software (Physical Electronics). Differences in binding energies between treatment groups were observed, and atomic weight percentages of carbon, fluorine, nitrogen, and oxygen were obtained.

High resolution scans for C1s, F1s, O1s, and N1s are shown in Figures 2.8-2.11. Binding energies from platelet population II samples are shown. XPS spectra of HA, HA-CTA, and silyl HA-CTA were previously collected by Zhang *et al*. The high resolution N1s spectra of HA contains one N1s peak at 399.8 eV, associated with the only nitrogen present in HA, an amide group. HA-CTA and silyl HA-CTA contain an amide peak, as well as a second N1s peak at 402.8 eV, representing the quaternary ammonium nitrogen from the CTA ammonium salt. As this second peak is not observed in the high resolution N1s spectra of any samples, the HA-treated samples have undergone complete hydrolysis through the removal of the trimethylsilyl and -CTA groups from silyl HA-CTA. [1]

In the C1s spectra, HA is expected to contain peaks at 284.8 eV (CHx, C-C), 826.5 eV (C-O, C-N), 287.8 eV (O-C-O, C=O), and 289.2 eV (HN-C=O). The peak present at 289.0 eV in the C1s spectra of the 3.5% HA + SD treatment group is attributed to an amide bond due to the high amount of surface HA.

The F1s spectra contains a distinct C-F peak at 689 eV associated with the F1s electron for all treatment groups except the 3.5% HA + SD sample. As XPS indicates that the 3.5% HA + SD sample only contains 0.4% fluorine and more carbon than the control ePTFE and sham, the HA coating is likely thick enough to obscure detection of the fluorine in the ePTFE. The F1s spectra is as expected, as the only fluorine bond present is the C-F bond of ePTFE.
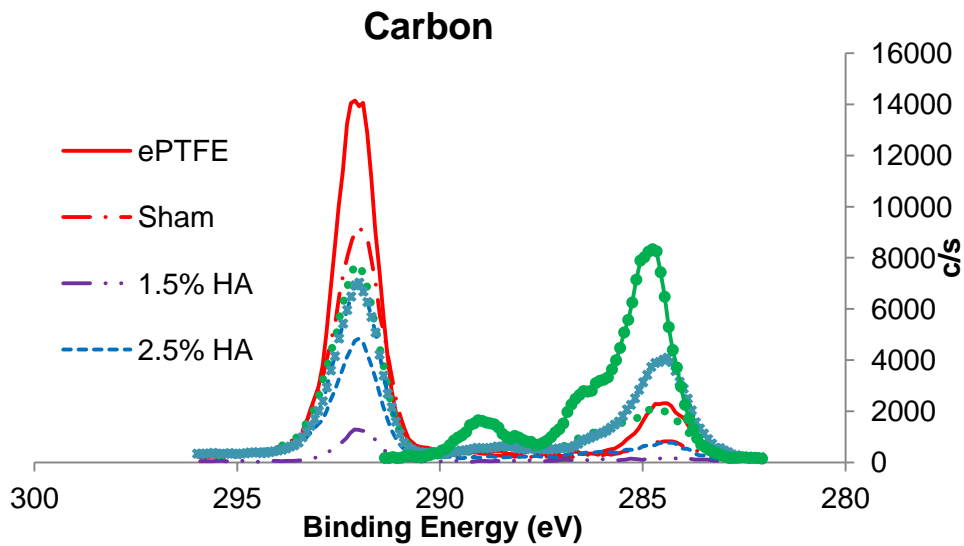
Figure 2.8: High resolution C1s spectra for ePTFE, sham, samples treated with a 1.5%, 2.5%, and 3.5% swelling solution, and samples treated with a 2.5% HA and 3.5% HA swelling solution that received an additional surface dip in an aqueous 1.0% HA solution.
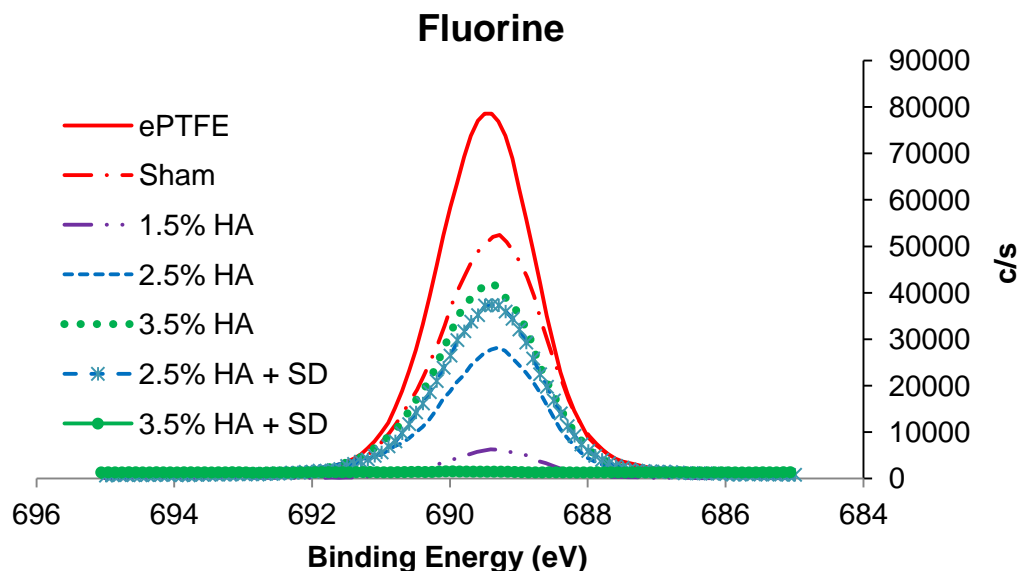
Figure 2.9: High resolution F1s spectra for ePTFE, sham, samples treated with a 1.5%, 2.5%, and 3.5% swelling solution, and samples treated with a 2.5% HA and 3.5% HA swelling solution that received an additional surface dip in an aqueous 1.0% HA solution.
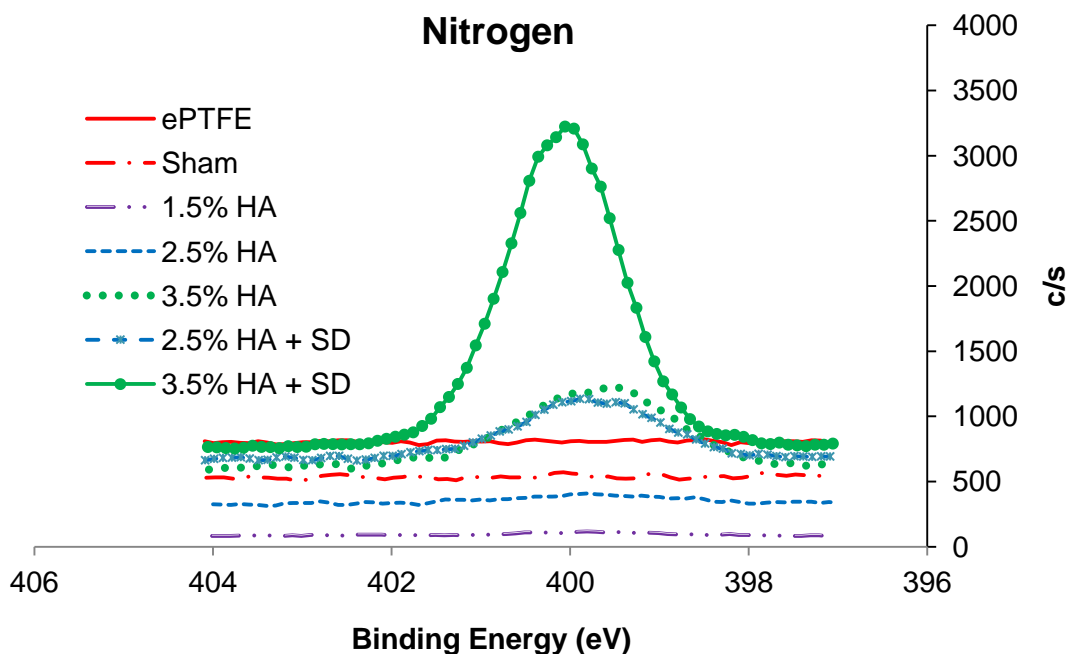
Figure 2.10: High resolution N1s spectra for ePTFE, sham, samples treated with a 1.5%, 2.5%, and 3.5% swelling solution, and samples treated with a 2.5% HA and 3.5% HA swelling solution that received an additional surface dip in an aqueous 1.0% HA solution.
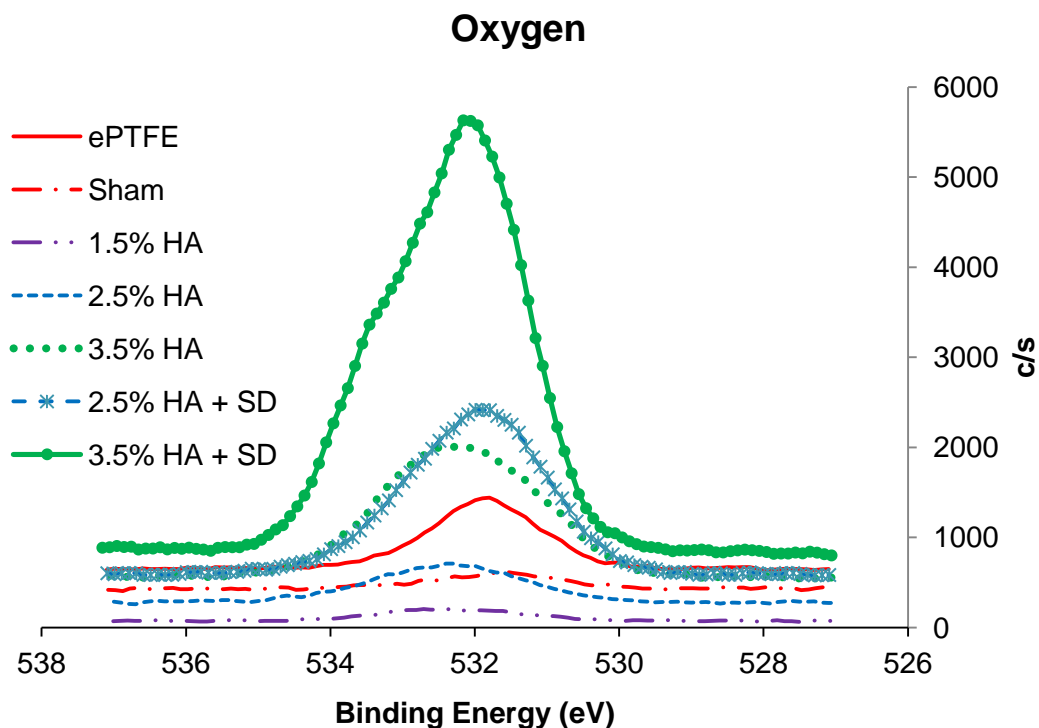
Figure 2.11: High resolution O1s spectra for ePTFE, sham, samples treated with a 1.5%, 2.5%, and 3.5% swelling solution, and samples treated with a 2.5% and 2.5% HA swelling solution that received an additional surface dip in an aqueous 1.0% HA solution.

The atomic weight percentages for carbon, fluorine, oxygen, and nitrogen were determined for each treatment group from the two platelet populations and are shown in Table 2.4 and

Table 2.5. Note that data for the same ePTFE sample is provided in both tables. There is little difference in atomic weight percentages between ePTFE and the sham for carbon, fluorine, oxygen, and nitrogen. This indicates that soaking the ePTFE in xylenes and the hydrolysis solutions does not dramatically alter the chemical composition of the ePTFE surface. The sham, however, has a lower hydrocarbon band than ePTFE.

There is a trend of increasing carbon composition as the concentration of HA in the swelling solution increases. There is an additional increase in carbon composition after the additional surface dip compared to an undipped sample prepared with the same concentration

swelling solution. Fluorine composition tends to decrease as the swelling solution concentration increases. Fluorine composition decreases further after a surface dip in an aqueous HA solution. Similarly, the amount of oxygen and nitrogen tends to increase as the swelling solution concentration increases, and it further increases after performing a surface dip in an aqueous HA solution. HA contains carbon, nitrogen in an amide bond, and oxygen, whereas ePTFE is composed of carbon and fluorine. As HA is added to samples, surface fluorine groups become covered by HA, and the number of hydrocarbon and nitrogen bonds increases. At a 45° takeoff angle, it is estimated that the XPS samples 10 nm into the surface, indicating the HA surface dip film is at least this thick in the area sampled. As fluorine is covered with HA, the atomic weight percent of fluorine at specimen surfaces decreases, and the atomic weight percentages of elements in HA (carbon, oxygen, and nitrogen) increase.

Table 2.4: Sample percent atomic weight percentages of carbon, fluorine, oxygen, and nitrogen for ePTFE samples used with platelet population I

	Atomic weight percent (%)			
	C1s	F1s	O1s	N1s
ePTFE	35.6	63.3	1.0	0.1
Sham	33.2	66.1	0.7	<0.1
1.5% HA	36.5	60.3	2.8	0.3
2.5% HA	34.3	64.0	1.5	0.2
3.5% HA	37.3	58.5	3.4	0.8
2.5% HA + SD	40.5	57.0	2.0	0.5

Table 2.5: Sample percent atomic weight percentages of carbon, fluorine, oxygen, and nitrogen for ePTFE samples used with platelet population II

	Atomic weight percent (%)			
	C1s	F1s	O1s	N1s
ePTFE	35.6	63.3	1.0	0.1
Sham	35.1	64.5	0.4	<0.1
1.5% HA	39.7	57.4	2.5	0.4
2.5% HA	35.3	62.6	1.8	0.4
3.5% HA	40.3	53.8	4.0	1.9
2.5% HA + SD	44.0	50.0	4.5	1.5
3.5% HA + SD	71.1	0.4	18.6	9.8

2.5.5 Static Contact Angle Goniometry

Static contact angles on dry and hydrated ePTFE, the sham control, 1.5% HA, 2.5% HA,

3.5% HA, 2.5% HA + SD, and 3.5% HA + SD samples were measured. Hydrated samples were

soaked in DI H_2O for at least 12 hours prior to testing to swell the HA. No statistically

significant differences within treatment groups were detected between dry and hydrated samples,

as seen in Figure 2.12. Hydrated samples typically had higher standard deviations than dry

samples due to the variation in HA surface coverage and surface wettability. While there were

no statistically significant differences found, the sham appears to decrease in contact angle more

than the ePTFE when hydrated compared to dry. Samples with a higher percent HA composition

also tend to decrease in contact angle when wet compared to dry, but these differences are not

statistically significant at the $p \leq 0.05$ level.
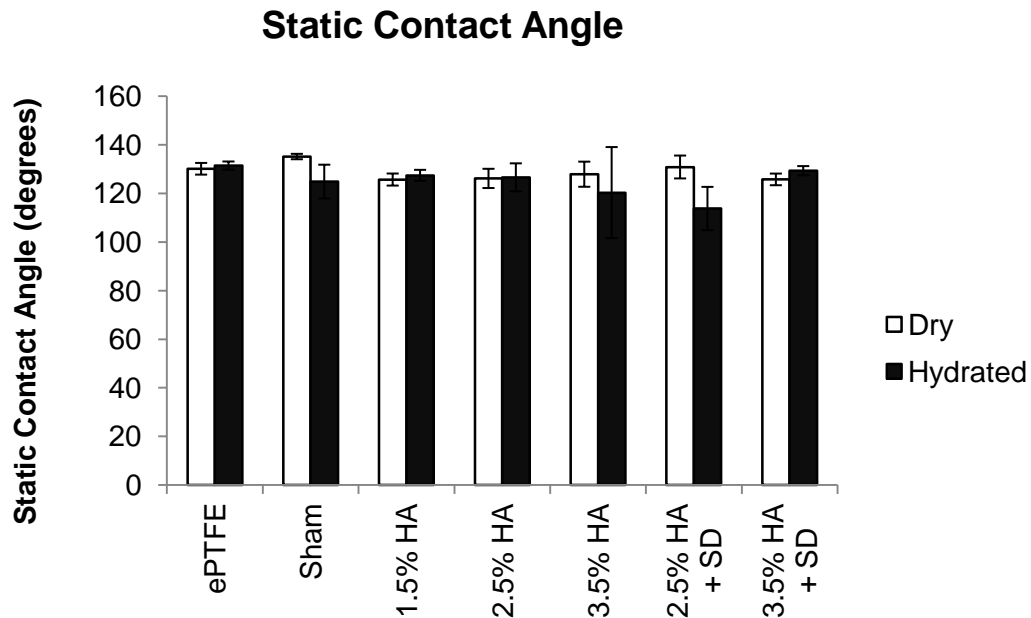
Figure 2.12: Static contact angle goniometry measurements for ePTFE, the sham control, 1.5% HA, 2.5% HA. 3.5% HA, 2.5% HA + SD, and 3.5% HA + SD samples in dry and hydrated states. Statistical analysis shows no statistical difference. Error bars represent standard deviation.

2.5.6 Scanning White Light Interferometry (SWLI)

Scanning White Light Interferometry (SWLI) was performed on dry and hydrated ePTFE, sham, 1.5% HA, 2.5% HA, 3.5% HA, 2.5% HA + SD, and 3.5% HA + SD samples. Three measurements were collected per sample, and the average resulting roughness values SR_z, SR_a, SP_k, SP_{vk}, and SP_{pk} of material surfaces were obtained across both sample ridges and channels. Roughness measurements R_a, R_q, R_z, R_t, and S_a were obtained on the ridge tops for the ePTFE, sham, and 3.5% HA + SD treatment groups.

SR_z is the base roughness profile depth and is the average base roughness depth (height of the third highest peak from the third lowest valley) of five sampling segments. R_k is the core roughness depth measured when the major peaks and valleys are removed. R_{pk} is the reduced peak height, or the peak height above the core roughness. R_{vk} is the reduced valley depth, or a measure of the valley depths below the core roughness. [9], [10]

The R_a is the mean deviation of all points from a plane fit to the sample surface. The R_q is the root mean square roughness parameter corresponding to R_a, or the average of the measured height deviations over sampling segments. The R_t is the mean peak-to-valley roughness determined by the difference between the highest peak and the lowest valley for five sampling lengths. The R_z is the average peak-to-valley separation. The S_m is the average spacing between peaks at a line of mean depth. [9]

The dry ePTFE and dry sham have a statistically significant difference in R_a (p=0.026). The increase in surface roughness of the dry sham compared to the dry ePTFE is caused by soaking in xylenes. The xylenes chemically etch the ePTFE, creating cavities and increasing pore size within the fibrous ePTFE channels. Xylenes also cause stress relaxation of ePTFE [15], [16].

The dry sham has a statistically significant difference in R_{vk} compared to the hydrated sham and the ePTFE. This indicates that the dry sham samples are rougher at a deeper pore depth than the ePTFE and hydrated sham.

SWLI images (Figures 14-19) indicated that the edges of the ridge walls were more rough and eroded on the sham but not the ePTFE. One measurement of this is the S_m value shown in Figure 2.23, which measures the average spacing of peaks. The spacing is larger for the sham than for ePTFE. There is inconsistent surface roughness on top of the sham ridges. Some ridges are smooth, while others are rough and appear pitted. Measurements were collected in the smoothest portion of the ridge tops. Additionally, the 3.5% HA + SD samples are more variable, with much narrower width of the ridge that is not pitted. Pitting increases the surface area.
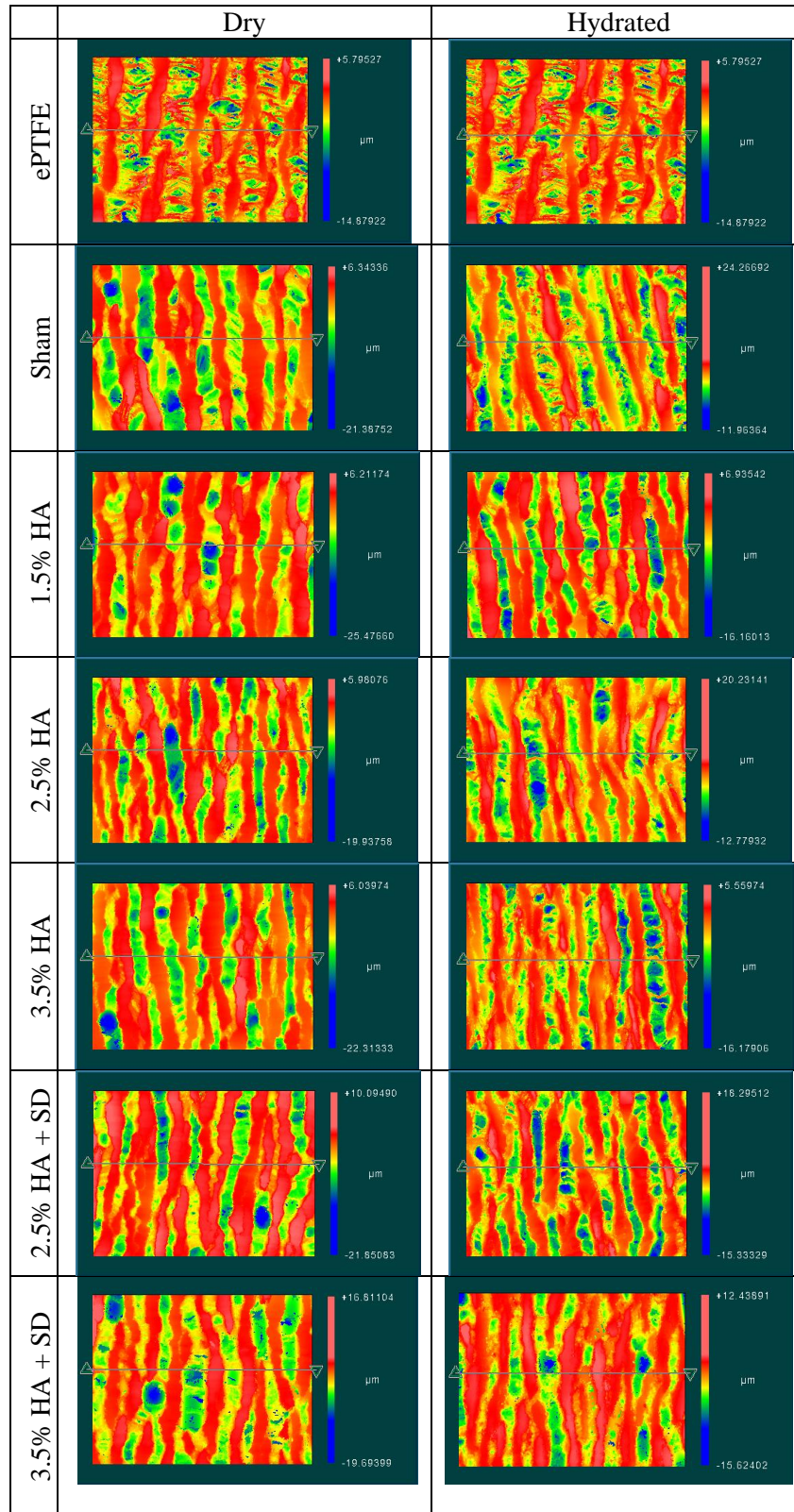
Figure 2.13: Fill maps at 50x magnification of ePTFE, the sham control, and 3.5% HA + SD samples in dry and hydrated states. The lines drawn on the ridge tops indicate where the roughness measurements SR_z, SR_a, SP_k, SP_{vk}, and SP_{pk} values were acquired.

	Dry	Hydrated
ePTFE		
Sham		
1.5% HA		
2.5% HA		
3.5% HA		
2.5% HA + SD		
3.5% HA + SD		
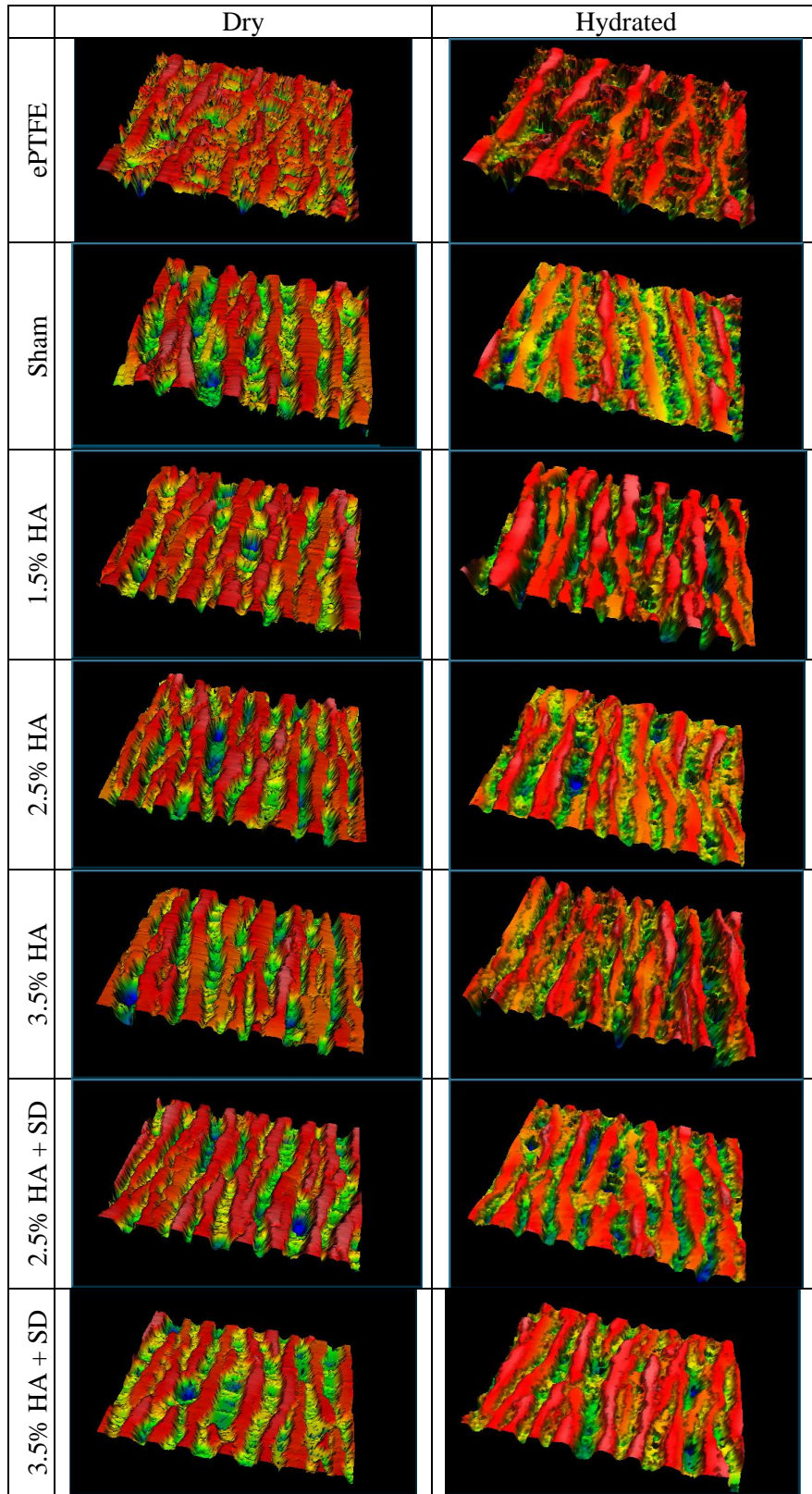
Figure 2.14: Three-dimensional models at 50x magnification of ePTFE, the sham control, and 3.5% HA + SD samples in dry and hydrated states. Increased surface texture is observed on the sham and 3.5% HA + SD samples compared to the ePTFE.
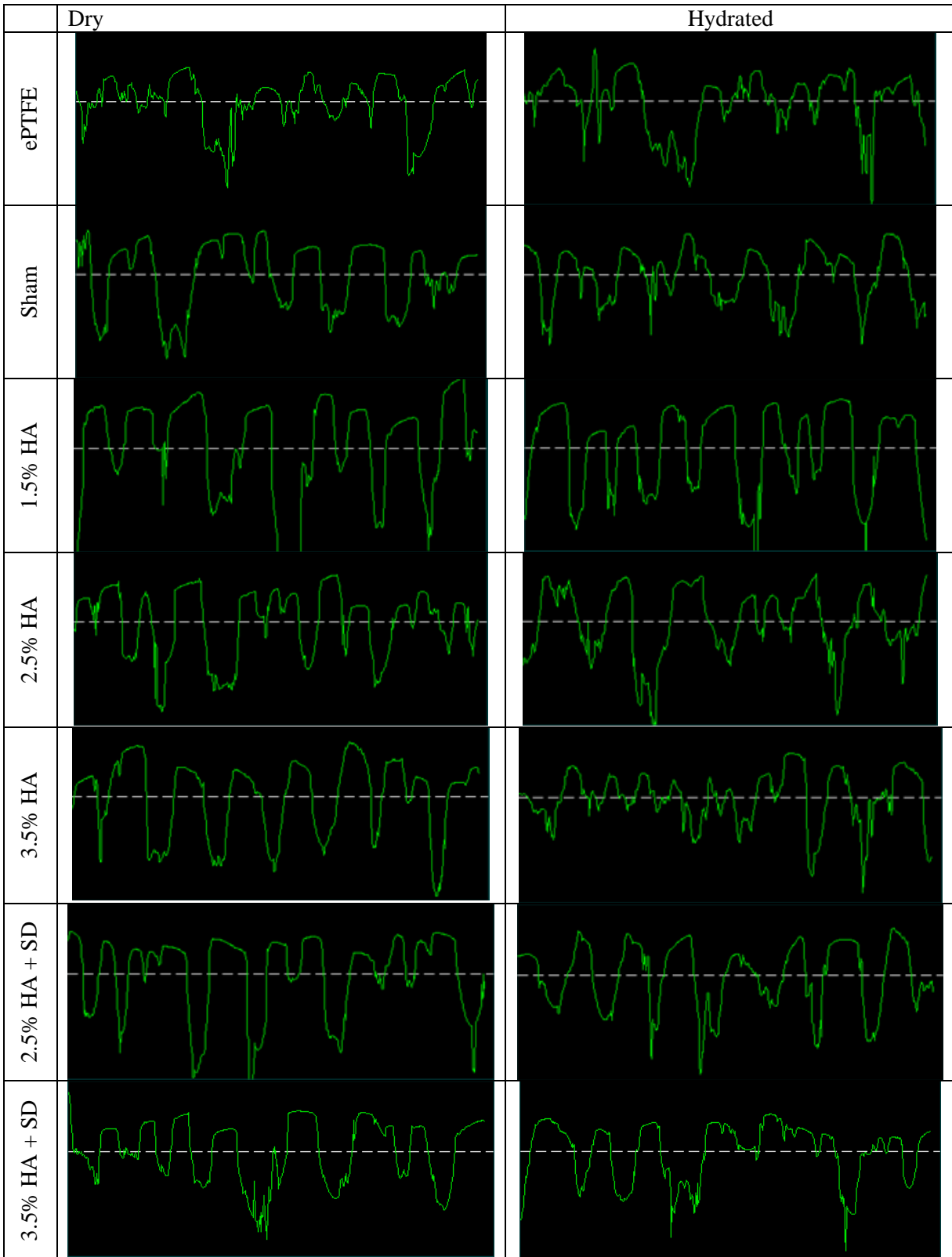
Figure 2.15: Two-dimensional profile at 50x magnification of ePTFE, the sham control, and 3.5% HA + SD samples in dry and hydrated states.
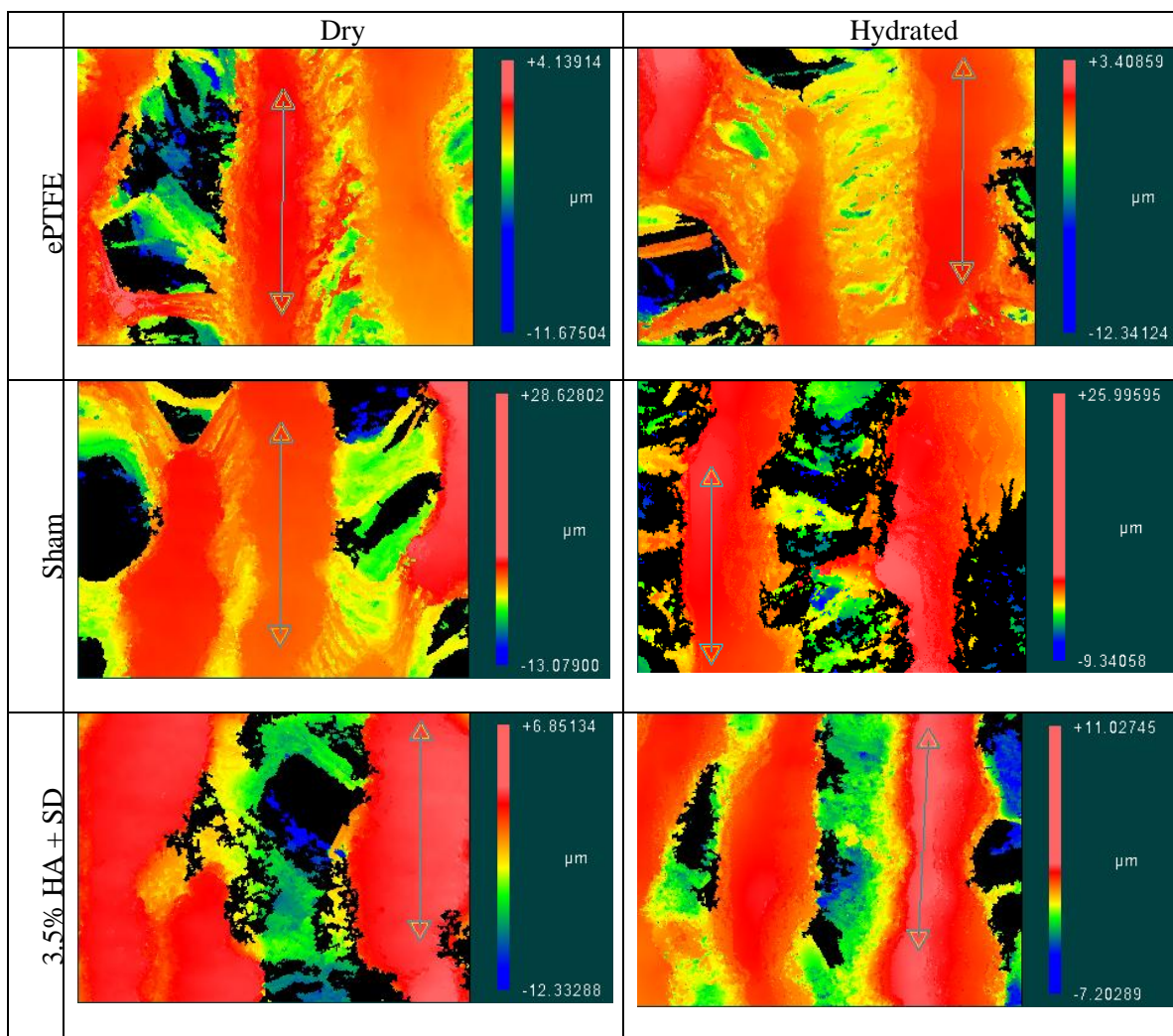
Figure 2.16: Fill maps at 100x magnification of ePTFE, the sham control, and 3.5% HA + SD samples in dry and hydrated states. The lines drawn on the ridge tops indicate where the roughness measurements R_a, R_q, R_z, R_t, and S_a values were acquired.

	Dry	Hydrated
ePTFE		
Sham		
3.5% HA + SD		
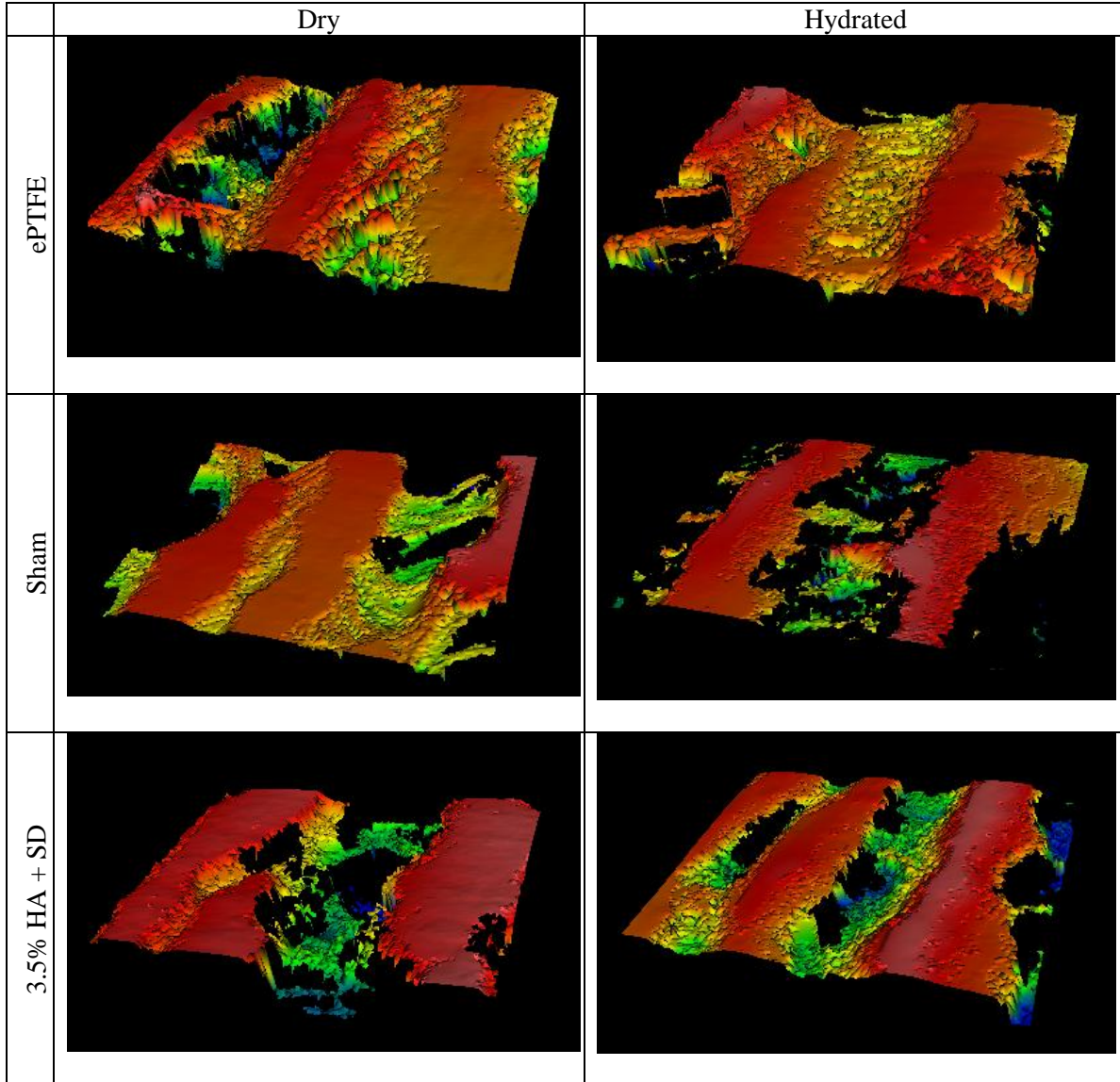
Figure 2.17: Three-dimensional models at 100x magnification of ePTFE, the sham control, and 3.5% HA + SD samples in dry and hydrated states. Increased surface texture is observed on the sham and 3.5% HA + SD samples compared to the ePTFE.
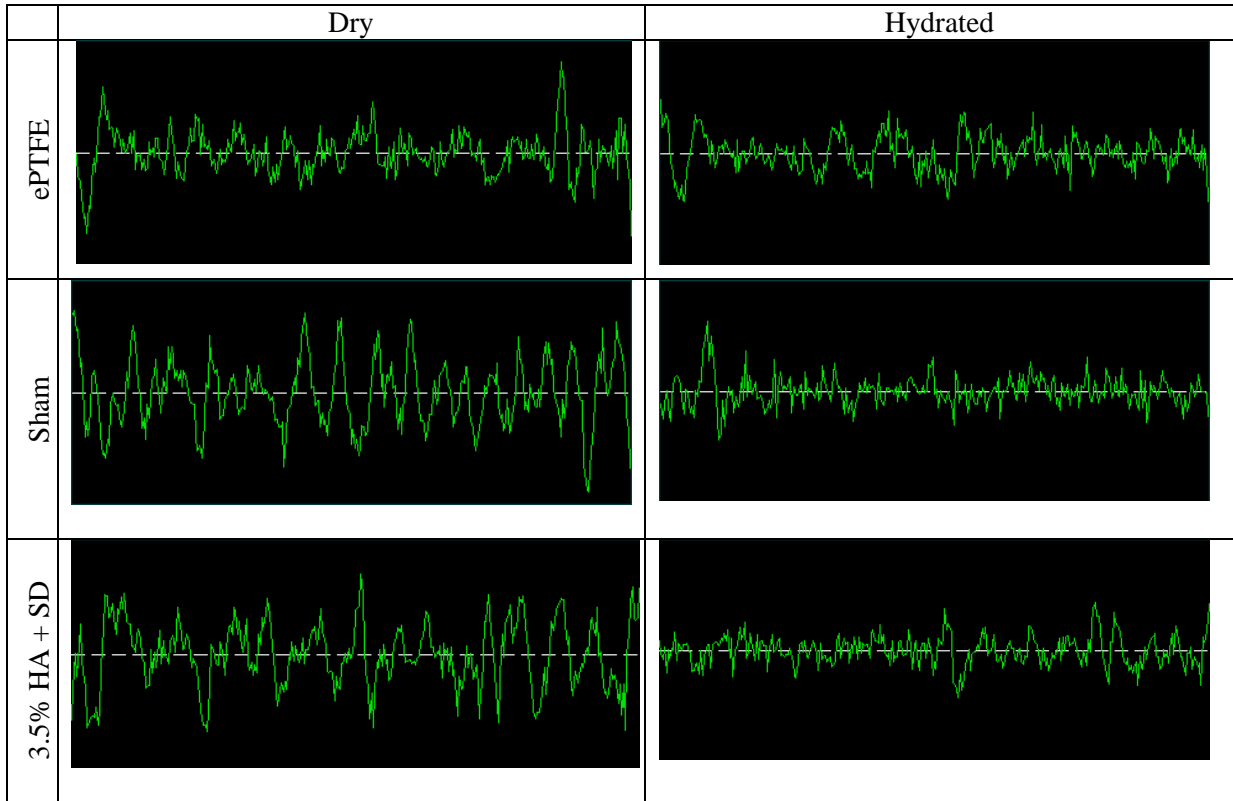
Figure 2.18: Two-dimensional depth profile plots at 100x magnification of ePTFE, the sham control, and 3.5% HA + SD samples in dry and hydrated states.
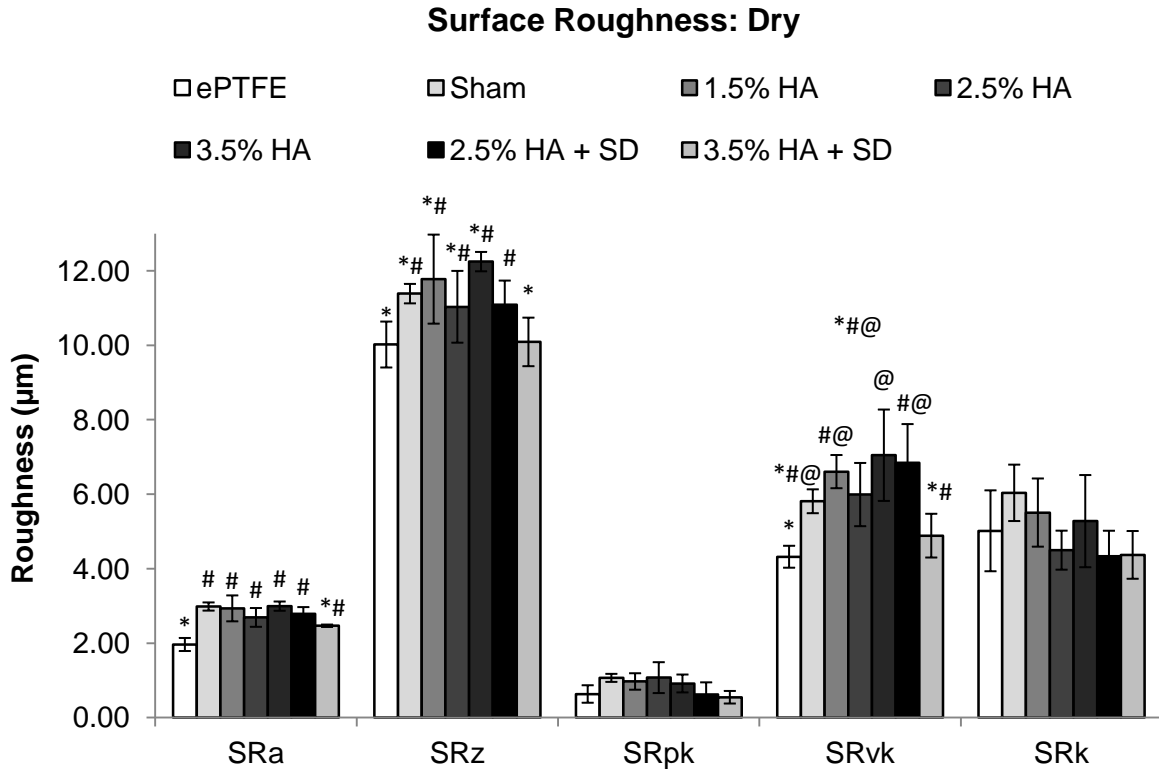
Figure 2.19: Quantification of surface roughness of dry samples across both ridges and valleys. Groups that do not share a symbol are significantly different. Error bars represent standard deviation.
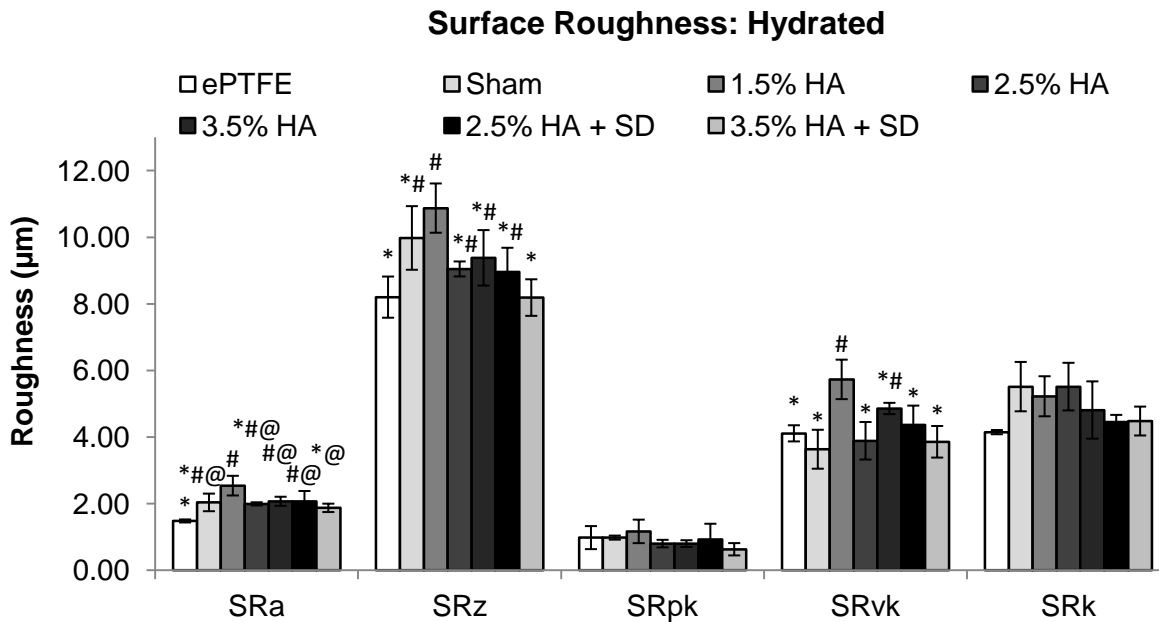
Figure 2.20 Quantification of surface roughness of hydrated samples across both ridges and valleys. Groups that do not share a symbol are significantly different. Error bars represent standard deviation.
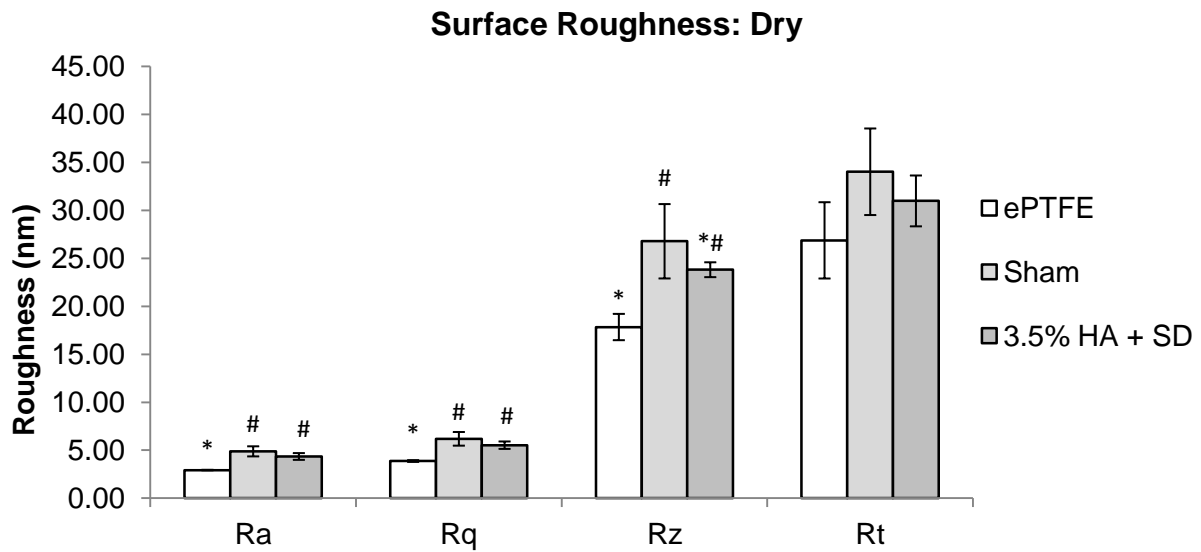
Figure 2.21 Quantification of surface roughness of dry samples for ridge tops only. Groups that do not share a symbol are significantly different. Error bars represent standard deviation.
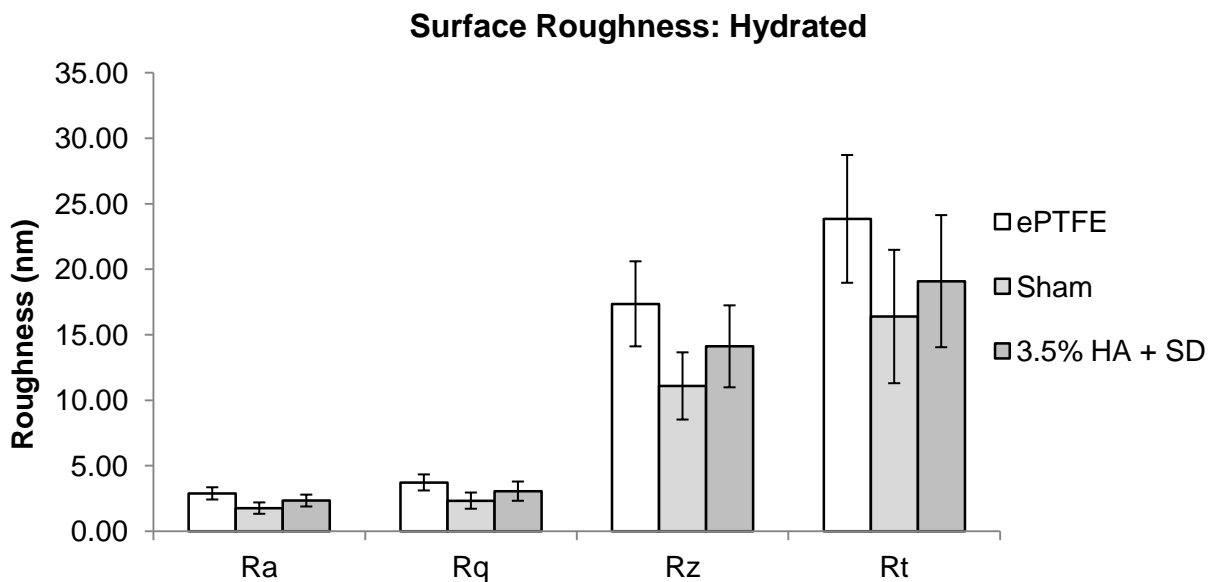
Figure 2.22: Quantification of surface roughness of hydrated samples for ridge tops only. Statistical analysis shows no statistical significance. Error bars represent standard deviation.
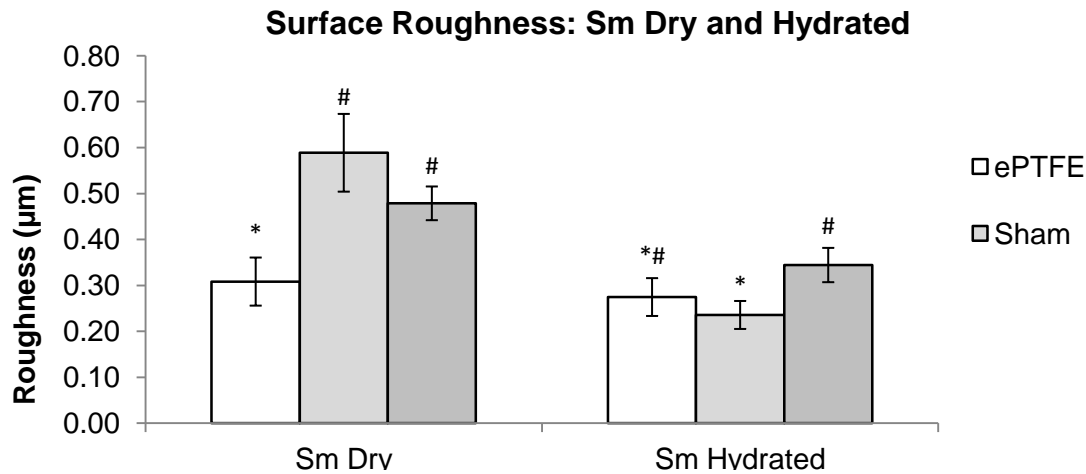
Figure 2.23 Quantification of surface roughness of dry and hydrated samples on ridge tops only. Groups that do not share a symbol are significantly different. Error bars represent standard deviation.

2.6 Conclusions

SEM images enable visualization of ePTFE material structure. HA was successfully incorporated into ePTFE materials through wicking in silyl HA-CTA and xylenes solutions. TGA results indicate that the 3.5% HA swelling solution concentration produces ePTFE materials with more HA than the 2.5% HA and 1.5% HA swelling solutions. Surface dipping further increased the percent weight composition of HA within ePTFE samples.

XPS results confirm that HA is present on samples surfaces, as determined by the atomic weight percentages of carbon, fluorine, oxygen, and nitrogen, as well as relative binding energy peak heights within a sample. For a given sample, as the amount of carbon increases, the amount of fluorine decreases because XPS sampling depth is less than the HA coating thickness on the ePTFE surface.

SWLI indicates that soaking samples in xylenes increases the surface roughness compared to the roughness of ePTFE, thereby increasing surface area. This affects cellular

adhesion, as will be shown in Chapter 3. The xylenes soak also increases the volume and depth

of pores.

REFERENCES

[1]   Zhang, M.; James, S.P. Silylation of hyaluronan to improve hydrophobicity and reactivity for improved processing and derivatization. *Polymer* **2005,** 46, 3639–3648.

[2]   Zhang, M. Surface Modification of Ultra High Molecular Weight Polyethylene With Hyaluronan For Total Joint Replacement Application. Ph.D. Dissertation, Colorado State University, Fort Collins, CO, 2005.

[3]   Kurkowski, R. The chemical crosslinking, compatibilization, and direct molding of ultra high molecular weight polyethylene and hyaluronic acid microcomposites. M.S. Thesis, Colorado State University, Fort Collins, CO, 2007.

[4]   Dean IV, H. Development of BioPoly(R) Materials for use in Prosthetic Heart Valve Replacements. M.S. Thesis, Colorado State University, Fort Collins, CO, 2012.

[5]   Beauregard, G.P. Synthesis and characterization of a biomimetic UHMWPE-based interpenetrating polymer network for use as an orthopedic biomaterial. Colorado State University, Fort Collins, CO, 1999.

[6]   Eastman, M.P.; Hughes, R.C.; Yelton, G.; Ricco, A.J.; Patel, S.V.; Jenkins, M.W. Application of the Solubility Parameter Concept to the Design of Chemiresistor Arrays. *J. Electrochem. Soc.* **1999,** 146, 3907–3913.

[7]   Hansen. *Journal of Paint Technology* **1967,** 39.

[8]   Patrick, R.L.Treatise on Adhesion and Adhesives. Marcel Dekker: New York, 1967; Vol. 1.

[9]   Zygo Corporation. Surface Texture Parameters. **2008**.

[10]   2D (Profile) Stylus Parameters. Michigan Metrology, LLC.

[11]   Socrates, G. Infrared and Raman Characteristic Group Frequencies: Tables and Charts. http://www.wiley.com/WileyCDA/WileyTitle/productCd-0470093072.html (accessed 2014).

[12]   Tzeng, G.S.; Chen, H.J.; Wang, Y.Y.; Wan, C.C. The effects of roughening on teflon surfaces. *Surf. Coat. Technol.* **1997,** 89, 108–113.

[13]   Kuo, J.W. Practical Aspects of Hyaluronan Based Medical Products. *CRC Press* **2005**.

[14]   Choi, J.; Kim, J.K.; Kim, J.H.; Kweon, D.K.; Lee, J.W. Degradation of hyaluronic acid powder by electron beam irradiation, gamma ray irradiation, microwave irradiation and thermal treatment: A comparative study. *Carbohydr. Polym.* **2010,** 79, 1080–1085.

[15] Hayes, M.J.; Lauren, M.D. Chemical stress relaxation of polyglycolic acid suture. *J. Appl. Biomater.* **1994,** 5, 215–220.

[16] Tobolsky, A.V. Stress Relaxation Studies of the Viscoelastic Properties of Polymers. *J. Appl. Phys.***2004,** 27, 673–685.

CHAPTER 3: STATIC HEMOCOMPATIBILITY OF ePTFE-HA MATERIALS

3.1 Introduction

Assessing hemocompatibility of a small diameter vascular graft material is important for the evaluation of whether graft patency will improve compared to current synthetic grafts. As small diameter grafts have low blood flow rates and a propensity to fail due to thrombosis, there is a need to find a graft material with a lower thrombogenic potential. A static hemocompatibility screen was performed on ePTFE, the sham control, 1.5% HA, 2.5% HA, 3.5% HA, 2.5% HA + SD, 3.5% HA + SD, and tissue culture polystyrene surfaces using a fluorescence stain and scanning electron microscopy to determine which swelling solution concentration produced samples with the lowest thrombogenic potential. After selecting a swelling solution concentration, additional studies were performed to further assess the antithrombogenic properties of ePTFE-HA materials. Specifically, protein adsorption, cell viability, whole blood clotting kinetics, and additional imaging were performed.

3.2 Materials and Methods

3.2.1 Hemocompatibility Screening

After performing SEM, ATR-FTIR, TGA, XPS, static contact angle goniometry, and SWLI, blood studies were performed to determine which swelling solution concentration produced samples with the lowest thrombogenic potential based on platelet and leukocyte adhesion, aggregation, activation, and morphology. Calcein-AM live fluorescence stain (Invitrogen) was used to quantify the number of adhered platelets on sample surfaces, and scanning electron microscopy (SEM) was used to assess platelet aggregation, activation, and morphology. [1], [2]

3.2.1.1 Sample Preparation

ePTFE tubes were dissected longitudinally, and tubes were folded open. Sterile biopsy punches (Acuderm Inc.) were used to acquire round (8mm diameter) specimens for testing. To prevent sample floating, samples were mounted to polytetrafluoroethylene (PTFE) white disc liners with 0.050" thickness and 8mm diameter (Berlin Packaging, LLC) using double sided carbon conductive tape (Ted Pella). Disc liners and 8mm samples were separately sterilized in 70% ethanol for 10 minutes, the ethanol was aspirated, and samples air dried. Disc liners were then placed on double sided carbon tape, and a sterile biopsy punch (8mm) was used to obtain a disc liner with matching size tape adhered to the surface. The exposed surface of tape was exposed to UV light for 30 mins. The ePTFE samples were mounted to the PTFE disc liners such that the inside surface of the tube was exposed for contact with blood. Mounted samples were placed in 48 well-plates, rinsed twice with PBS, and then hydrated for at least 12 hours prior to incubation with blood plasma. When HA is hydrated, it can swell to 1,000 times its dry size [3]. The sample preparation protocol can be found in Appendix 1.

Tissue culture polystyrene (TCPS) control samples were obtained using polystyrene cell culture petri dishes (Cell Star) and a drill press. TCPS samples were subsequently cleaned using an ultrasonic cleaner in solutions of 2% Liquinox in DI H_2O, DI H_2O, and 70% ethanol for fifteen minutes in each solution. Samples were rinsed with DI H_2O after sonicating in 2% Liquinox to remove excess soap.

3.2.1.2 Plasma Isolation from Whole Blood

Whole blood was drawn from healthy individuals free of medicine, painkillers, or vitamin supplements for at least two weeks was obtained through venopuncture and collected into 10 mL vacuum tubes coated with an anticoagulant, ethylenediaminetetraacetic acid (EDTA). The first

10 mL tube was discarded to eliminate effects of the skin plug and platelet activation due to the needle insertion. Vacuum tubes were centrifuged at 300 g for 15 min to separate the plasma from red blood cells, and the upper plasma layer was pooled into a fresh centrifuge tube. Collected blood was used within two hours of venopunture. [1]

3.2.1.3 Calcein-AM

Sample treatment groups included in the calcein-AM screening tests are ePTFE, the sham control, 1.5% HA, 2.5% HA, 3.5% HA, 2.5% HA + SD, 3.5% HA + SD, and TCPS. Three samples per treatment group were used. Additional controls include one sample from each treatment group that was stained but not incubated with blood plasma to assess stain interaction with samples. Calcein-AM was performed with two sample sets using plasma from two different platelet populations.

Platelet and leukocyte adhesion and aggregation was assessed using a calcein-AM live fluorescence stain. Samples were incubated in 500µl of pooled blood plasma in a 48 well-plate for two hours at 37°C and 5% CO_2 on a horizontal shaker plate (100rpm). The plasma was removed, and samples were rinsed twice with PBS to remove any un-adhered cells. Samples were transferred to a clean 48 well-plate and incubated with 500µL of 5µM calcein-AM solution in PBS at room temperature for 30 minutes in the dark. Samples were then rinsed in PBS and imaged using a Zeiss fluorescence microscope with a 62 HE BP 474/28 filter set. Five images per sample were obtained at 50x, and one image per sample was obtained at 10x. ImageJ software was used to quantify the number of platelets and leukocytes from 50x images. [1]

3.2.1.4 Scanning Electron Microscopy

Scanning electron microscopy (SEM) was used to further assess platelet and leukocyte aggregation, activation, and morphology on HA-modified ePTFE surfaces compared to control

ePTFE. After incubating pooled blood plasma on sample surfaces at 37°C and 5% CO_2 on a horizontal shaker plate (100rpm) for two hours, the plasma was aspirated, and samples were rinsed twice with PBS to remove un-adhered cells. Adherent cells were then fixed by placing samples in a primary fixative solution (6% gluteraldeyde (Sigma Aldrich), 0.1M sodium cacodylate (Polysciences), and 0.1M sucrose (Sigma)) for 45 mins. Samples were then placed in a secondary fixative solution for 10 mins. The secondary fixative solution is the same as the primary fixative solution but without gluteraldehyde. Next, samples were dehydrated by placing in a series of ethanol solutions (35%, 50%, 70%, and 100%) for 10 mins each. An additional dehydration step was performed by placing samples in hexamethyldisilazane ($\geq$ 97%, Sigma Aldrich) for 10 mins. This was followed by air drying, and samples were stored in a dessicator until ready to image using SEM. [1] Note that the HMDS dehydration was not performed on samples incubated with the second platelet population because fibrin formation on samples from the first platelet population was thought to be observed and caused by interaction of HMDS with the ePTFE material.

Prior to imaging, samples were coated with a 10nm layer of gold. A scanning electron microscope model JEOL JSM-6500F (Thermo Electron) with 5.0kV and working distance 10.1mm was used to obtain one image of each sample at 500x, five images at 2,000x, and one image at 5,000x magnification.

Sample treatment groups included in the SEM screening tests are ePTFE, the sham control, 1.5% HA, 2.5% HA, 3.5% HA, 2.5% HA + SD, 3.5% HA + SD, and TCPS. Three samples per treatment group were used. SEM was performed with two sample sets using plasma from two different platelet populations.

After performing the static hemocompatibility screen, SEM imaging was also performed on protein adsorption samples exposed to protein solutions. Three separate protein solutions, each containing a different protein, were used. These samples were not exposed to blood and therefore did not undergo the fixation procedure.

3.2.2 Sample Preparation

Based on plasma studies and measurement of platelet adhesion and activatio from the static hemocompatibility screening with calcein-AM and SEM, a 3.5% HA swelling solution was selected for use in additional static hemocompatibility testing. Both 3.5% HA and 3.5% HA + SD samples were prepared and tested. Specimens were mounted on PTFE disc liners as described in Section 3.2.1.1. TCPS controls were included in additional hemocompatibility tests. Refer to Chapter 2 for sample preparation processes.

3.2.3 Protein Adsorption

After implantation of a biomaterial, blood and tissue proteins adsorb onto material surfaces within seconds to minutes after an implant is placed in the body. Cell adhesion is mediated by interactions with adsorbed proteins. The quantity, density, orientation, and conformation of adsorbed proteins depend on chemical and physical characteristics of a surface. Surface chemistry and Van der Waals bonds, hydrogen bonds, hydrophobicity, and electrostatic interactions affect adsorption. Cells bind when specific protein geometries are present. [4] Protein adsorption on ePTFE-HA materials is therefore an indicator of material hemocompatibility. Albumin (ALB), fibrinogen (FIB), and immunoglobulin-G (IgG) are three blood serum proteins.

ALB is the most abundant protein in blood plasma and transports fatty acids and small molecules throughout the circulatory system. Its primary function is to regulate and maintain

colloidal osmotic pressure of blood. It is a globular protein and can become distorted upon

interaction with material surfaces. [2], [4]

Thrombin is a key protein in the initiation of the coagulation cascade and platelet

activation. Thrombin transforms the glycoprotein FIB into fibrin monomers, which can then

form a polymeric network resulting in a clot. Quantification of FIB can be used to assess the

pro-coagulant activity of surfaces. [1] FIB is the most abundant protein involved in the

coagulation cascade and has a Y shaped structure with two identical halves linked by a globular

domain at the center. IgG also has a Y shape and is less elongated than FIB. It is the most

abundant antibody isotype in blood and functions to control infection of body tissues. [2], [4]

Protein adsorption on material surfaces was measured using a micro-BCA assay kit

(Thermo Scientific). Three samples per treatment group (ePTFE, the sham control, 3.5% HA,

3.5% HA + SD, and TCPS) were used for each of the proteins analyzed. Samples were sterilized

in 70% ethanol for 10 mins, mounted on PTFE discs, placed in a 48 well-plate, and rinsed twice

with PBS. Samples were then incubated in a 48 well-plate in a 100 µg/ml solution of FIB, ALB,

or IgG in PBS on a horizontal shaker plate at 100rpm in an incubator at 37°C and 5% CO_2.

Separate samples were used for each of the three proteins tested. After incubating for two hours,

the protein solution was removed and samples were rinsed with PBS three times to remove

unattached protein from sample surfaces. Samples were moved to a new well plate and

incubated with 1% sodium dodecyl sulfate (SDS) in PBS for one hour on a horizontal shaker

plate. SDS is an anionic detergent that was used to solubilize the adsorbed protein. The SDS

solution was then collected into new wells, and fresh SDS solution was placed in wells

containing samples to incubate again for one hour on a horizontal shaker plate. The SDS

solution was collected again and pooled with the previous SDS wash. The SDS incubation and

pooling was performed once more (three times total). The absorbance of the pooled SDS

solution containing solubilized proteins was measured using a plate reader (BMG Labtech) at

562nm. A standard curve for each protein was prepared with protein concentrations of 200

µg/mL, 40 µg/mL, 20 µg/mL, 10 µg/mL, 5 µg/mL, 2.5 µg/mL, 1 µg/mL, 0.5 µg/mL, and 0

µg/mL and the absorbance at a wavelength of 562nm was measured. Absorbance of SDS

collected from samples was then compared to the standard curve for each protein to determine

the amount of protein adsorbed on each sample.   [2], [5], [6]

SEM imaging was also performed for ePTFE, the sham control, 3.5% HA, and 3.5% HA

+ SD specimens incubated in FIB, ALB, and IgG solutions (100 µg/mL) for two hours at 37°C

and 5% CO_2. Separate samples were prepared for SEM and absorbance. One sample per

treatment group per protein was imaged. Samples were air dried and stored in a vacuum

dessicator until ready to image. Specimens were coated with a thin layer of gold (~3nm) and

imaged at 5 kV. Images at 1,000x and 5,000 magnifications were obtained.

3.2.4 Direct Immunofluorescence

Immunofluorescence staining and microscopy was performed to identify adherent

platelets and leukocytes on sample surfaces. Samples were stained with 4'6-diamidino-2-

phenylindole-dihydrochloride (DAPI, Invitrogen) nucleus stain and the F-actin cytoskeleton stain

rhodamine-conjugated phalloidin (RHO, Cytoskeleton). DAPI was used to identify adherent

leukocytes, as platelets do not have nuclei. The cytoskeleton stain was used to identify both

platelets and leukocytes. [1]

Three samples per treatment group (ePTFE, the sham control, 3.5% HA, 3.5% HA + SD,

and TCPS) were used. Additional controls include one sample from each treatment group that

was stained but not incubated with blood plasma to assess stain interaction with samples. DAPI

and RHO staining and imaging was performed with two sample sets using plasma from two different platelet populations.

After incubating samples with blood plasma in a 48 well-plate for two hours, blood plasma was aspirated, samples were rinsed twice with PBS to remove unadhered cells, and samples were moved to a new 24-well plate. Adherent cells were fixed in a 3.7% solution of gluteraldehyde for 15 minutes at room temperature and subsequently washed with PBS three times for five minutes each wash. Cell membranes were permeabilized using a 1% Triton-X solution in PBS for three minutes at room temperature and subsequently washed with PBS three times for five minutes each wash. Next, samples were incubated with a 1:40 dilution of rhodamine-conjugated phalloidin in PBS for 25 minutes at room temperature in the dark. Samples were then incubated in a 0.2 µg/ml DAPI in PBS solution for 5 minutes. Fluorescence imaging was performed with a fluorescence microscope equipped with a blue 49 DAPI BP 445/50 blue filter and 62 HE BP 585/35 red filter set (Zeiss). Five images per sample were obtained at 50x, and one image per sample was obtained at 10x. ImageJ software was used to quantify the number of platelets and leukocytes from 50x images. [1]

3.2.5 MTT Cell Viability Assay

Platelet and leukocyte viability was evaluated using the Vybrant® MTT Cell Proliferation Assay Kit (Invitrogen). The water soluble (3-(4, 5-dimethylthiazol-2-yl)-2,5-diphenyltetrazolium bromide) (MTT) is converted to an insoluble formazan crystal by metabolically active cells. A detergent is then added to solubilize the formazan, and the optical density of solutions was measured at 570nm. [2], [7]

Three samples per treatment group (ePTFE, the sham control, 3.5% HA, 3.5% HA + SD, and TCPS) were used. Samples were incubated in 500µl of blood plasma for two hours at 37°C

and 5% CO_2 on a horizontal shaker plate at 100rpm. Then, the non-adherent cells were removed by aspirating the cell rich media from the surfaces and samples were rinsed twice with PBS, and samples were moved to a new 48 well-plate. A 12 mM MTT stock solution was prepared by adding 1 mL of sterile PBS to one vial of MTT powder. The MTT stock solution was mixed by pipetting and vortexing until the powder dissolved. The solution was diluted further by adding it to 10mL of PBS. Next, 500 µL of solution was placed on each specimen, and samples were incubated in a 48 well-plate for four hours at 37°C and 5% CO_2. One bottle of SDS (1g) was dissolved in 10 mL of DI H_2O and 8.27 µL of 12.1M hydrochloric acid to prepare the formazan solvent. The solution was mixed until dissolved and 500 µL of the SDS solvent solution was transferred directly to sample wells still containing the MTT solution. Samples were incubated an additional 4.5 hours at 37°C and 5% CO_2. The absorbance of the resulting solution was measured using a plate reader at a wavelength of 570 nm (BMG Labtech). The absorbance values are used as an indirect measurement of cell viability on substrates. [1], [2], [7]

3.2.6 Whole Blood Clotting Kinetics

The thrombogenic potential of ePTFE, the sham control, 3.5% HA, 3.5% HA + SD, and TCPS samples was further assessed by whole blood clotting kinetics. As the concentration of free hemoglobin increases, the absorbance directly increases.

Whole blood was drawn from healthy individuals through venopuncture and collected into 15 mL centrifuge tubes that were not coated. The first 10 mL tube was discarded to eliminate effects of the skin plug and platelet activation due to the needle insertion. Whole blood was used immediately after collection. Whole blood (5µl) was placed onto sample surfaces for 15, 30, and 60 minutes. Three samples per treatment group were tested at each time point. The concentration of free hemoglobin was measured by transferring samples to a new well-plate

86

containing 500 µl of DI H_2O, gently agitating for 30 seconds, and sitting in the DI H_2O for 5 minutes for red blood cells not trapped in the thrombus to release free hemoglobin. Absorbance of the DI H_2O containing the free hemoglobin was measured using a plate reader at 540nm. Samples from the 60min time point were then air dried and stored in a vacuum dessicator until ready to image with SEM. To image, samples were coated with a thin layer of gold (~3nm) and imaged with SEM at 5 kV. [5], [8]

3.2.7 Statistical Analysis

Each experiment was performed on at least three samples per treatment group. Experiments were performed using blood from two different platelet populations. Quantitative results were analyzed with a one way analysis of variance (ANOVA) with a statistical significance level of $p<0.05$. Tukey tests were performed post hoc, and outliers were removed using a Grubb's test for outliers.

3.3 Results and Discussion

3.3.1 Static Hemocompatibility Screening

Samples from each swelling solution concentration and surface dipped samples were used in blood plasma studies to assess hemocompatibility based on calcein-AM (Invitrogen) fluorescence staining and scanning electron microscopy (SEM). The swelling solution used to treat the samples with the lowest thrombogenicity as determined by calcein-AM and SEM was used for additional hemocompatibility testing, as well as mechanical testing.

3.3.1.1 Calcein-AM

Platelet and leukocyte adhesion and aggregation were assessed after sample incubation with blood plasma for two hours. Calcein-AM live fluorescence staining and imaging was

performed on ePTFE, a sham control, 1.5% HA, 2.5% HA, 3.5% HA, 2.5% HA + SD, 3.5% HA + SD, and TCPS samples. Calcein-AM is a stain that permeates into live cells, where it is converted to a green fluorescent calcein by hydrolyzation of intracellular acetoxymethylesterases. [1] Staining was performed on three samples each from two platelet populations. Note that the 3.5% HA + SD treatment group was not included in testing with the first platelet population. The number of adherent platelets was quantified using ImageJ software, and average total cell counts per area were determined for each sample treatment group. Grubb's test for outliers was performed and outliers removed. Representative fluorescence images are shown in Figure 3.1, and adherent cell densities from platelet populations I and II are shown in Figure 3.3 and Figure 3.4, respectively. Representative SEM images from platelet populations I and II are shown in Figure 3.5 and Figure 3.7, respectively.

Statistically significant differences between treatment groups were found in both platelet populations I and II. The ePTFE treatment group has a statistically significant difference from HA and TCPS groups in platelet population I, where samples containing HA have more adhesion. The 3.5% HA treatment group in platelet population I has statistically lower adhesion than the other groups prepared with HA. In platelet population II, ePTFE has significantly lower platelet adhesion than the 3.5% HA + SD group, where the remaining treatment groups are not significant from either ePTFE or the 3.5% HA + SD group.

Error bars represent standard error. A surface with nonuniform HA coverage could contribute to the standard error observed. Residual sample curvature from the initial ePTFE tube shape could also result in plasma pooling at the centerline of samples, resulting in higher cell counts along the centerline than along the edges of specimens.

There are similar trends in average total cell counts between the two platelet populations. The sham has higher cell counts than the ePTFE, indicating that soaking in xylenes decreases hemocompatibility of the ePTFE surface. This could be due to the increase in surface roughness as measured by SWLI. Additionally, as the percentage of HA in samples increases from 1.5% HA, 2.5% HA, to 3.5% HA samples, the average total cell count generally decreases as shown in Figure 3.3 and Figure 3.4. As HA percentage increases, HA likely fills in voids and cavities formed by soaking in xylenes, effectively decreasing surface roughness and decreasing surface area.

Samples with a surface dip in aqueous HA have higher cell count than samples without the surface dip. Variability in cell count could also be attributed to variation in HA composition across the ePTFE surface. The roughness of surface dipped samples further increases compared to the same swelling concentration samples without the surface dip. The increase in roughness increases the surface area, which could cause an increase in the number of adhered platelets on samples with a surface dip compared to samples prepared at the same concentration but without a surface dip. An example high magnification image is shown in Figure 3.2. Surface dipped samples exhibit an increase in leukocyte-platelet complexes.

These results do not indicate reduction in platelet and leukocyte adhesion on HA modified ePTFE materials for controlling the thrombogenic effects of the material surfaces. However, sample preparation using a higher HA swelling concentration could further reduce the number of adhered platelets. More HA could decrease thrombogenic potential of surfaces to that of the control ePTFE. With a low amount of HA, the HA can become trapped within the material pores and is not as exposed on the ePTFE surface. It is possible that enough HA could decrease the thrombogenic potential of surfaces to below that of ePTFE.
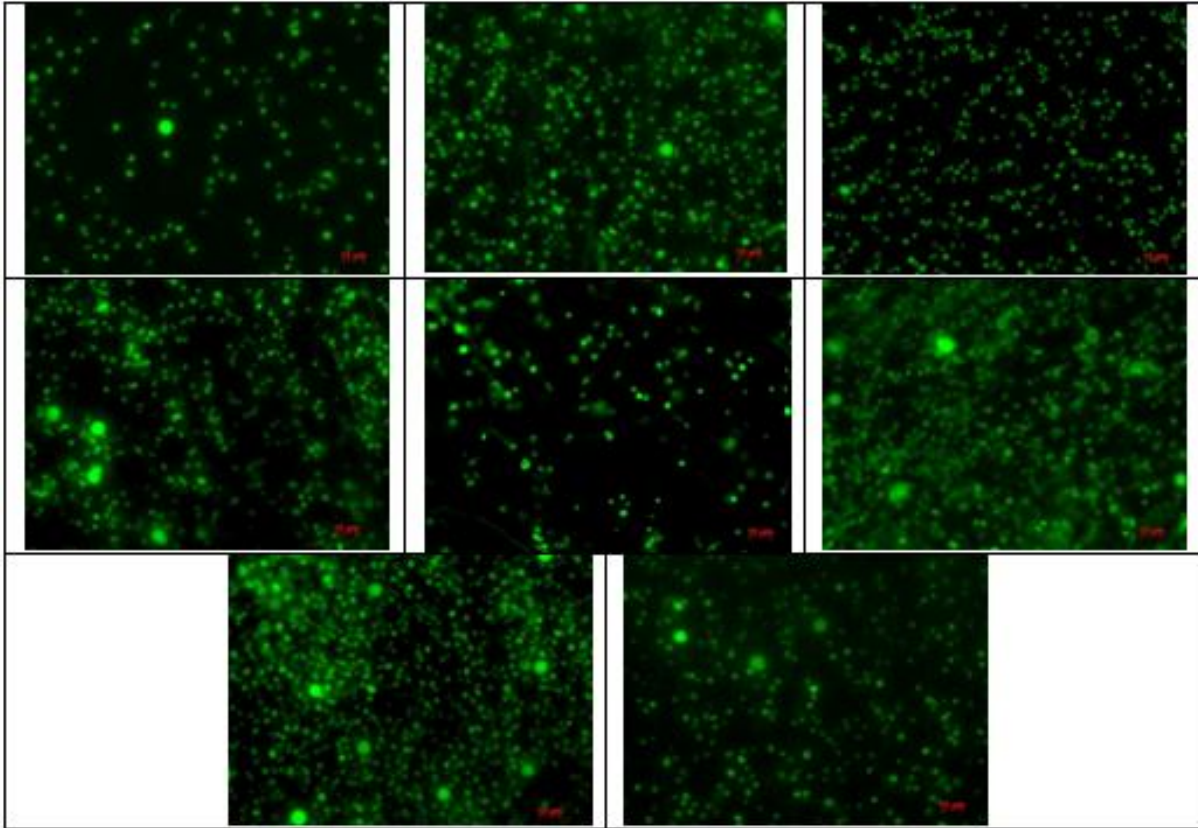
Figure 3.1: Representative fluorescence microscopy images of adhered platelets and leukocytes stained with calcein-AM on ePTFE (top left), the sham (top center), TCPS (top right), 1.5% HA (middle left), 2.5% HA (middle center), 3.5% HA (middle right), 2.5% HA + SD (bottom left), and 3.5% HA + SD (bottom right) surfaces after 2 hours of incubation in whole blood plasma.
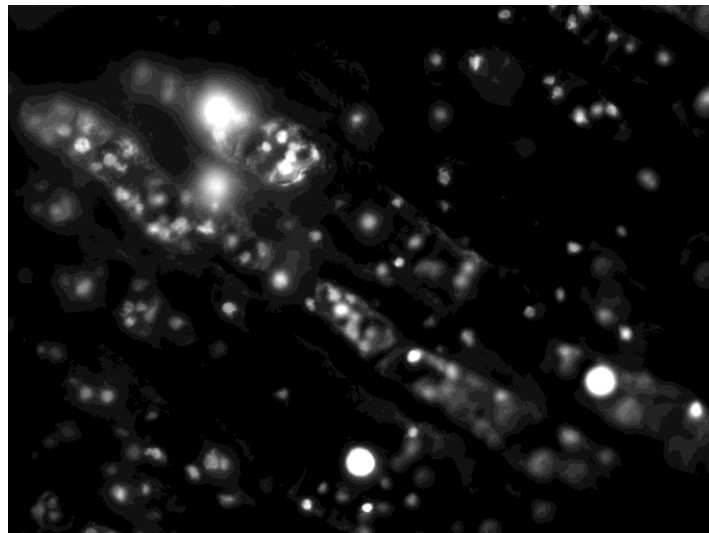
Figure 3.2: An example Calcein-AM 50x image of a 2.5% HA sample.

Calcein: Platelet Population I

Figure 3.3: Average total calcein cell counts per area for ePTFE, a sham control, 1.5% HA, 2.5% HA, 3.5% HA, 2.5% HA + SD, and TCPS surfaces for platelet population I. Groups that do not share a symbol are significantly different. Error bars represent standard error.

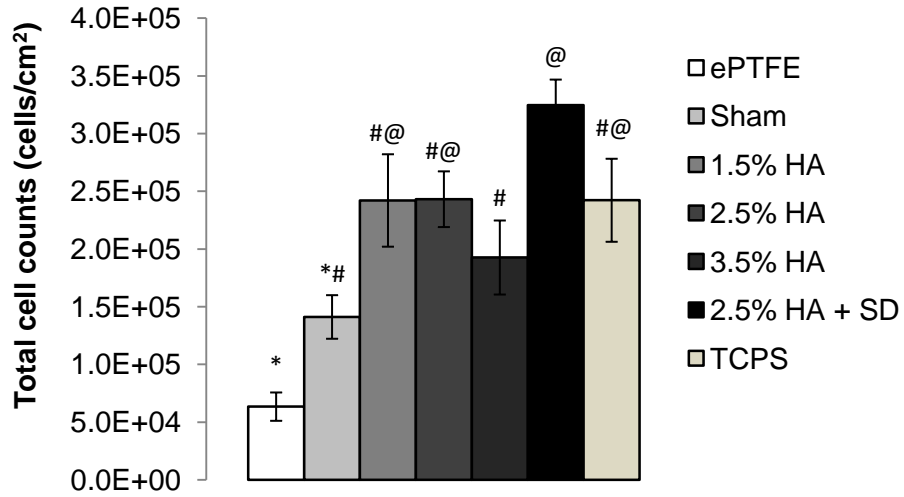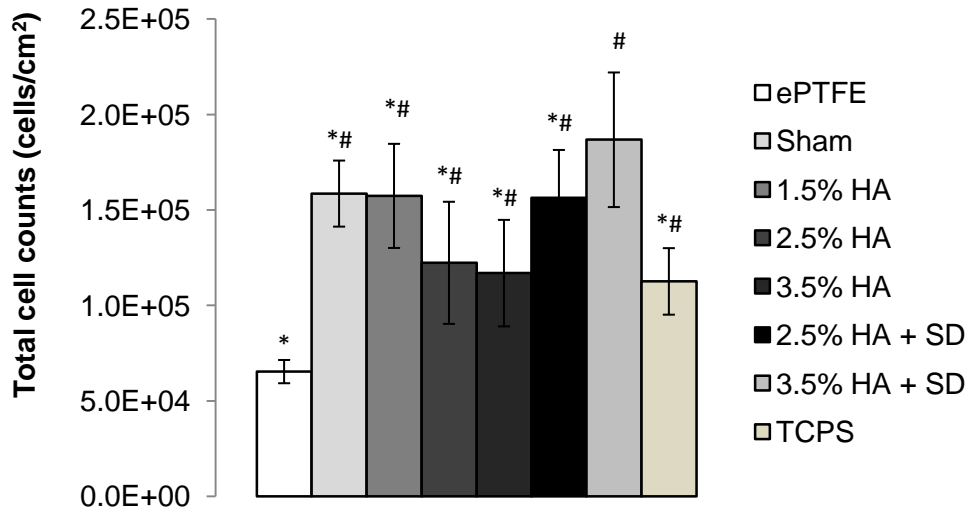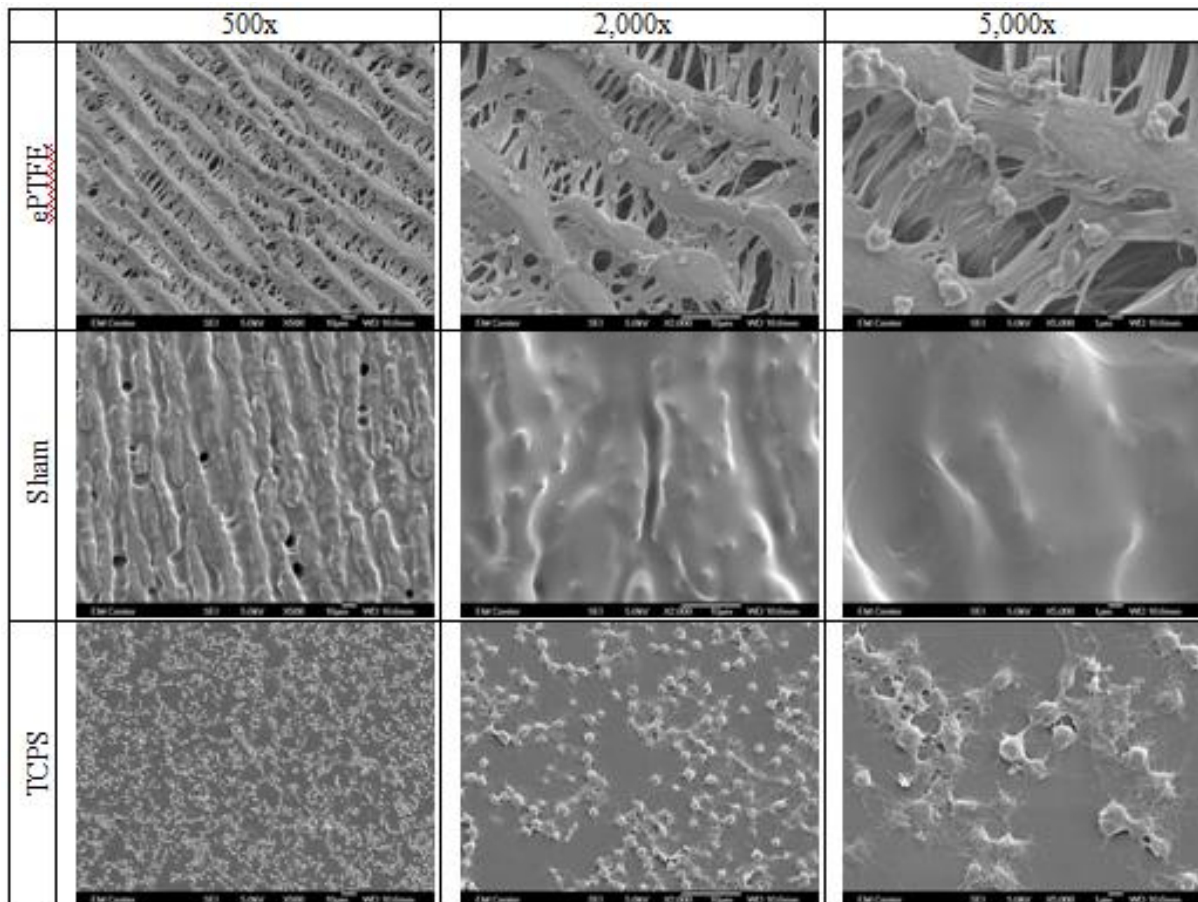# Calcein: Platelet Population II

Figure 3.4: Average total calcein cell counts per area for ePTFE, a sham control, 1.5% HA, 2.5% HA, 3.5% HA, 2.5% HA + SD, 3.5% HA + SD, and TCPS surfaces for platelet population II. Groups that do not share a symbol are significantly different. Error bars represent standard error.

3.3.1.2 Scanning electron microscopy

Scanning electron microscopy images were collected at 500x, 2000x, and 5000x magnification for ePTFE, a sham control, 1.5% HA, 2.5% HA, 3.5% HA, 2.5% HA + SD, 3.5% HA + SD, and TCPS samples from each of two platelet populations to visualize platelet and leukocyte aggregation, morphology, and interaction. Morphological changes of cells are often attributed to interaction with other cells or with biomaterial stimulation. Cellular interactions affect the degree of cellular functionality and thrombogenic potential. Cell adhesion, aggregation, morphology, and interaction were imaged by SEM.

Plain ePTFE surfaces exhibit platelet aggregation and platelet-leukocyte interactions. Aggregated platelets display a high degree of dendritic extension, and some individual platelets express some short dendritic extensions. In platelet population II, less platelet aggregation and decreased platelet-leukocyte interaction is observed on the sham compared to the ePTFE control. In platelet population II, the 1.5% HA group shows more platelet adhesion and aggregation than the 2.5% HA and 3.5% HA groups, which is in agreement with calcein data. Short dendritic extensions are observed in the 2.5% HA and 3.5% HA groups. The 2.5% HA + SD and 3.5% HA + SD treatment groups in platelet population II appear to have minimal platelet aggregation and activation. Less activation is observed on surface dipped samples compared to samples without the surface dip. TCPS results are as expected, with a high degree of adhesion and activation. There appears to be an interaction between the HMDS used during the cell fixation procedure in platelet population I and the sample surfaces in the sham, 1.5% HA, 2.5% HA, and 3.5% HA groups. The HMDS step was omitted during fixation of platelet population II specimens, and this interaction was not observed.

Figure 3.5: SEM images (500x, 2000x, and 5000x magnification) for ePTFE, a sham control, and TCPS surfaces for platelet population I.
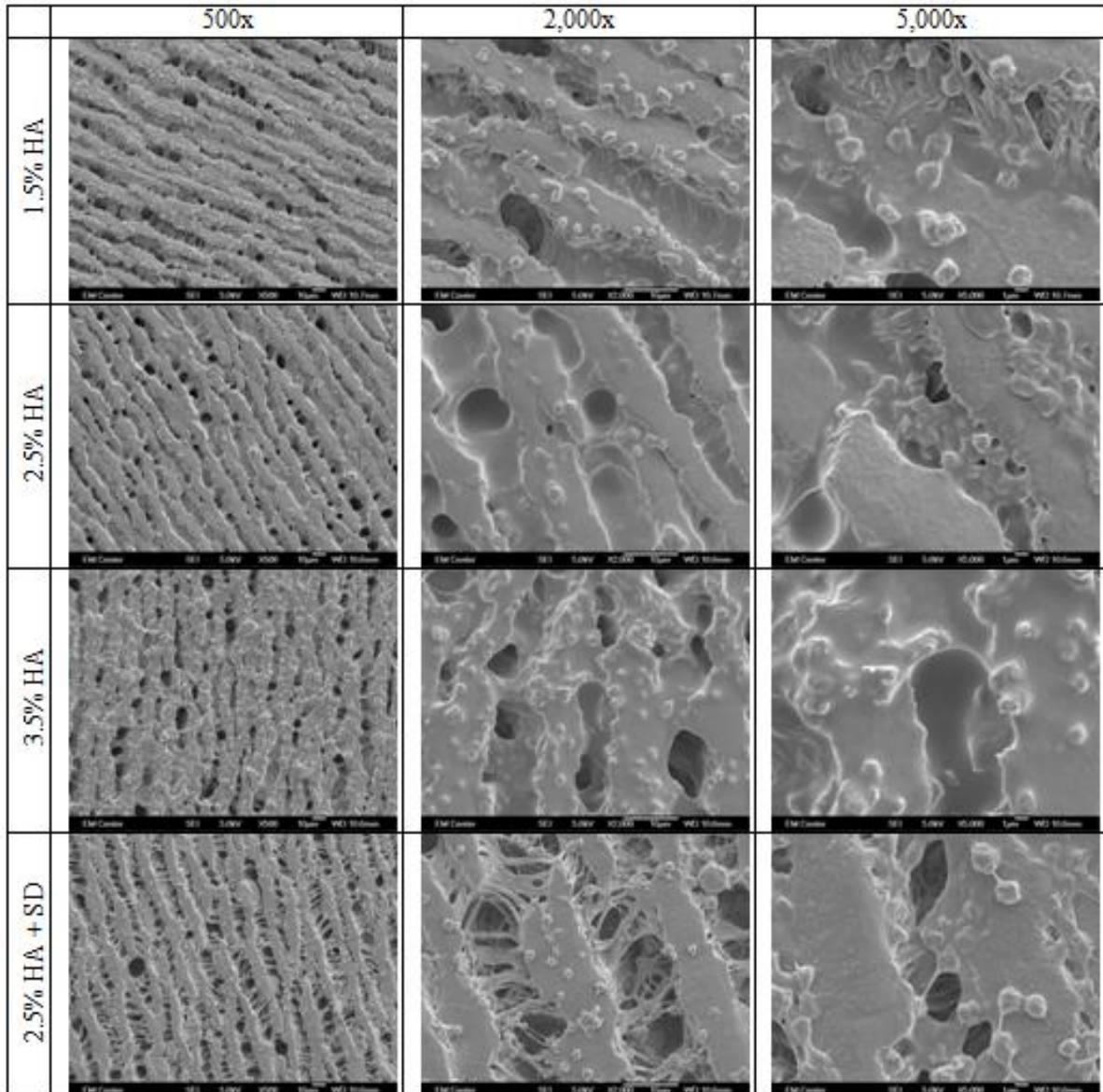
Figure 3.6: SEM images (500x, 2000x, and 5:000x magnification) for 1.5% HA, 2.5% HA, 3.5% HA, 2.5% HA + SD, and 3.5% HA + SD surfaces for platelet population I.
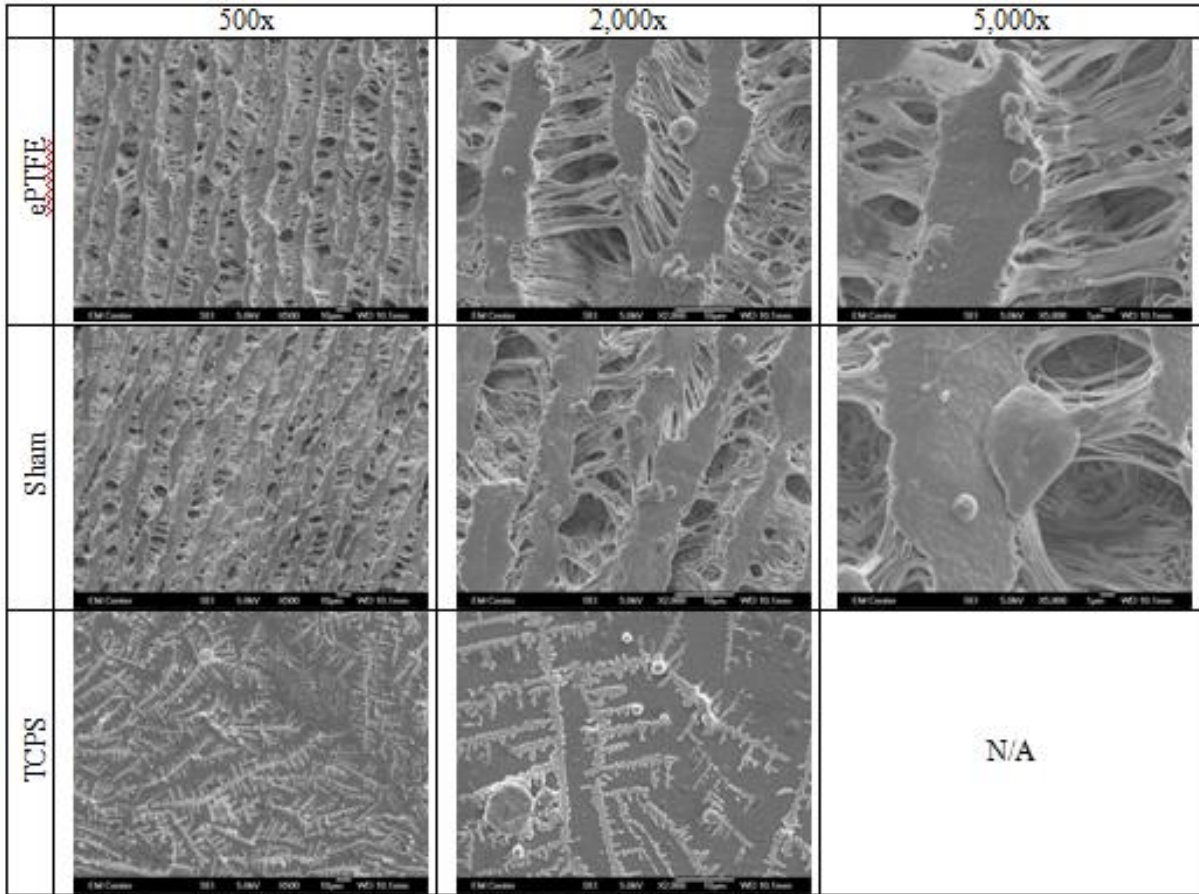
Figure 3.7: SEM images (500x, 2000x, and 5000x magnification) for ePTFE, a sham control, and TCPS surfaces for platelet population II.

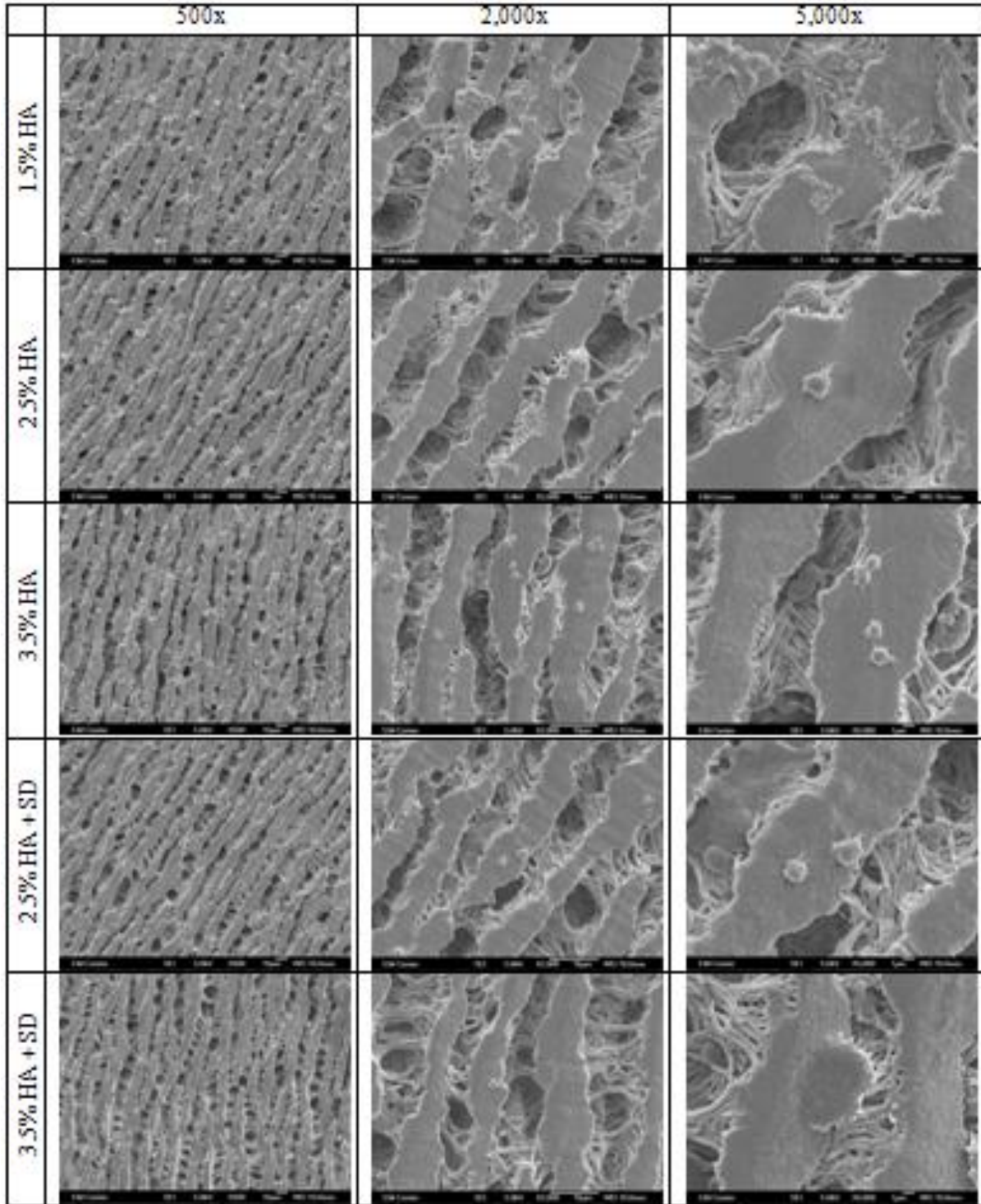**Figure 3.8: SEM images (500x, 2000x, and 5000x magnification) for 1.5% HA, 2.5% HA, 3.5% HA, 2.5% HA + SD, 3.5% HA + SD, and TCPS surfaces for platelet population II.**

3.3.2 Protein Adsorption

Total protein adsorption was measured using the micro-BCA assay kit. Samples were incubated in either FIB, ALB, or IgG solutions (100µg/mL) in PBS for two hours at 37°C and 5% CO_2 on a horizontal shaker plate at 100rpm. Adsorbed proteins were removed using the anionic detergent SDS, and the absorbance of the adsorbed proteins was measured using a plate reader. Protein concentrations were calculated from standard curves for each of the three proteins and shown in Figure 3.9. Adsorbed protein in sample surfaces was additionally visualized using SEM, and representative images are shown in Figure 3.10, Figure 3.11, and Figure 3.12 for ALB, FIB, and IgG, respectively. Total protein adsorption results indicate that IgG adsorbed the most on all surfaces, followed by FIB, then ALB, respectively. There is no significant difference in ALB, FIB, or IgG adsorption between treatment groups.

ALB can act as a passivating protein, preventing material interaction with other proteins and cellular components. As seen in the SEM images in Figure 3.10, the 3.5% HA + SD group has the least adsorbed ALB, followed by the 3.5% HA, then the sham, with the most adsorbed ALB on the ePTFE. Visually, HA appears to decrease the adsorption of ALB. ALB has been shown to have high adsorption on fluoropolymers such as ePTFE. Latour et al found that increasing hydrophillicity decreases the amount of ALB adsorbed, and increases conformation change of proteins. [9], [10] This is in contrast to the quantitative results seen in Figure 3.9. Quantitatively, ePTFE has the lowest measured absorbance. However, this difference is not significant. ALB is more hydrophobic than hydrophilic [11], which may prevent interaction of ALB and ePTFE surfaces due to a hydrophopic effect, decreasing the adsorbed protein on ePTFE. Similarly, the increased hydrophillicity of the 3.5% HA and 3.5% HA + SD surfaces

97

could increase surface interaction with ALB. It can also be difficult to fully remove adsorbed protein from porous surfaces using SDS.

Quantitatively, plain ePTFE has a slightly higher adsorbed FIB concentration than the other treatment groups. The sham and 3.5% HA + SD groups have the lowest adsorbed protein concentration. The quantitative results match those as observed in SEM images in Figure 3.11. These results may identify the sham and 3.5% HA + SD as having the most reduction in fibrin clot formation below that of ePTFE, increasing material hemocompatibility. Fibrinogen can exist in multiple orientations and conformations. Depending on the specific orientation and conformation, FIB can bind nonspecifically with hydrophobic or hydrophilic surfaces. The orientation and binding sites available for cell adhesion then have an effect on the amount of platelet adhesion on a surface. [12] Latour et al have investigated whether platelet adhesion to fibrinogen is the result of the amount of adsorbed protein or the conformation of the protein. Their work concludes that platelet adhesion is determined by the conformation of fibrinogen, where adsorption-induced unfolding of the protein exposes two types of platelet binding sites. One binding site was shown to induce platelet adhesion, while the other binding site was shown to induce both platelet adhesion and activation. [9], [10]

IgG adsorbed the most on 3.5% HA, 3.5% HA + SD, and TCPS surfaces as measured by absorbance. SEM images of adsorbed IgG in Figure 3.12 correlate with quantitative results. The lowest adsorption was observed on the sham control, followed by ePTFE.   IgG has a planar Y shape where FIB is more elongated than IgG. IgG can bind preferentially with hydrophilic of hydrophobic surfaces depending on the pH. Results in Figure 3.9 indicate that IgG bound more preferentially with surfaces that are more hydrophillic. [13], [14]
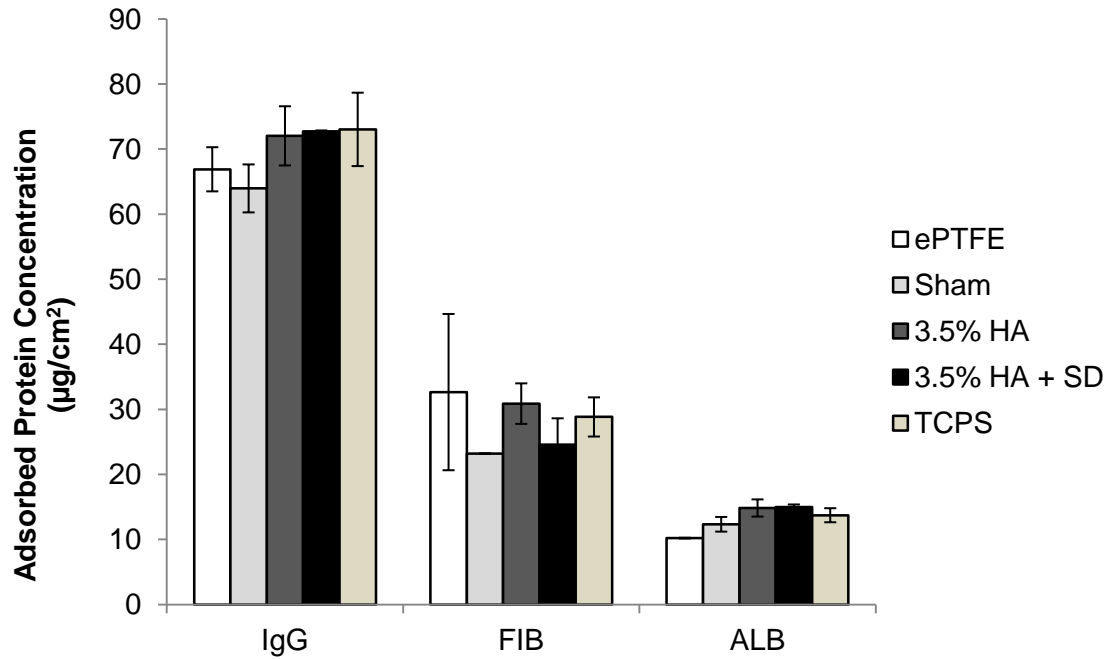
Figure 3.9: Adsorbed protein concentration (µg/mL) of IgG, FIB, and ALB on ePTFE, sham, 3.5% HA, 3.5% HA + SD, and TCPS surfaces after two hours of incubation in 100µg/mL protein solutions in PBS. Statistical analysis shows no significant differences. Error bars represent standard error.
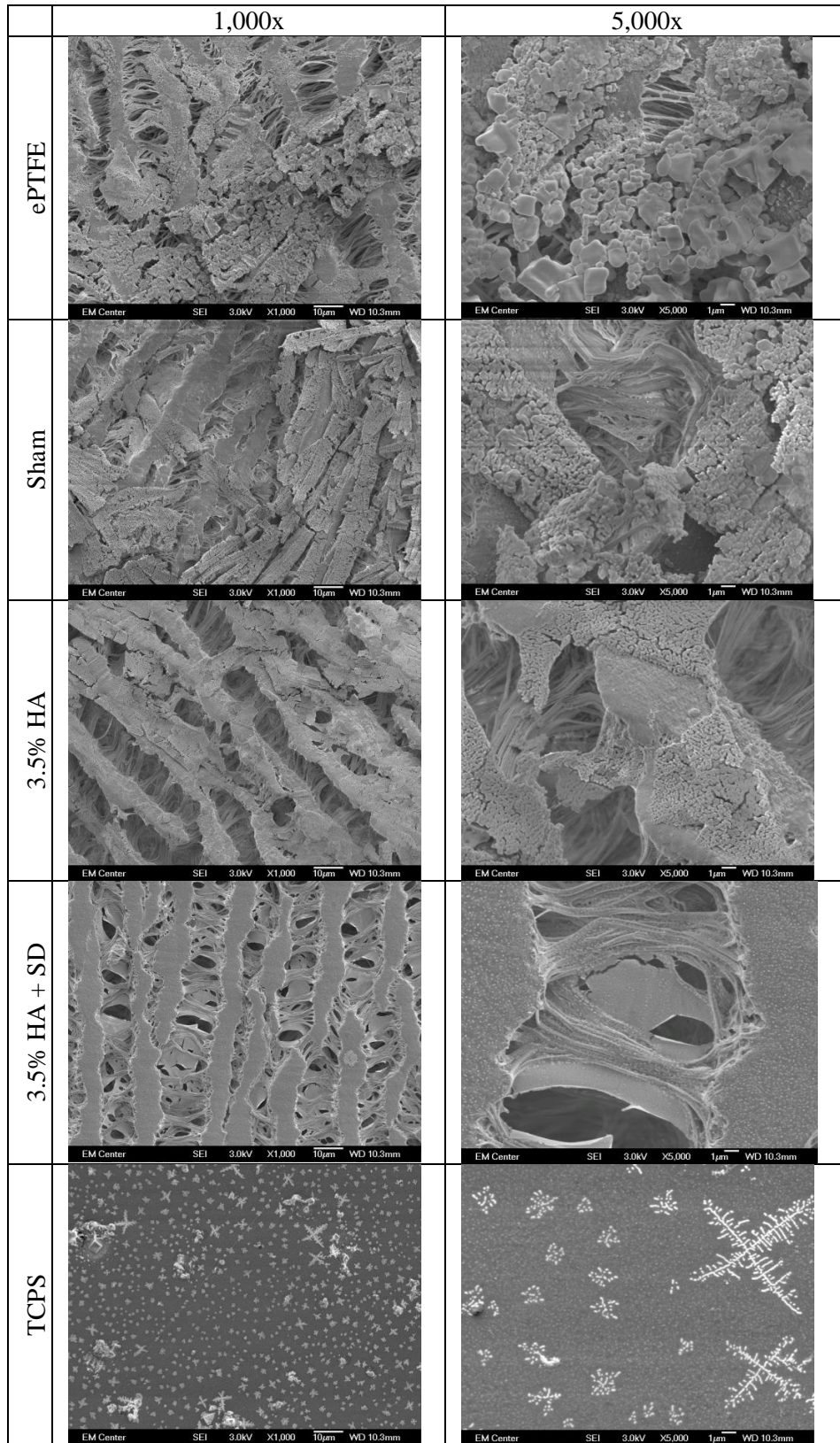
Figure 3.10: SEM images (1,000x, and 5,000x magnification) for ePTFE, a sham control, 3.5% HA, 3.5% HA + SD, and TCPS surfaces for adhered ALB.
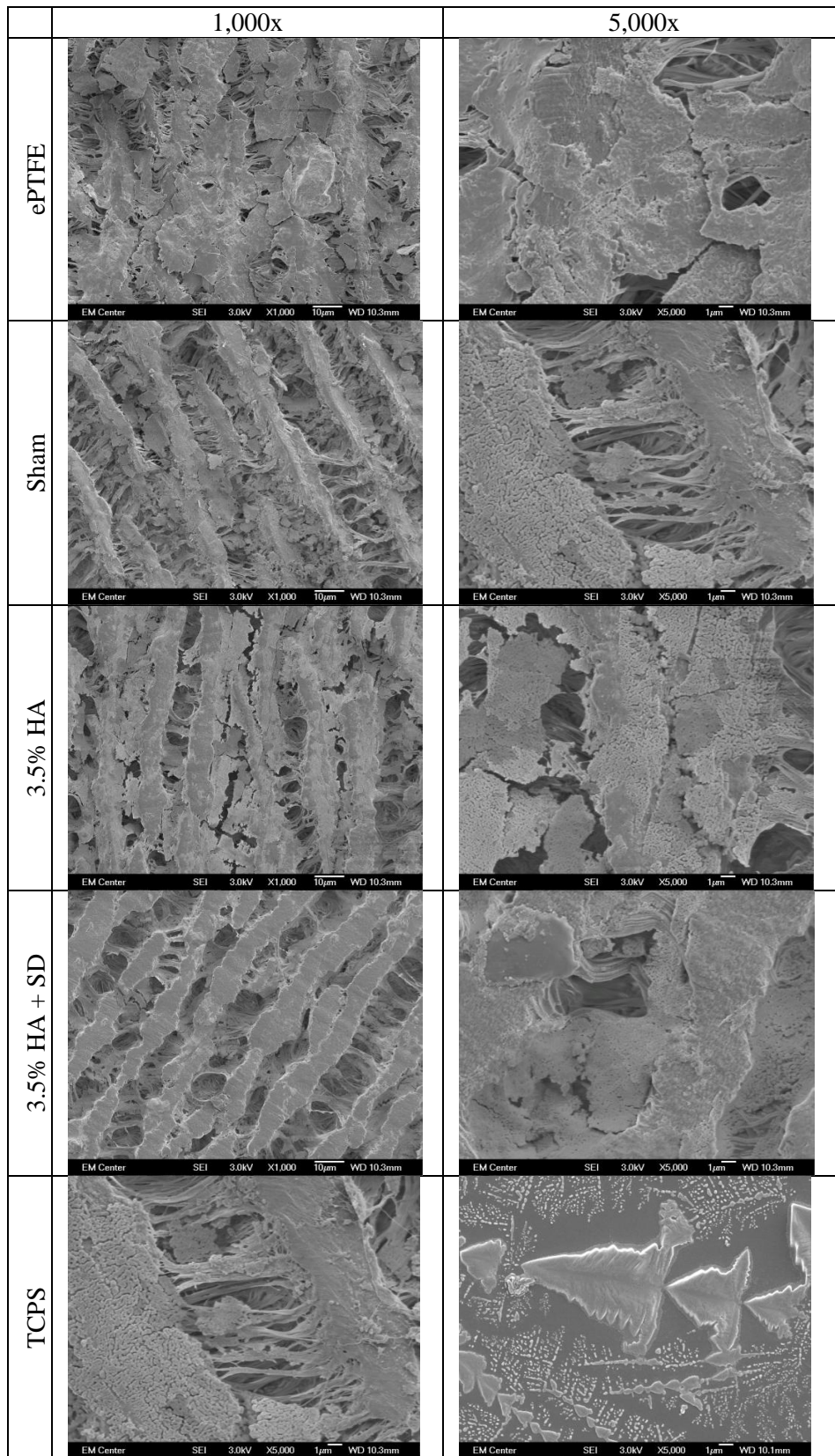
Figure 3.11: SEM images (1,000x, and 5,000x magnification) for ePTFE, a sham control, 3.5% HA, 3.5% HA + SD, and TCPS surfaces for adhered FIB.
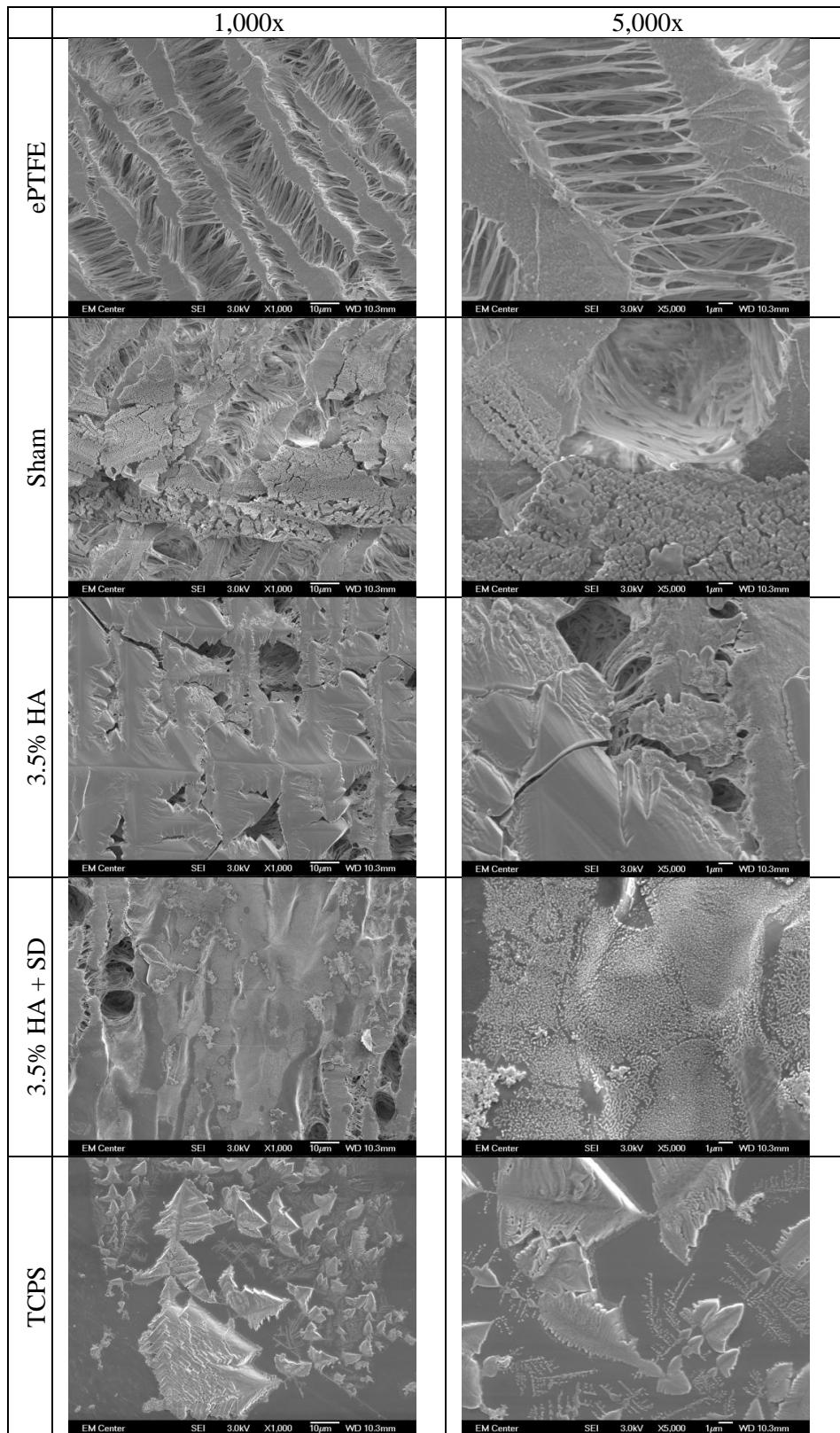
Figure 3.12: SEM images (1,000x, and 5,000x magnification) for ePTFE, a sham control, 3.5% HA, 3.5% HA + SD, and TCPS surfaces for adhered IgG.

3.3.3 Direct Immunofluorescence

DAPI nucleus staining and RHO cytoskeletal staining were performed on plasma isolated from whole blood. Results for DAPI from platelet populations I and II are shown in Figure 3.13 and Figure 3.15, respectively. Results for RHO from platelet populations I and II are shown in Figure 3.14 and Figure 3.16, respectively. Statistically significant differences were only present in RHO platelet population II, where ePTFE has significantly higher platelet and leukocyte adhesion than the 3.5% HA, 3.5% HA + SD, and TCPS samples. This is in contrast with platelet population I, where the sham and TCPS have the highest number of adhered platelets and leukocytes. Trends in DAPI staining seem similar between populations with the exception that platelet population I has more similar adhesion on ePTFE and the sham than in platelet population II. DAPI and RHO results seem inconsistent with calcein, as samples with HA have lower platelet and leukocyte adhesion than the sham control.

DAPI: Leukocyte Population I
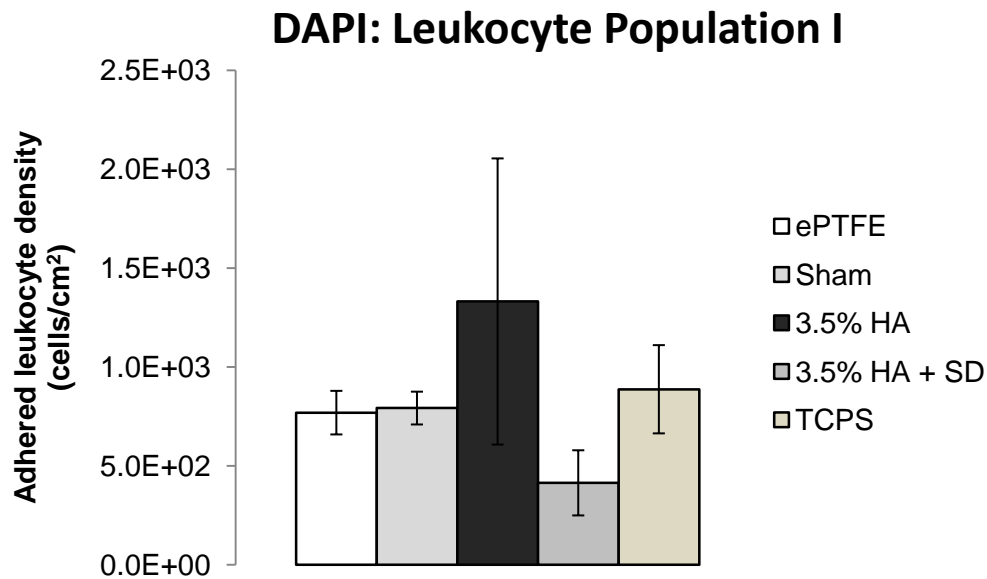
Figure 3.13: Average total cell counts per area for ePTFE, a sham control, 1.5% HA, 2.5% HA, 3.5% HA, 2.5% HA + SD, 3.5% HA + SD, and TCPS surfaces stained with DAPI for platelet population I. Statistical analysis shows no statistically significant differences between surfaces. Error bars represent standard error.

RHO: Platelet Population I
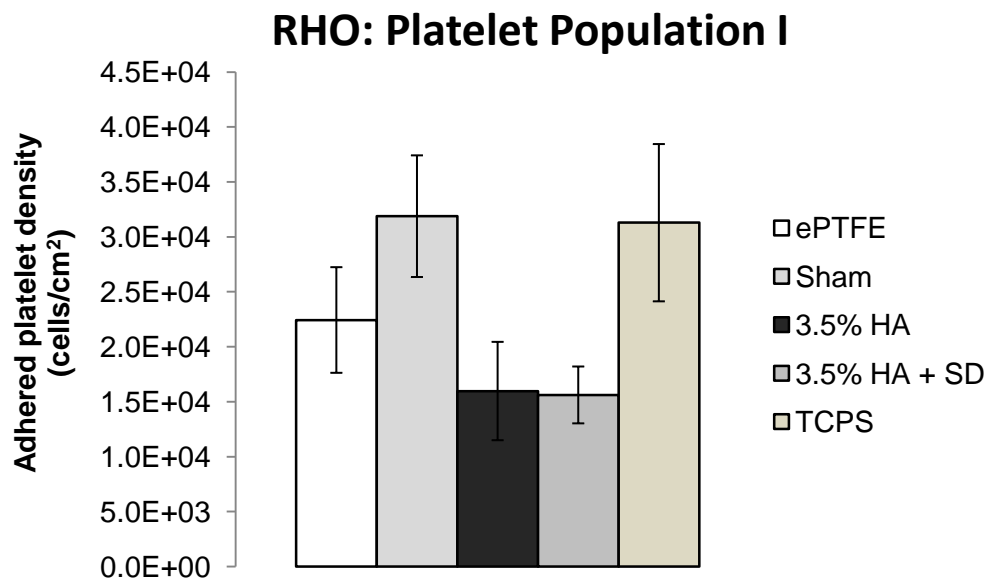
Figure 3.14: Average total cell counts per area for ePTFE, a sham control, 1.5% HA, 2.5% HA, 3.5% HA, 2.5% HA + SD, 3.5% HA + SD, and TCPS surfaces stained with RHO for platelet population I. Statistical analysis shows no statistically significant differences between surfaces. Error bars represent standard error.

DAPI: Leukocyte Population II
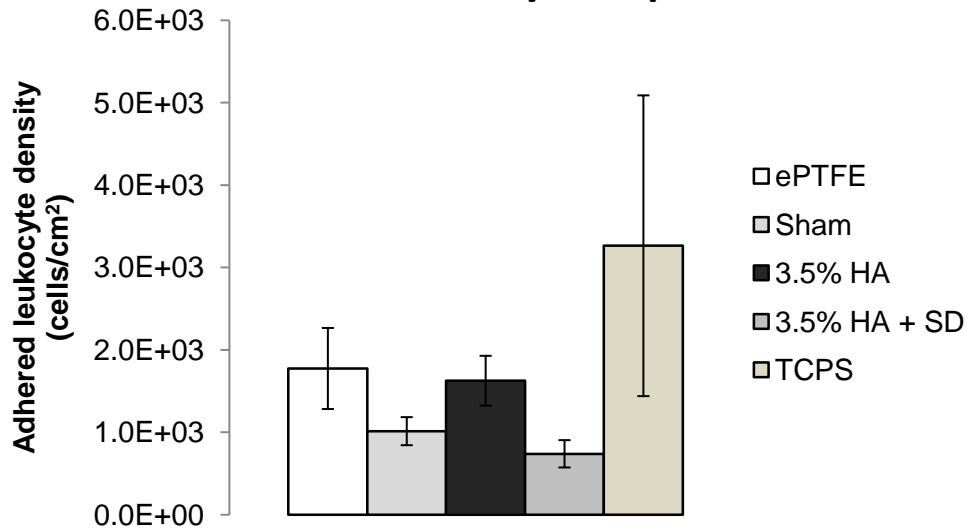
Figure 3.15: Average total cell counts per area for ePTFE, a sham control, 1.5% HA, 2.5% HA, 3.5% HA, 2.5% HA + SD, 3.5% HA + SD, and TCPS surfaces stained with DAPI for platelet population II. Statistical analysis shows no statistically significant differences between surfaces. Error bars represent standard error.

RHO: Total Cell Count Population II

Figure 3.16: Average total cell counts per area for ePTFE, a sham control, 1.5% HA, 2.5% HA, 3.5% HA, 2.5% HA + SD, 3.5% HA + SD, and TCPS surfaces stained with RHO for platelet population II. Groups that do not share a symbol are significantly different. Error bars represent standard error.

3.3.4 MTT Cell Viability Assay

The viability of platelets was indirectly measured using a MTT Cell Viability Assay. Viable cells enzymatically convert tetrazolium dye to formazan through cellular metabolic activity [15]. Absorbance of the purple formazan was determined using a spectrophotometer. Formazan was dissolved using an SDS solution for colorimetric absorbance measurement and quantification at a wavelength of 570nm. The absorbance of formazan corresponds to the amount of metabolic activity, which correlates to the number of adhered platelets.

Results indicate that there are no statistically significant differences between treatment groups within platelet population I, as shown in Figure 3.17. However, platelet population II indicates that the ePTFE and sham control groups have a statistically significant difference from the 3.5% HA, 3.5% HA + SD, and TCPS treatment groups, as shown in Figure 3.18. There is an additional statistical difference between the 3.5% HA + SD treatment group and the 3.5% HA and TCPS treatment groups. This indicates that the 3.5% HA + SD sample has the most metabolic activity, followed by the 3.5% HA and TCPS samples, followed by ePTFE and the sham control. These results correlate with calcein-AM, DAPI, and RHO results because the most cells were observed on the surface dipped sample, and the lowest number of cells was observed on the ePTFE samples. The sham control had a lower adherent cell density than the HA treated samples and TCPS control. Samples containing HA are no more cytotoxic to blood plasma than ePTFE.

MTT: Platelet Population One
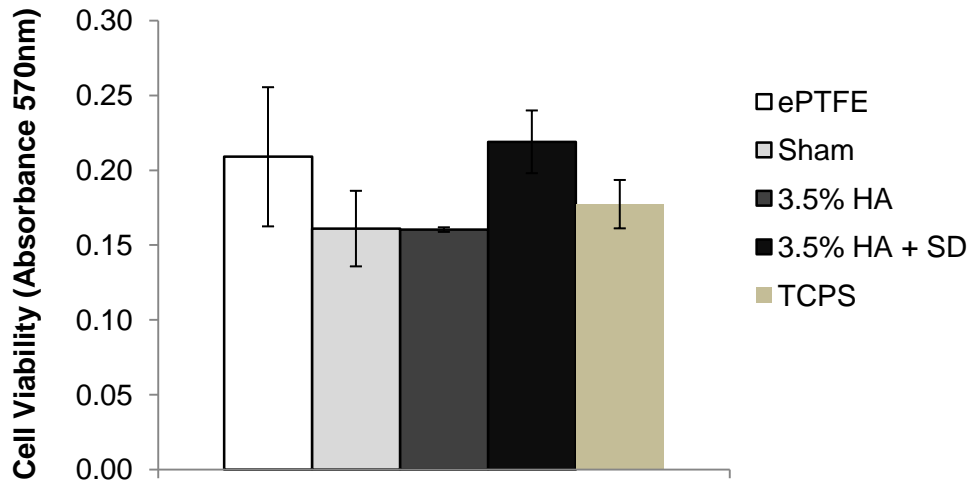
Figure 3.17: MTT absorbance as an indirect measurement of cell viability on ePTFE, the sham control, 3.5% HA, 3.5% HA + SD, and TCPS surfaces from platelet population I. Statistical analysis shows no statistically significant differences between surfaces. Error bars represent standard error.
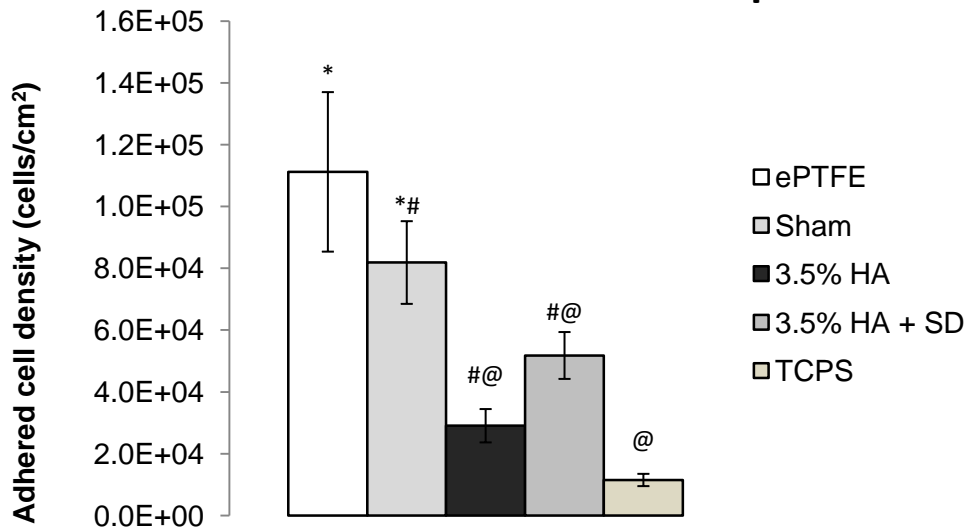
MTT: Platelet Population Two
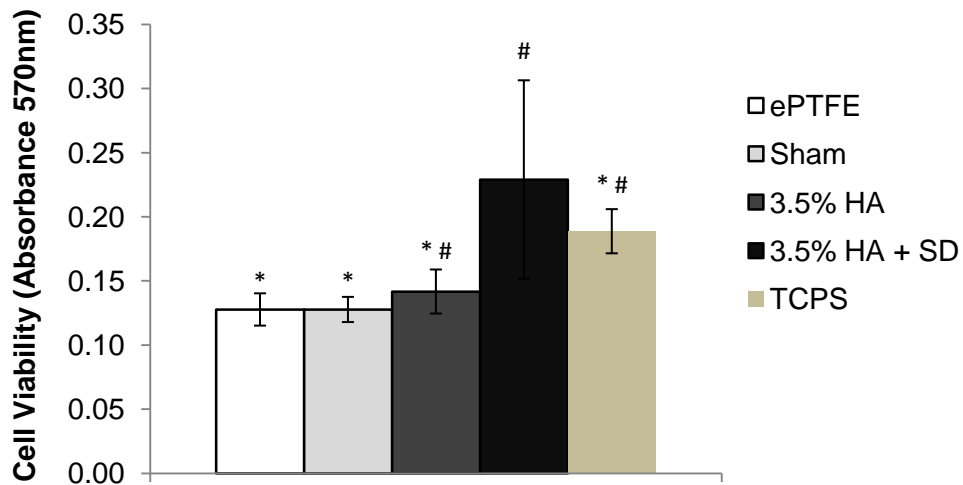
Figure 3.18: MTT absorbance as an indirect measurement of cell viability on ePTFE, the sham control, 3.5% HA, 3.5% HA + SD, and TCPS surfaces from platelet population II. Groups that do not share a symbol are significantly different. Error bars represent standard error.

3.3.5 Whole Blood Clotting Kinetics

The presence of a blood clot on a material implant can lead to the formation of an embolism or cause an immune reaction. [5] Whole blood clotting kinetics were measured at 15, 20, and 60 minutes to compare lysis of erythrocytes between ePTFE, sham, 3.5% HA, 3.5% HA + SD, and TCPS samples. Upon cell lysis, red blood cells release hemoglobin. The absorbance of free hemoglobin was used as a measurement of cell lysis. As seen in Figure 3.19 and Figure 3.20, there are no statistically significant differences in the amount of free hemoglobin between treatment groups at any time point. SEM images of the blood clot at 60 minutes are shown in Figure 3.21 and show that there are still erythrocytes present on the 3.5% HA and 3.5% HA + SD samples but not on the sham or the ePTFE samples. This could indicate that surfaces with HA had cellular adhesion but caused less cell lysis than surfaces without HA. This also correlates with the quantitative hemolysis data, where the 3.5% HA + SD treatment group had the lowest rate of hemolysis.
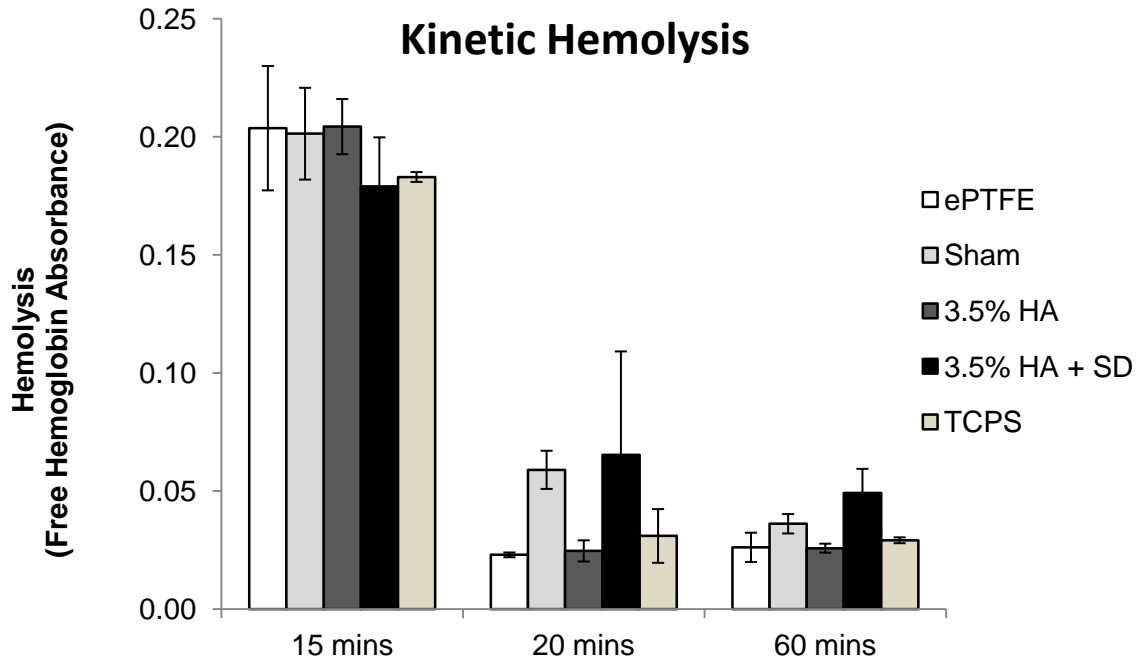
Figure 3.19: Clotting resistance kinetics as measured by the absorbance of free hemoglobin for donor population I. Statistical analysis shows no statistically significant differences between surfaces. Error bars represent standard error.
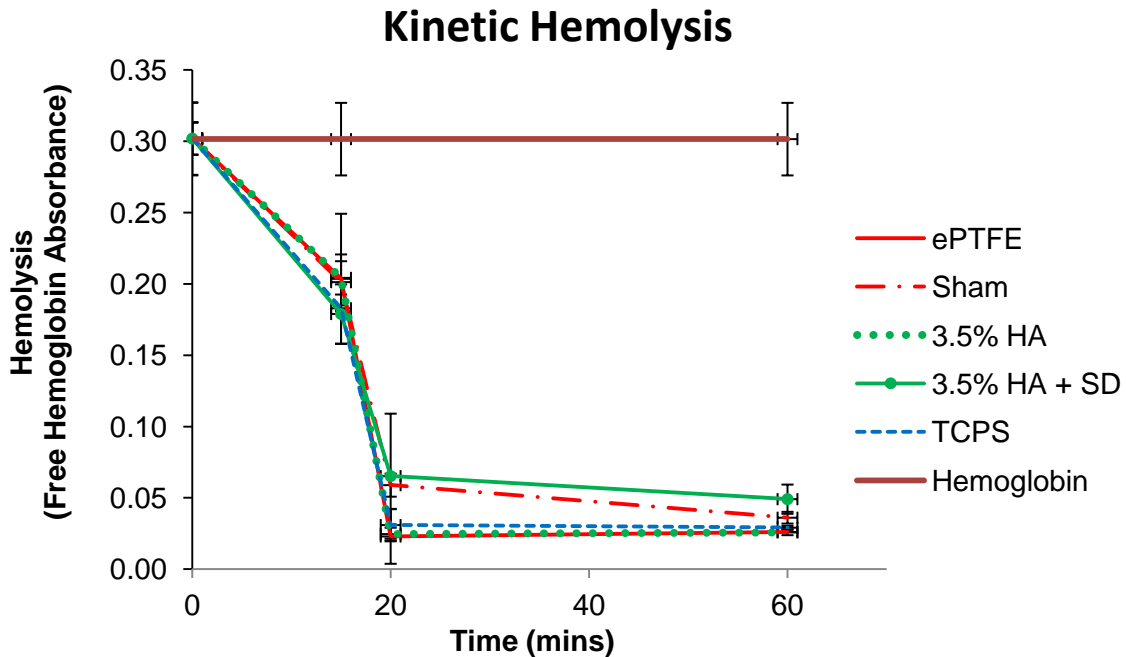
Figure 3.20: Clotting resistance kinetics as measured by the absorbance of free hemoglobin for donor population I. Statistical analysis shows no statistically significant differences between surfaces. Error bars represent standard error.
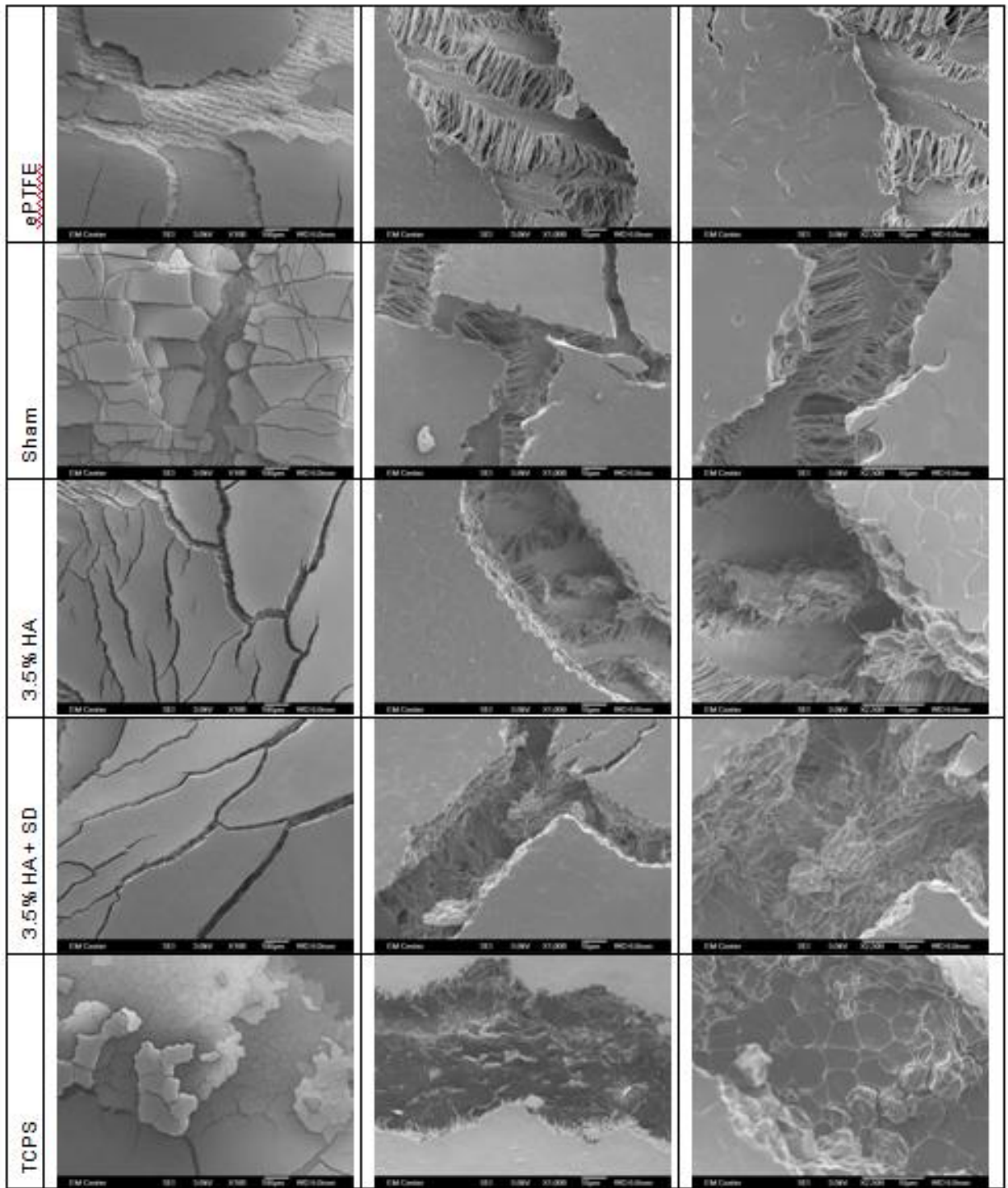
Figure 3.21: SEM images (100x, 1,000x, and 2,500x magnification) for ePTFE, a sham control, 3.5% HA, 3.5% HA + SD, and TCPS surfaces for whole blood clotting resistance.

3.4 Conclusions

The thrombogenic effects of ePTFE materials have been evaluated for use in small diameter vascular grafts. A decrease in thrombogenic potential of ePTFE could lead to higher patency rates of synthetic small diameter vascular grafts. Results do not indicate a definite decrease in the thrombogenic potential of ePTFE materials prepared with HA, but perhaps the selection of a different swelling solvent to prevent surface roughening and chemical stress relaxation of the ePTFE, as well as a higher percent composition of HA within ePTFE materials, has the potential of reducing ePTFE thrombogenicity.

A hemocompatibility screen was performed to determine which HA swelling solution concentration to use for additional hemocompatibility testing and mechanical property testing described in Chapter 4. Differences were observed in adhered platelet density between treatment groups, where the 3.5% HA group had a lower adherent cell density than the 1.5% HA and 2.5% HA groups for both platelet populations. The 3.5% HA treatment group also consistently had a higher weight percent HA than the 1.5% HA and 2.5% HA treatment groups as determined by TGA. The 3.5% HA swelling solution concentration was therefore selected for the remainder of testing.

Platelet and leukocyte adhesion as evaluated by fluorescence microscopy and ImageJ software increased on surfaces modified with HA. SEM does not indicate an increase in platelet activation or platelet-leukocyte complex formation on surfaces, however. The MTT assay results are in agreement with fluorescence staining, indicating that surfaces are not cytotoxic and that there is more metabolic activity and a larger number of cells on surfaces with HA. Hemolysis results show no significant difference in clotting kinetics between treatment groups. However, the 3.5% HA + SD group had the lowest rate of cell lysis of all groups tested, and erythrocytes

111

were observed on 3.5% HA + SD and 3.5% + HA surfaces but not on the sham or ePTFE. This may indicate that while more cells adhere to surfaces with HA, there may be less activation and hemolysis.

REFERENCES

[1]   Smith, B.S.; Popat, K.C. Titania nanotube arrays as interfaces for blood-contacting implantable devices: a study evaluating the nanotopography-associated activation and expression of blood plasma components. *J. Biomed. Nanotechnol* **2012,** 8, 642–658.

[2]   Leszczak, V.; Smith, B.S.; Popat, K.C. Hemocompatibility of polymeric nanostructured surfaces. *J. Biomater. Sci. Polym. Ed.* **2013,** 24, 1529–1548.

[3]   Zhang, M. Surface Modification of Ultra High Molecular Weight Polyethylene With Hyaluronan For Total Joint Replacement Application. Ph.D. Dissertation, Colorado State University, Fort Collins, CO, 2005.

[4]   Roach, P.; Farrar, D.; Perry, C.C. Interpretation of Protein Adsorption: Surface-Induced Conformational Changes. *J. Am. Chem. Soc.* **2005,** 127, 8168–8173.

[5]   Smith, B. Titania Nanotube Arrays: Interfaces for Implantable Devices. Colorado State University, Fort Collins, CO, 2012.

[6]   Micro BCA (TM) Protein Assay Kit. Thermo Scientific. http://www.fishersci.com/ecomm/servlet/itemdetail?catnum=PI23235&storeId=10652 (accessed 2014).

[7]   Vybrant(R) MTT Cell Proliferation Assay Kit. Life Technologies. http://www.lifetechnologies.com/us/en/home/references/protocols/cell-culture/mtt-assay-protocol/vybrant-mtt-cell-proliferation-assay-kit.html (accessed 2014).

[8]   Dean IV, H. Development of BioPoly(R) Materials for use in Prosthetic Heart Valve Replacements. M.S. Thesis, Colorado State University, Fort Collins, CO, 2012.

[9]   Sivaraman, B.; Latour, R.A. The relationship between platelet adhesion on surfaces and the structure versus the amount of adsorbed fibrinogen. *Biomaterials* **2010,** 31, 832–839.

[10] Sivaraman, B.; Fears, K.P.; Latour, R.A. Investigation of the Effects of Surface Chemistry and Solution Concentration on the Conformation of Adsorbed Proteins Using an Improved Circular Dichroism Method. *Langmuir* **2009,** 25, 3050–3056.

[11] He, X.M.; Carter, D.C. Atomic structure and chemistry of human serum albumin. *Nature* **1992,** 358, 209–215.

[12] Wertz, C.F.; Santore, M.M. Fibrinogen Adsorption on Hydrophilic and Hydrophobic Surfaces: Geometrical and Energetic Aspects of Interfacial Relaxations. *Langmuir* **2002,** 18, 706–715.

[13] Buijs, J.; W. van den Berg, P.A.; Lichtenbelt, J.W.T.; Norde, W.; Lyklema, J. Adsorption Dynamics of IgG and Its F(ab′)2and Fc Fragments Studied by Reflectometry. *J. Colloid Interface Sci.***1996,** 178, 594–605.

[14] Buijs, J.; White, D.D.; Norde, W. The effect of adsorption on the antigen binding by IgG and its F(ab′)2 fragments. *Colloids Surf. B Biointerfaces* **1997,** 8, 239–249.

[15] Cell Viability and Proliferation. *Sigma-Aldrich*. http://www.sigmaaldrich.com/technical-documents/articles/biofiles/cell-viability-and-proliferation.html. (accessed Apr 7, 2014).

CHAPTER 4: MECHANICAL PROPERTIES AND DURABILITY

4.1 Introduction

Mechanical properties of vascular grafts are important for the functionality and patency of the graft *in* vivo. Matching mechanical properties of the graft to those of the natural artery it replaces can reduce or prevent the formation of intimal hyperplasia. Graft tensile properties, including UTS and elastic modulus, as well as graft compliance were determined for ePTFE, sham, 3.5% HA, and 3.5% HA + SD samples. The water entry pressure for these treatment groups was also determined to evaluate whether tubes would leak under pressurized flow conditions. Additionally, the durability of HA when crosslinked to form a microcomposite with ePTFE was evaluated qualitatively through enzymatic degradation by hyaluronidase. The stability of HA is important for any long term hemocompatibility benefits that the HA may confer.

Vascular graft compliance is the degree of elastic expansion and contraction in the circumferential direction during pulsatile pressure. [1] A goal regarding graft compliance in the design of a vascular graft is to match the compliance of the graft with the vessel it replaces. A mechanical mismatch in compliance can cause a change in velocity of blood flow and potentially create stagnant flow regions. Also, the discontinuity in flow occurs at the anastomosis sites, causing pulsatile stress on the arterial wall near the anastomosis sites, leading to arterial hypertrophy. These changes in blood flow result in an unfavorable physiological response. [2]

An experiment investigating the effects of graft compliance compared to vessel compliance of small diameter arteries was performed by Stewart and Lyman. Urethane grafts with a range of compliance values that were less than, equal to, and greater than the compliance

of a natural vessel were implanted in dogs. Dogs receiving grafts with low compliance had local

pulsatile stresses at the anastomotic regions and developed arterial hypertrophy severe enough to

cause early graft failure. When the graft compliance matched that of vessels, graft failure

occurred later than when the graft compliance did not match that of the natural artery. Currently,

synthetic grafts are 5-10 times less compliant than the natural vessels they replace.

The percent compliance as calculated in the Cardiovascular implants – tubular vascular

prostheses ANSI/AAMI/ISO 7198:1998/2001/(R)2010 standard is shown in Equation 1 below,

where P_1 is the low pressure, P_2 is the high pressure, R_1 is the internal radius at the low pressure,

and R_2 is the internal radius at the high pressure. Mechanical compliance of arteries, as a percent

change in diameter divided by initial diameter for a pressure range from 80-120mmHg, range 9-

15%, and compliance of vein grafts ranges from 1.5-2.0%. [2]

$$\% \ compliance = \frac{\frac{R_{P_2}(-R_{P_1})}{R_{P_1}}}{P_2 - P_1} x \ 10^4 \qquad\qquad Equation \ 1$$

4.2 Materials and Methods

4.2.1 Material Preparation and HA Concentration

Samples of ePTFE were prepared through a wicking and hydrolysis procedure as previously

described in Chapter 2. An ePTFE control that was not exposed to xylenes, HA, crosslinker, or

hydrolysis solutions was used. A sham control that underwent the swelling procedure except

without silyl HA-CTA in the swelling solution and without HMDI in the crosslinking solution

was also used to assess the effect of solvents on the ePTFE material. The 3.5% HA swelling

solution was selected for sample preparation for mechanical testing based on initial testing of

thrombogenic potential assessed from calcein-AM and SEM data. The 3.5% HA samples also

contained the highest weight percent of HA compared to samples prepared with a 1.5% HA and 2.5% HA swelling solution. The surface dip in a 1.0% aqueous HA solution was also performed on samples that were swelled in a 3.5% HA swelling solution.

4.2.2 Tensile Testing

The elastic modulus is defined as the ratio of applied stress on a material to the resultant strain in the elastic region of the quasi-static tensile test curve, and is a material property independent of the sample geometry. The maximum engineering stress, or the ultimate tensile strength, was also determined. Tensile testing of ePTFE tubes in the longitudinal and radial directions was tested to analyze changes in tensile properties of ePTFE after enhancement with HA. Three ePTFE, sham, 3.5% HA, and 3.5% HA + SD samples were tested per treatment group. An ASTM D638 Type V dogbone shape specimen punch (World of Test) was used to acquire samples used for longitudinal tensile testing. Samples were dissected longitudinally, and an arbor press was used in conjunction with the dog bone punch. Final sample length was 63.5mm with a gage width of 3.18mm and gage length of 9.53mm. Radial specimens were tested in tube form with 11mm length. Samples were soaked in PBS for at 12 hours prior to testing to hydrate the hyaluronan.

An MTS Landmark Bionix Servohydraulic Test System was used for longitudinal and radial testing. An MTS System Corporation model 662.20D-04 15 load cell (15kN) was used for both longitudinal and radial testing. This load cell was used on the bottom of the radial testing setup. Additionally, a MFG model 1210AFS-2K load cell (2000 lb) was used as the top interface for radial testing. MTS model 647.02B-22 thin film grips were used for holding tensile specimens during testing.

A preload of 1N was applied to longitudinal and radial samples prior to elongation. A Flea 3 firewire camera model FL3-FW-14S3M-C (Point Grey) and ImageJ software were used to measure sample length and gage width for longitudinal samples and inner and outer tube diameters for radial test samples. Dimensions were used to calculate longitudinal strain rate based on a sample 50mm long with a strain rate of 50mm/min in accordance with the American National Standard Cardiovasular implants – tubular vascular prostheses. [1] For radial tensile tests, the centerline diameter of each tubular sample was divided by two and multiplied by 0.2 to obtain strain rate between 50-200mm/min in accordance with the American National Standard Cardiovascular implants – tubular vascular prostheses. [1] A custom-designed sample fixture was machined for testing in the radial direction, as shown in Figure 4.2. Tubular specimens (11cm length) were placed on the fixture. Samples were elongated until failure or maximum displacement of the MTS system was reached.
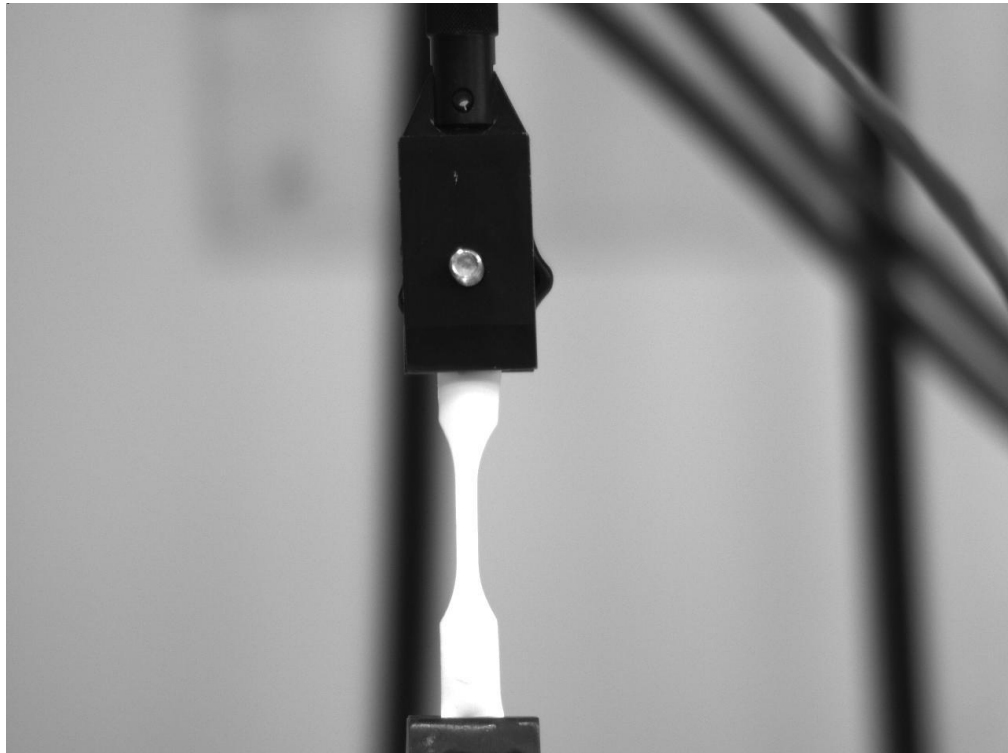
Figure 4.1: A longitudinal tensile test using an ASTM D638 Type V shape specimen.
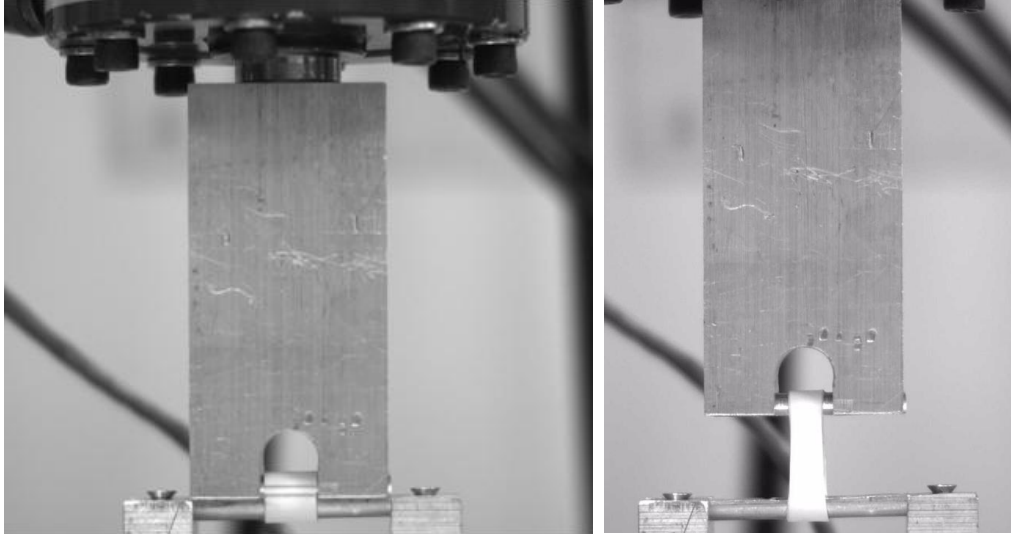
Figure 4.2: Radial tensile testing was performed using a custom machined fixture.

4.2.3 Water Entry Pressure

The water entry pressure is the pressure at which water passes from the inside of the vascular graft, through the graft wall, to the outside of the graft. The custom flow setup shown in Figure 4.3 was used to measure graft water entry pressure. The flow setup included a custom built piston to control flow and a compliance chamber. Tubular ePTFE (Bard Peripheral Vascular OEM), sham, 3.5% HA, and 3.5% HA + SD samples were cut to 9cm lengths. One sample per treatment group was tested. Tubes were placed in the flow system setup as shown in Figure 4.3. A longitudinal preload of 0.441N was applied by placing a spacer to hold tubes at a fixed strain. Samples were pressurized to 60 beats per minute using a custom built piston and water at room temperature. A linear actuator (Linmot) was used to activate the piston. A high speed camera model SA3 (Photron Fastcam) was used for imaging. Samples were incrementally pressurized using tap water and the same system design as used to test graft compliance. Water pressure inside the tubes was gradually increased until water was observed on the outside of the graft surface. The pressure at which water was observed was recorded as the water entry pressure. [1]

119
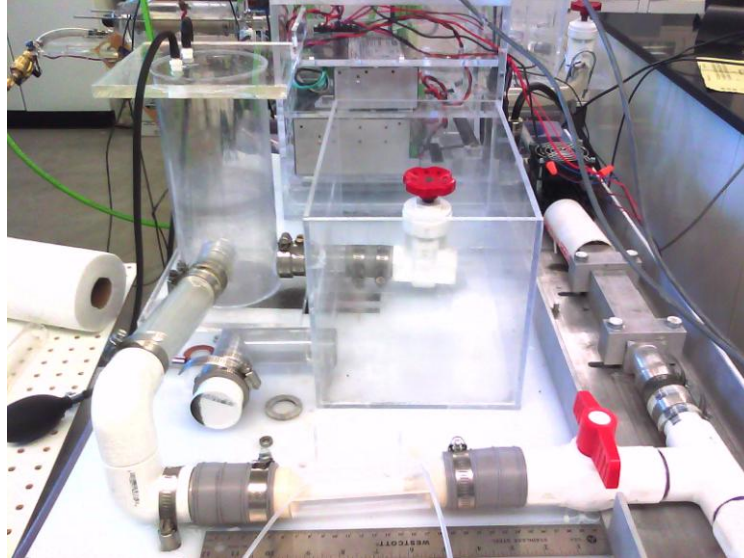
Figure 4.3: Custom flow system used for water entry pressure testing.

4.2.4 Degradation of HA by Hyaluronidase Enzyme Solution

Enzymatic degradation of HA on ePTFE surfaces was qualitatively assessed using a toluidine blue o stain (TBO, Sigma Aldrich). Samples were soaked in a hyaluronidase in PBS solution (150 units/ml) for 0, 1, and 7 days and imaged to determine whether there was a visible change in the amount of TBO, and therefore HA, between the three time points.

Samples (ePTFE, the sham control, 3.5% HA, and 3.5% HA + SD) were obtained using sterile biopsy punches (8mm diameter), sterilized in 70% ethanol for 10 mins followed by exposure to UV light for 30 mins, rinsed twice with PBS, and soaked in PBS for at least 12 hours. The PBS was removed, and 5ml of the 150units/ml enzyme solution was transferred to each tube for day 1 and day 7. Centrifuge tubes containing the samples and enzyme solution were placed in a 37°C water bath for the designated amounts of time. At days 1 and 7, samples were removed from the enzyme solutions, rinsed with DI H_2O, rinsed with 70% ethanol, placed in a 0.1% TBO solution in 8M urea for 10 minutes, and rinsed with DI H_2O until TBO stain was

no longer visibly removed. Samples were then air dried and stored in a vacuum dessicator until photographed.

To check whether the enzyme was active throughout the three time points, the 10ml of enzyme solution was additionally placed in the 37°C water bath alongside the samples. A fresh 0.1% HA solution in DI H_2O was prepared in a sterile centrifuge tube and inverted and vortexed to dissolve on days 0 and 7. The enzyme and aqueous HA solution were combined in a 1:1 volume ratio, mixed using a vortexer, and placed in a 37°C water bath for 30 minutes. The viscosity of the combined enzyme/HA solution and of the HA solution only was measured using a VISCOLAB 4000 viscometer and 1-20cp spindle (Cambridge Viscosity). A decrease in viscosity indicates a decrease in molecular weight of the HA and that the enzyme is active.

4.2.5 Statistical Analysis

Quantitative results were analyzed using Minitab software with a one-way analysis of variance (ANOVA) with a statistical significance level of $p<0.05$.

4.3 Results and Discussion

4.3.1 Tensile Testing

The measured ultimate tensile strength and elastic modulus in the longitudinal direction for ePTFE, the sham, 3.5% HA, and 3.5% HA + SD samples are shown in Figure 4.4, and stress-strain graphs are shown in Figures 7-10. The longitudinal tensile strength of ePTFE specified by the manufacturer, Bard Peripheral Vascular OEM), is greater than or equal to 600gF/mm^2, or 5.8 MPa. The average measured value and standard deviation of the longitudinal ultimate tensile strength of ePTFE was 21.09 ± 1.21 MPa. While these values of UTS are similar, there could be a discrepancy between test methods, such as a difference in strain rate, which could result in such a difference. The specification also states greater than or equal to, and the measured values are

greater than the longitudinal UTS specification. Comparisons are made between sample groups tested using the same methods. A longitudinal elastic modulus specification is not known.

The measured ultimate tensile strength and elastic modulus in the radial direction for ePTFE, the sham, 3.5% HA, and 3.5% HA + SD samples are shown in Figure 4.5 and 4.6, respectively, and stress-strain graphs are shown in Figures 11-14. The radial tensile strength of ePTFE specified by the manufacturer, Bard Peripheral Vascular OEM), is greater than or equal to 400psi, or 2.76 MPa. The average measured value and standard deviation of the radial ultimate tensile strength of ePTFE is 1.40 ± 0.08 MPa. These numbers are quite similar despite the measured average being lower than the specification. Again, this discrepancy could be the result of differences in test methods. Comparisons are made between sample groups tested using the same methods for each group. A radial elastic modulus specification is not known.

There is no significant difference between treatment groups for the longitudinal or radial UTS. The UTS is lower in the radial direction than in the longitudinal direction. The UTS depends on fiber strength. Despite the resulting etching and stress relaxation from material exposure to xylenes, enough material remains that the UTS does not significantly change.

Significant differences in the modulus of elasticity were found for both longitudinal and radial treatment groups. In the longitudinal direction, the modulus of elasticity of ePTFE is significantly higher than of the sham, 3.5% HA, and 3.5% HA + SD samples. In the radial direction, the modulus of elasticity of the ePTFE and sham are not shown to be statistically different from each other and are both statistically different from the 3.5% HA samples. Statistical difference between the 3.5% HA + SD samples is not shown between the ePTFE and sham or the 3.5% HA samples. A decrease in elastic modulus is favorable, as ePTFE is stiffer than natural arteries. The elastic modulus of the carotid artery in humans ranges from $0.4\text{-}9\text{x}10^{6}$

dynes/cm^2. The compliance of veins is slightly higher than the compliance of the carotid artery. [2]

The decrease in longitudinal elastic modulus in samples exposed to xylenes and HA is due the alignment of channel fibers parallel to the direction of force and a loss in fiber alignment after exposure to xylenes. This also explains why the UTS is higher in the longitudinal direction than in the radial direction. The modulus of elasticity in the radial direction also decreases with exposure to HA, where xylenes and HA could act as a plasticizer, lower the glass transition temperature, alter viscoelastic properties, and thereby lower the elastic modulus. Xylenes have less of an effect in the radial than the longitudinal direction because xylenes do not have as much effect on the ridges, where there is less fiber alignment, as seen by the significant decrease in modulus from ePTFE to the sham in the longitudinal direction but not the radial direction.

The elastic modulus is also influenced by the porosity of a material as in the rule of mixtures. If ePTFE is considered a composite between air and solid Teflon, and xylene etching increases the porosity of the Teflon, then etching increases the amount of air in the composite. Air has an elastic modulus of zero, thereby decreasing the elastic modulus as the porosity increases. However, the elastic modulus in the radial direction shows a somewhat different trend, where the 3.5% HA samples have a lower modulus than the 3.5% HA + SD samples.

Additionally, there is evidence of strain hardening in both longitudinal and radial tensile testing, where increased stress is required to produce plastic deformation beyond the yield point until the ultimate tensile strength is reached at fracture.
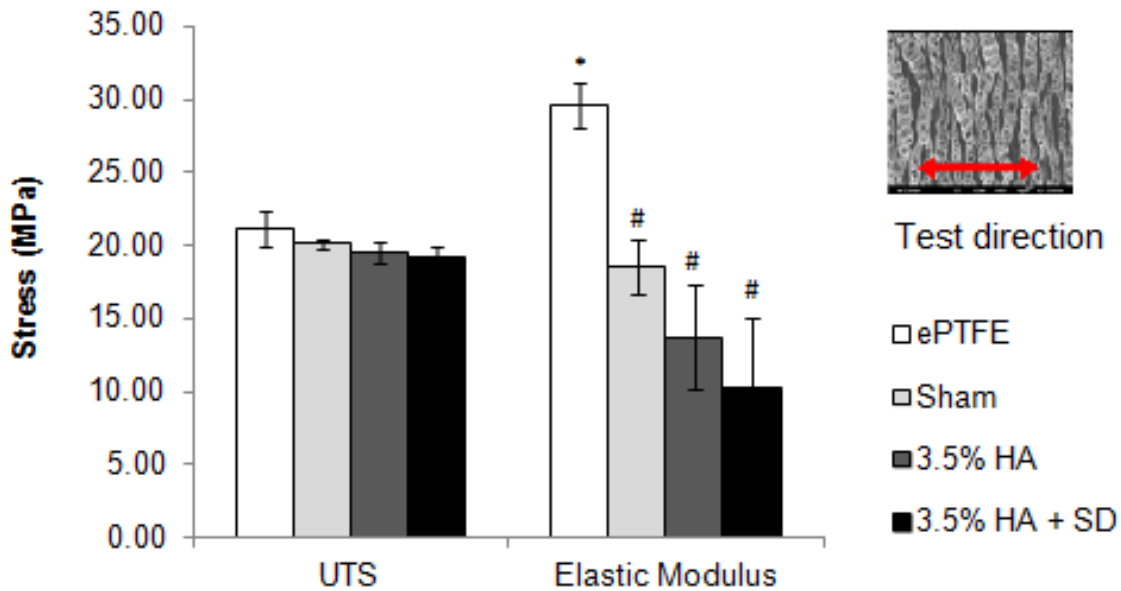
Figure 4.4: Ultimate tensile strength and modulus of elasticity in the longitudinal direction as calculated for ePTFE, the sham, 3.5% HA, and 3.5% HA + SD samples. Elastic modulus groups that do not share a symbol are significantly different. Statistical analysis shows no statistically significant differences in UTS. Error bars represent standard deviation.
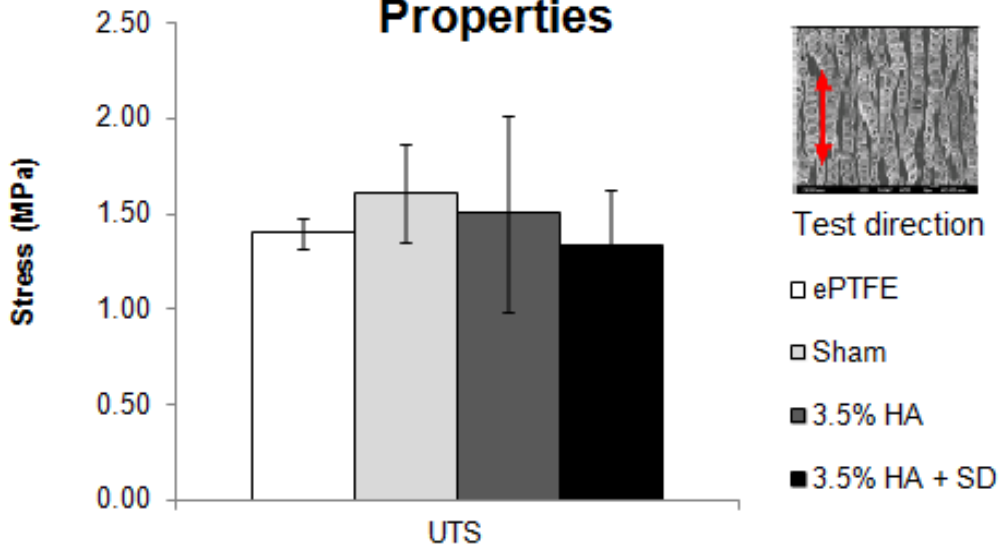
Figure 4.5: Ultimate tensile strength in the radial direction as calculated for ePTFE, the sham, 3.5% HA, and 3.5% HA + SD samples. Statistical analysis shows no statistically significant differences in UTS. Error bars represent standard deviation.
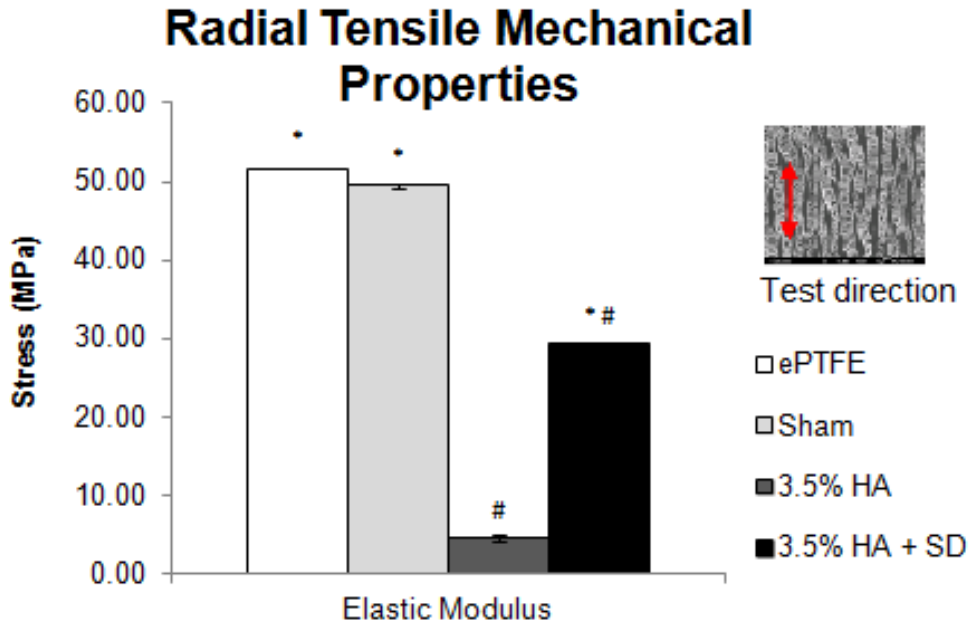
Figure 4.6: Modulus of elasticity in the radial direction as calculated for ePTFE, the sham, 3.5% HA, and 3.5% HA + SD samples. Groups that do not share a symbol are significantly different. Error bars represent standard deviation.
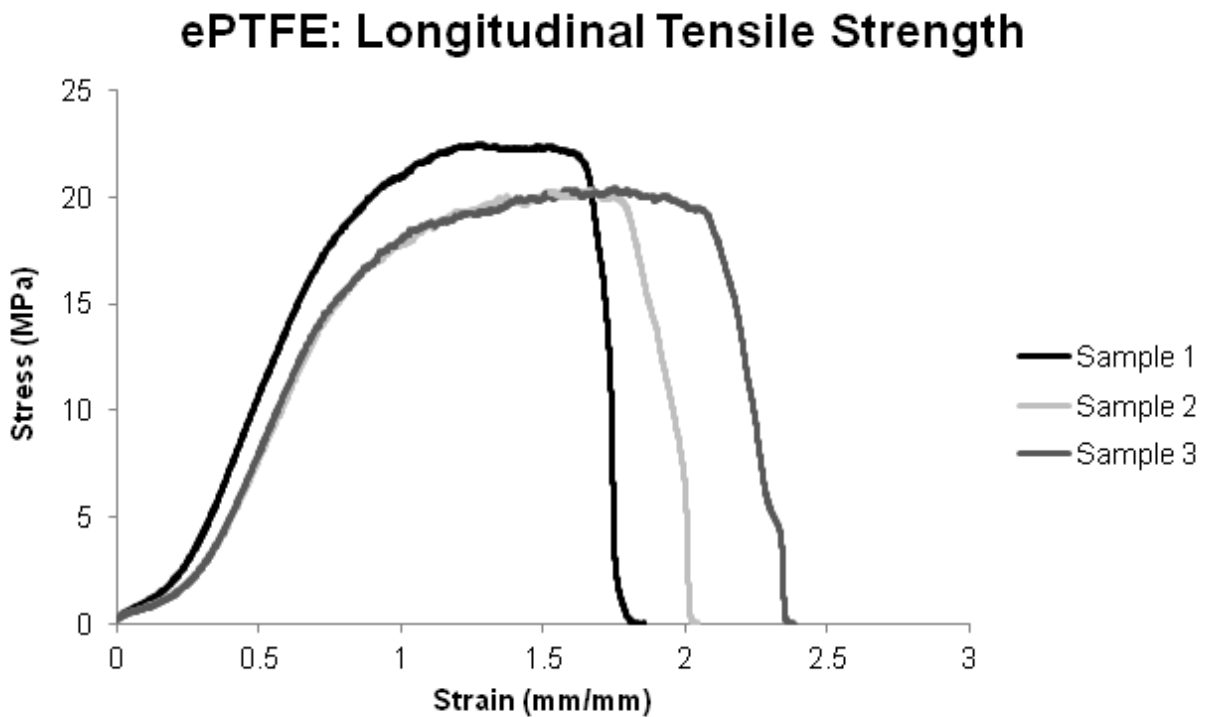
Figure 4.7: Stress-strain plots of three ePTFE control samples in the longitudinal direction.
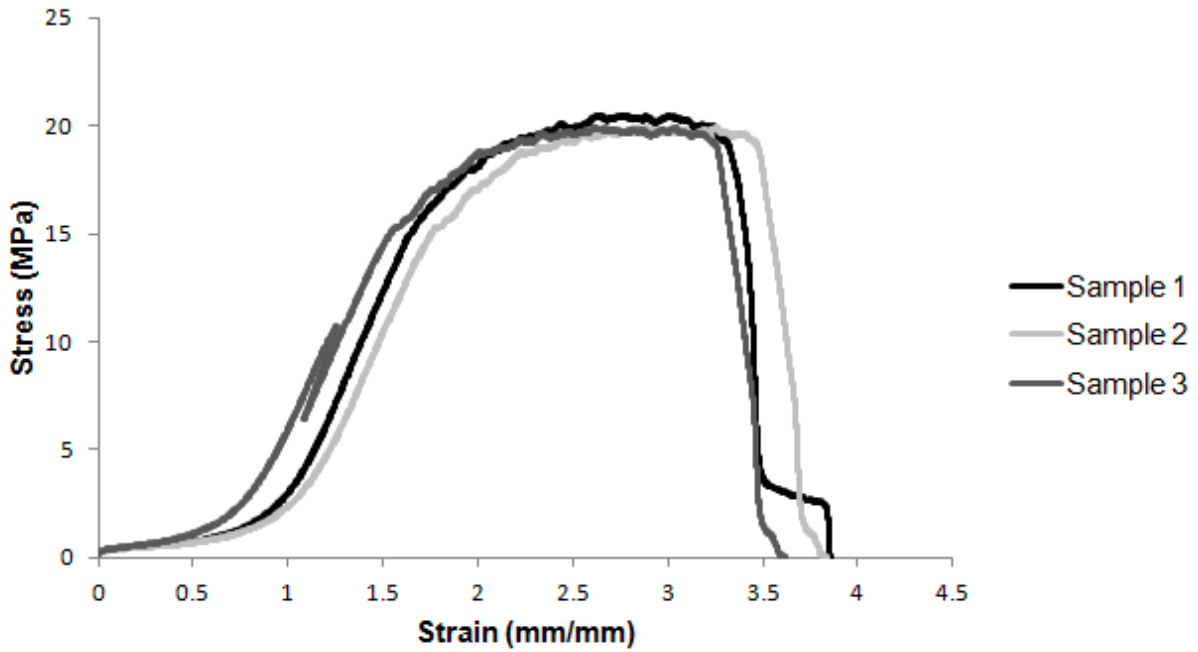
Figure 4.8: Stress-strain plots of three sham control samples in the longitudinal direction.
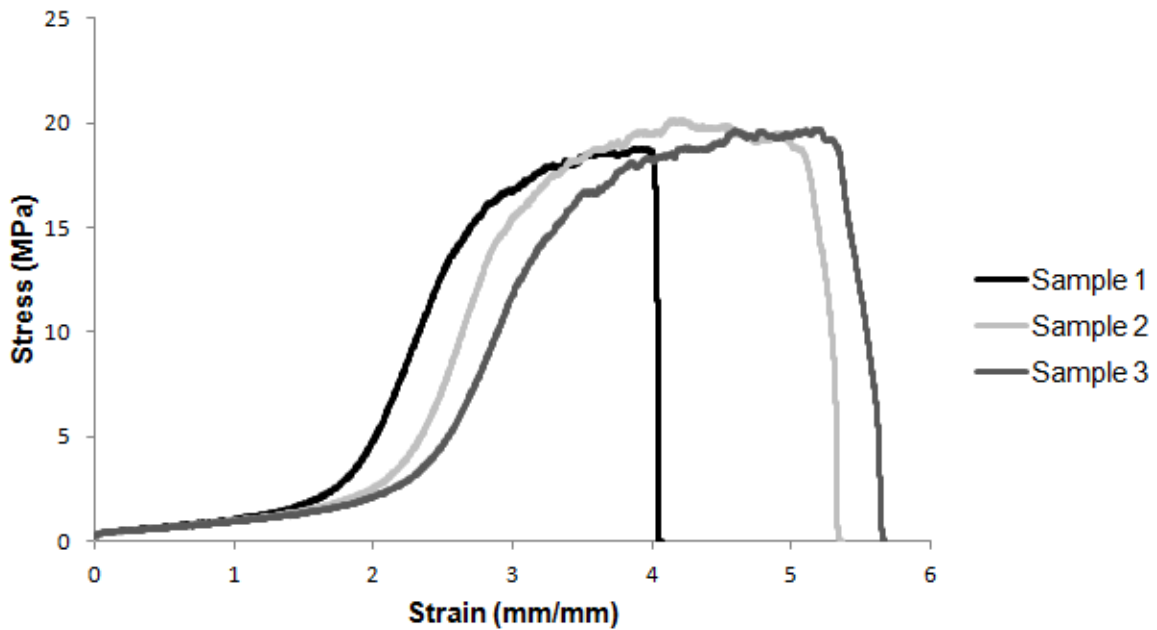
Figure 4.9: Stress-strain plots of three 3.5% HA samples in the longitudinal direction.

126
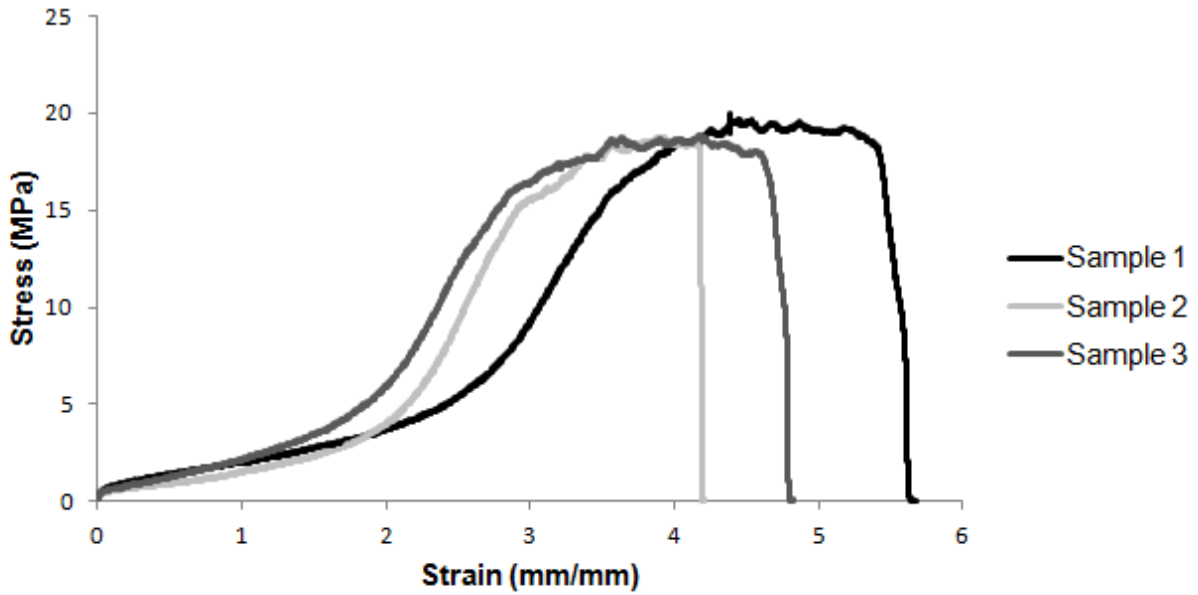
Figure 4.10: Stress-strain plots of three 3.5% HA + SD samples in the longitudinal direction.
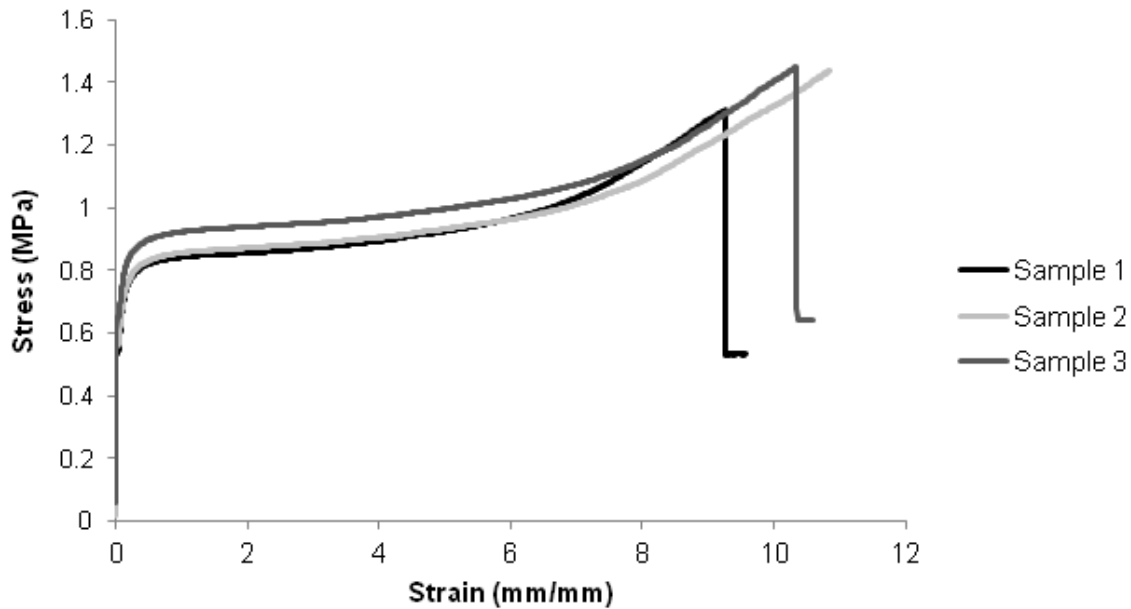
Figure 4.11: Stress-strain plots of three ePTFE control samples in the radial direction.

127
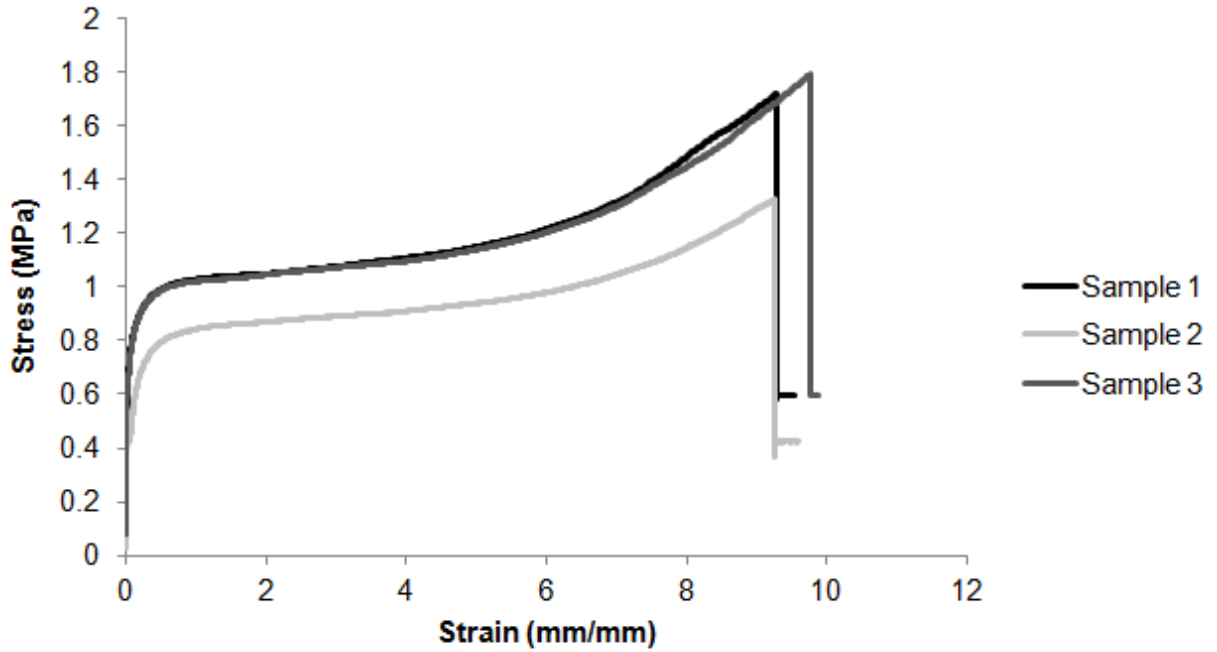
Figure 4.12: Stress-strain plots of three sham control samples in the radial direction.

Figure 4.13: Stress-strain plots of three 3.5% HA samples in the radial direction.

3.5% HA + SD: Radial Tensile Strength
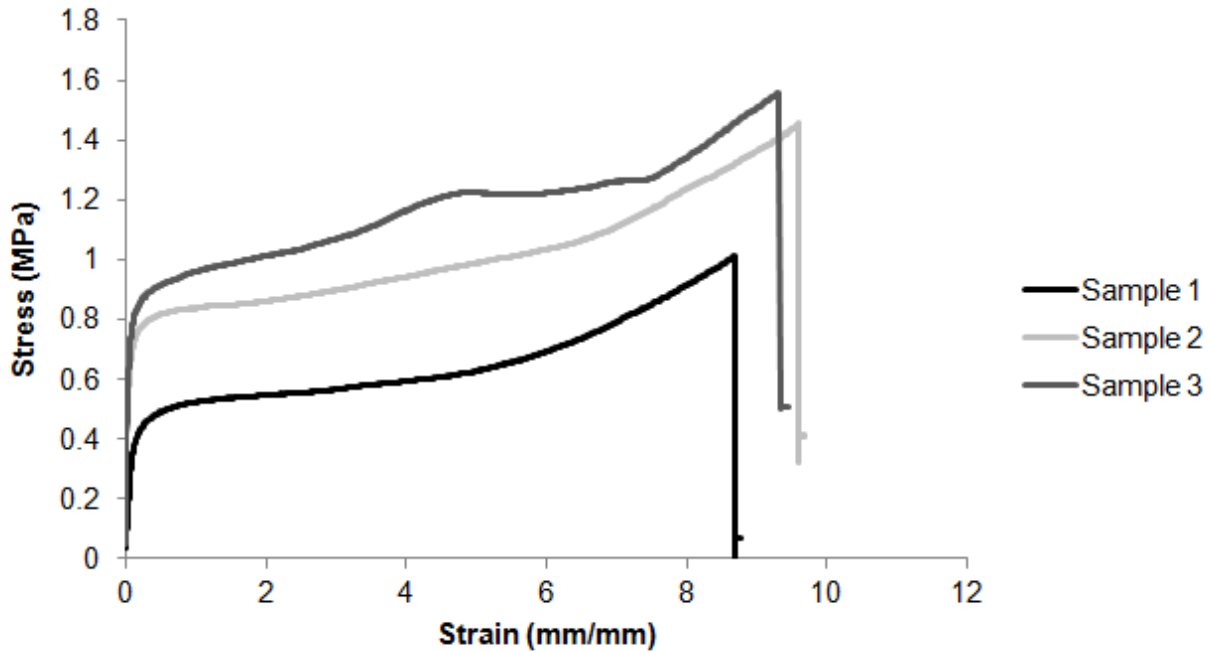
Figure 4.14: Stress-strain plots of three 3.5% HA + SD samples in the radial direction.

4.3.2 Water Entry Pressure

To prevent leakage of blood through the wall of a vascular graft, it is important for the water entry pressure to be higher than expected blood pressures. The water entry pressure of ePTFE as specified by the manufacturer, Bard Peripheral Vascular OEM, is greater than or equal to 3.5psi, or 181mmHg. When pressurized to 300mmHg, no water was observed on the outside wall of the ePTFE control graft. Water was observed on the outside of the sham control graft beginning above 240mmHg. The 3.5% HA and 3.5% HA + SD tubes began to leak between 240-260mmHg and 260mmHg, respectively. The 3.5% HA sample developed larger leaks around 280mmHg and tended to leak water droplets around the circumference of the tube, as shown in Figure 4.15. The 3.5% HA + SD sample exhibited water leakage more uniformly across the longitudinal length of the graft, as shown in Figure 4.16. This is due to the ePTFE

129

morphology where the fibrous channels are oriented parallel to the circumferential direction. Also, after a tube leaked once at these relatively high pressures, the tube would continue to leak after reducing pressure to approximately 30mmHg. No leaking was observed until pressurized above the specification of 181mmHg.

No leaking was observed for the ePTFE sample, while leaking was observed for samples exposed to xylenes and HA. As the sham exhibited the lowest water entry pressure, chemical etching from xylenes, and contained no HA, it can be concluded that the increase in porosity enabled water to pass through the graft wall at a lower pressure than untreated ePTFE. The 3.5% HA and 3.5% HA + SD samples contained HA to partially fill in pores, decreasing the water transfer through the graft wall. The 3.5% HA + SD sample has a higher water entry pressure than the 3.5% HA sample because it contained more HA.
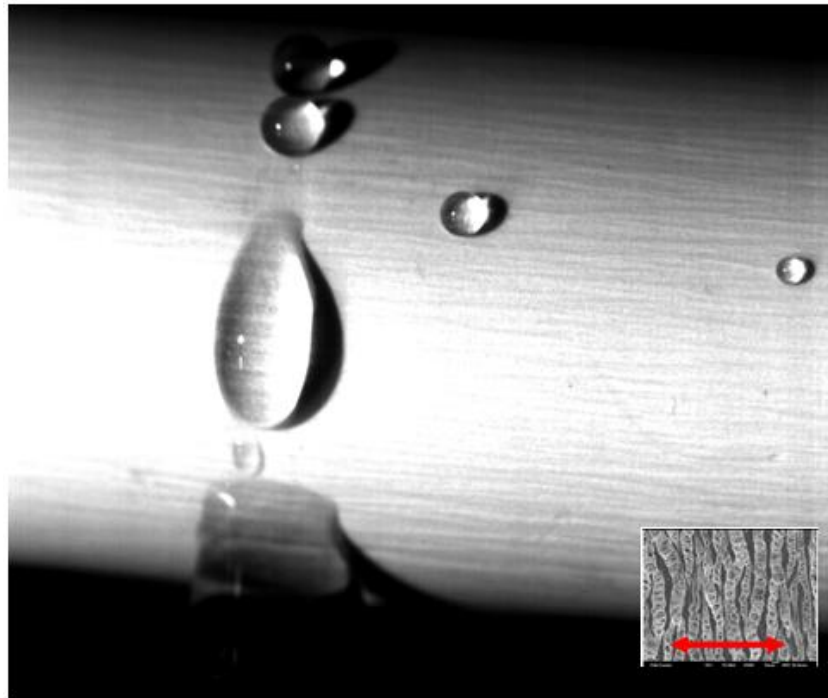
Figure 4.15: Water droplets were observed on the 3.5% HA ePTFE tube when pressurized to approximately 240-260mmHg.
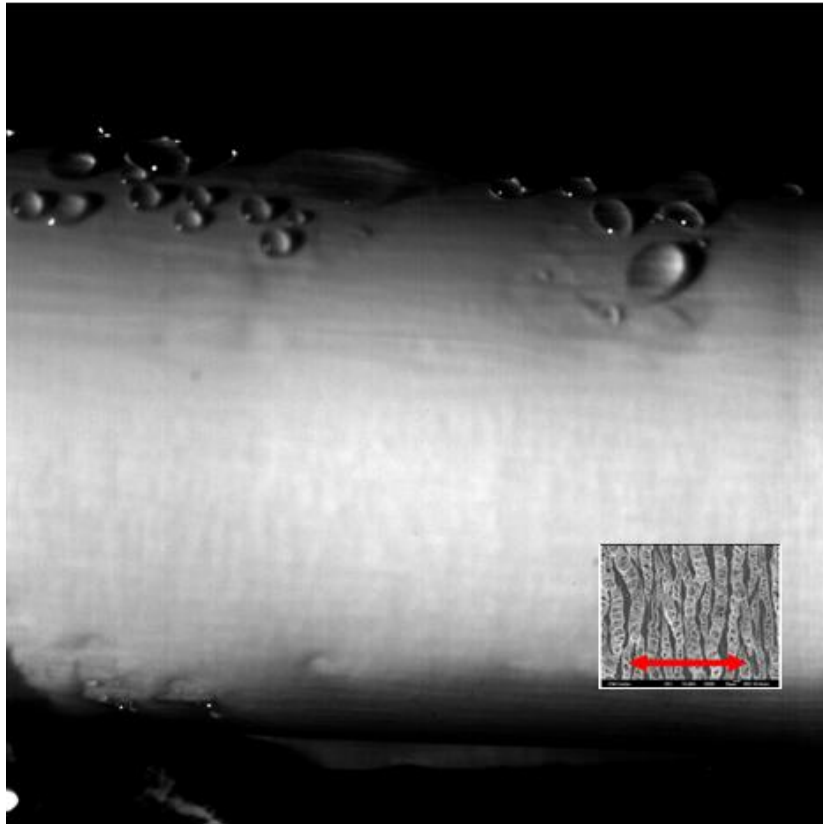
Figure 4.16: Water droplets were observed on the 3.5% HA + SD ePTFE tube when pressurized to approximately 260mmHg.

4.3.3 Degradation of HA by Hyaluronidase Enzyme

TBO is a cationic dye that binds to negatively charged carboxyl groups. A purple color change indicates binding of the dye. [3] HA is a negatively charged glycosaminoglycan with carboxyl groups. The control ePTFE is composed of carbon and fluorine only. There is minimal white to purple color change on the ePTFE and sham controls. Staining of ePTFE and the sham controls is consistent between the three time points. The color present is likely due to contamination from tweezers used to transfer samples between solutions. The 3.5% HA and 3.5% HA + SD samples have a distinct purple color change compared to the ePTFE and sham controls. No differences between the 3.5% HA and 3.5% HA + SD samples are observed at the same time point. Based on the purple color, there does not appear to be a decrease in the amount

131

of surface HA between days 0, 1, or 7 for either treatment group. Due to the difficulty in removing TBO from the pores of ePTFE and high amount of bound TBO, a quantitative evaluation was not performed. The enzyme was active throughout the experiment, as evidenced by the decrease in viscosity of HA when exposed to the enzyme solution. Based on this data, HA appears to be present in the same surface quantity for all time points within treatment group, and it can be inferred that the HA is not degrading. The crosslinked HA appears to be stable against enzymatic degradation when exposed to solutions of hyaluronidase at concentrations 60 times higher than those found in human blood serum [4], [5].
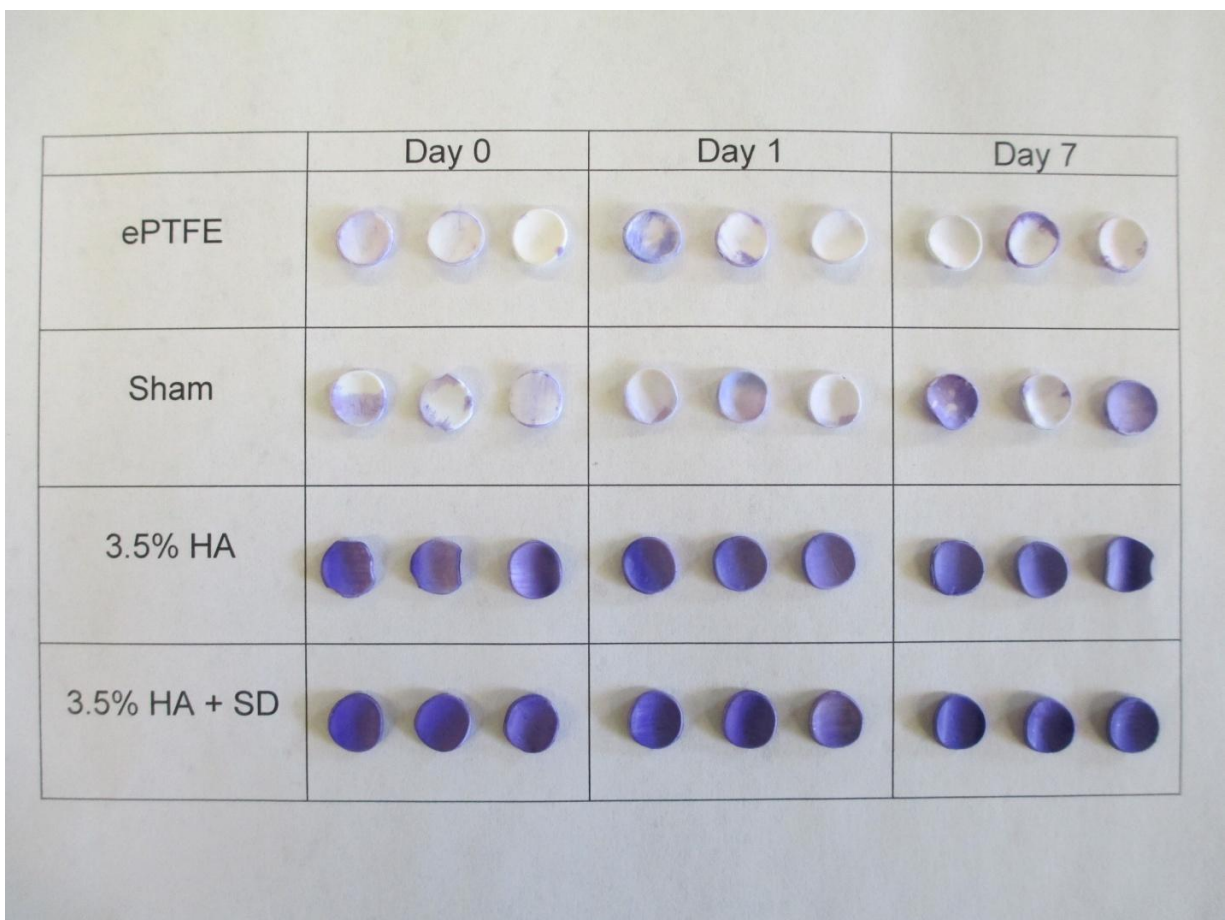
Figure 4.17: Samples (ePTFE, sham, 3.5% HA, and 3.5% HA + SD) stained with TBO at days 0, 1, and 7.

4.4 Conclusions

Tensile testing in the longitudinal and radial directions was performed, and UTS and elastic modulus were determined. Data shows no significant differences in UTS between treatment groups. The radial UTS is lower than the longitudinal UTS. Significant differences in elastic modulus values were identified. Longitudinally, the ePTFE has a significantly higher elastic modulus than the sham, 3.5% HA, and 3.5% HA + SD samples. Radially, the ePTFE and sham are not statistically different from each other and are both statistically different from the 3.5% HA samples. The 3.5% HA + SD samples are not significantly different from either group. The elastic modulus decreases longitudinally with exposure to xylenes and further decreases with increased HA composition as the xylenes and HA act as plasticizers and lower the glass transition temperature. Chemical etching has less impact on the radial sham compared to the ePTFE because the fibers within the fibrous channels are parallel to the longitudinal test direction.

Water entry pressure was tested on ePTFE, sham, 3.5% HA, and 3.5% HA tubes by pressurizing the lumen of the graft with water until leaking was observed. No leakage was observed on ePTFE. The sham had the lowest water entry pressure, followed by the 3.5% HA sample, with the 3.5% HA having the largest measured water entry pressure. This is likely the result of chemical etching in the sham control. The 3.5% HA sample had some increased resistance to leaking compared to the sham due to the presence of HA in pores. The 3.5% HA + SD sample had a higher composition HA and increased resistance to water leakage through the graft walls. All samples had a water entry pressure greater than 181mmHg, indicating that none of the treatment groups should exhibit leakage *in vivo*.

Enzymatic degradation was qualitatively tested using a TBO stain. No HA degradation was observed between the time points 0, 1, and 7 days. Results indicate that the HA was effectively crosslinked and not susceptible to enxymatic degradation. This is important for long term stability of HA in a vascular graft implanted *in vivo*.

REFERENCES

[1]   Cardiovascular implants - Tubular vascular prostheses. Association for the Advancement of Medical Instrumentation. (accessed 2011).

[2]   Roeder, R.A.; Lantz, G.C.; Geddes, L.A. Mechanical remodeling of small-intestine submucosa small-diameter vascular grafts: A preliminary report. *Biomed. Instrum. Technol.,* 35, 110–120.

[3]   Hoshi, R.A.; Van Lith, R.; Jen, M.C.; Allen, J.B.; Lapidos, K.A.; Ameer. The blood and vascular cell compatibility of heparin-modified ePTFE vascular grafts. *Biomaterials* **2013,** 34, 30–41.

[4]   Zhang, M. Surface Modification of Ultra High Molecular Weight Polyethylene With Hyaluronan For Total Joint Replacement Application. Ph.D. Dissertation, Colorado State University, Fort Collins, CO, 2005.

[5]   Lowry, K.M.; Beavers, E.M. Resistance of hyaluronate coatings to hyaluronidase. *J. Biomed. Mater. Res.***1994,** 28, 861–864.

CHAPTER 5: RESEARCH SUMMARY, LIMITATIONS, AND FUTURE WORK

5.1 Research Summary

Tubular ePTFE samples were successfully prepared by wicking and crosslinking of silyl HA-CTA dissolved in xylenes into the pores of ePTFE materials to form a microcomposite. The silyl and CTA groups were removed through a hydrolysis procedure. Selected samples prepared with 2.5% HA and 3.5% HA solutions were additionally dipped in 1.0% HA aqueous solutions. TGA and XPS confirmed the presence of HA in ePTFE samples. TGA results indicates that the percent composition of HA increased as the silyl HA-CTA/xylenes solution concentration increased. However, variation in HA composition across the length of sample tubes likely increased variability in data, particularly the hemocompatibility data. XPS also indicates that there is more HA on sample surfaces prepared with a higher concentration of HA as evidenced by changes in atomic weight percentages. However, static contact angle goniometry results indicate little change in hydrophobicity after sample preparation with HA.

The xylenes used during the sample preparation procedure were found to change the morphology of the ePTFE materials based on surface texture parameters. In particular, SR_a and S_m parameters indicate that the sham control exposed to xylenes is rougher and has wider channels than the ePTFE that was not exposed to xylenes. The xylenes chemically etch the ePTFE material preferentially from the walls of the ridges. There is also a trend towards decreasing roughness as HA composition increases for samples without the aqueous HA dip.

A static hemocompatibility screen was performed to determine the concentration of HA used to prepare samples that exhibited the lowest number of adhered platelets. While samples prepared with HA had significantly higher platelet adhesion than the untreated ePTFE, the

samples prepared with a 3.5% HA solution had the fewest adhered platelets compared to other HA treatment groups. Therefore, the 3.5% HA and 3.5% HA + SD samples were selected for further static hemocompatibility and mechanical testing.

Further static hemocompatibility testing indicates that surfaces are not cytotoxic to cells in blood plasma. Protein adsorption results show no statistically significant differences between surfaces. Hemolysis kinetics indicate no significant difference in clotting rate between surfaces but may indicate less erythrocyte lysis on the 3.5% HA and 3.5% HA + SD surfaces. The hemolysis kinetics, together with SEM images of adhered platelets and protein adsorption, may indicate less cellular activation on surfaces prepared with HA.

The sample treatment process, as well as soaking in xylenes only, changes the mechanical properties of the ePTFE grafts. Statistical analysis showed no significant differences in ultimate tensile strength in the longitudinal or radial directions. The modulus of elasticity in the longitudinal direction was significantly higher for the ePTFE compared to other treatment groups. This is due the alignment of channel fibers parallel to the direction of force and a loss in fiber alignment after exposure to xylenes. Significant differences in elastic modulus were also observed in the radial direction, where xylenes could act as a plasticizer, lower the glass transition temperature, alter viscoelastic properties, and lower the elastic modulus. The decrease in elastic modulus is favorable for matching mechanical properties to those of natural arteries.

The water entry pressure was the highest for the ePTFE, followed by the 3.5% HA + SD, 3.5% HA, and sham samples, respectively. The pressures measured were high enough to be suitable for graft implantation. The crosslinked HA within ePTFE materials appears to be stable against enzymatic degradation.

5.2 Limitations and Future Work

5.2.1 Solvent Selection

Xylenes chemically etch ePTFE materials, increasing surface roughness, deepening

pores, and effectively increasing the surface area of materials. ePTFE materials also shorten

when soaked in xylenes due to chemical stress relaxation with less chain alignment in the fibrous

regions. While xylenes were selected based on previous success with assisting in the infiltration

of silyl HA-CTA into polyethylene materials [1]–[3] and because of the similarity in Hildebrand

solubility parameters between xylenes and ePTFE, the selection of a different solvent is

desirable. A solvent that silyl HA-CTA dissolves into that does not degrade the ePTFE could

maintain the surface morphology of the base ePTFE material to improve hemocompatibility. A

smoother surface with lower surface area has potential to more effectively reduce the

thrombogenic properties of small diameter vascular grafts.

5.2.2 Molecular Weight of HA

Hyaluronic acid with a molecular weight of 700kDa was used in this research based on

previous success with polyethylene materials. However, the molecular weight of HA used for

various applications has an effect on mechanical properties.

5.2.3 Uniformity of HA

On average, the amount of HA within ePTFE tubes increased as the swelling solution

concentration of silyl HA-CTA in xylenes increased. However, the amount of HA within a tube

varied across the length of the tube. A more consistently robust technique should be used to

ensure the homogeneous incorporation of HA within materials.

Additionally, ePTFE is more porous and has a higher surface area than linear low density

polyethylene (LLDPE) as used in prior work with heart valve leaflets. Using a material like

ePTFE that is initially less thrombogenic than LLDPE is more challenging to improve

hemocompatibility. The higher surface area of ePTFE compared to LLDPE may also increase

the adhesion of platelets within the pores of the material. Furthermore, the high surface area may

require a higher concentration of HA in the swelling solution to achieve similar surface coverage

as obtained with LLDPE using the same swelling solution concentration.

5.3 Swelling Solution Concentration and Viscosity

Previous work by Dean et al using LLDPE with 0.5%, 1.5%, and 2.5% HA swelling

solution concentrations resulted in LLDPE sample with the highest HA composition using the

1.5% HA swelling solution. The 2.5% HA swelling solution was believed to have a high

viscosity and limit the swelling of HA into the LLDPE, lowering the final HA composition. The

1.5% HA LLDPE samples were believed to have the highest HA composition swelling was not

as limited by viscosity.

The ePTFE-HA materials did not exhibit a decrease in HA composition with increasing

swelling solution concentration. ePTFE in a xylenes and silyl HA-CTA solution can be

considered a polymer solution where the viscosity depends on the concentration and size

(molecular weight) of the polymer. The viscosity of ePTFE in silyl HA-CTA and xylenes is

effectively lower than a solution without ePTFE, relative to the ePTFE. It may therefore be

possible to use a higher concentration swelling solution, such as a 10% HA solution, to further

increase the HA composition within samples without encountering a viscosity limitation.

Preparing ePTFE samples with a wider range of HA swelling solutions would be beneficial.

5.3.1 Dynamic Flow Hemocompatibility Testing

Blood plasma and whole blood studies described in this work were performed in the

static environment of polystyrene well-plates. Arteries are part of a dynamic system with

flowing blood. Pulsatile blood flow changes the shear stress and other properties that influence

cellular interactions with other cells and with material surfaces. Dynamic flow testing is needed

to more closely understand the effectiveness of ePTFE grafts as small diameter artery conduits at

reducing thrombogenicity and matching mechanical properties to natural arteries.

5.3.2 Degradation of HA with Dynamic Flow Conditions

As a polymer, HA degrades into monomers through multiple physical and chemical

mechanisms, including shear stress, heat degradation, radiation, acidic or alkaline hydrolysis,

oxidation, and enzymatic digestion. [4] A brief enzymatic degradation study was presented in

this work. However, a dynamic and quantitative test may be beneficial to understanding the long

term stability of crosslinked HA within ePTFE materials present in fluid flow conditions.

5.3.3 Endothelial and Smooth Muscle Cells

Endothelialization of the lumen of small diameter vascular grafts has been shown to play

an important role in increasing graft hemocompatibility. Further, preventing smooth muscle cell

migration from the tunica media to the tunica intima of the graft reduces plaque formation, vessel

narrowing, and intimal hyperplasia. Evaluation of endothelial cell growth and morphology under

shear stress of fluid flow [5], as well as evaluation of smooth muscle cell proliferation, is

necessary for a synthetic small diameter vascular graft. [6]–[10]

5.3.4 Viscoelastic Mechanical Properties

Solid materials may have elastic and plastic deformation. Stress applied to a fluid causes

viscous flow. Blood vessel walls have viscoelastic properties because the graft wall is naturally

elastic and the blood flow confers viscous properties. The graft compliance is a simplified

method for measuring viscoelastic properties and expresses circumferential dimension changes at various pressures. [11]

Graft compliance, depends on the graft wall thickness and inner diameter. [11] As compliance testing was performed with a large diameter (10mm) graft, changes between the ePTFE, sham, and samples prepared with HA can be determined to infer how HA alters graft compliance. Furthermore, the elastic modulus has been documented to vary nonlinearly with pressure, where the modulus has been shown to increase exponentially with increasing pressure [12].

REFERENCES

[1]   Zhang, M.; James, S.P. Silylation of hyaluronan to improve hydrophobicity and reactivity for improved processing and derivatization. *Polymer* **2005,** 46, 3639–3648.

[2]   Zhang, M. *S*urface Modification of Ultra High Molecular Weight Polyethylene With Hyaluronan For Total Joint Replacement Application. Ph.D. Dissertation, Colorado State University, Fort Collins, CO, 2005.

[3]   Dean IV, H. Development of BioPoly(R) Materials for use in Prosthetic Heart Valve Replacements. M.S. Thesis, Colorado State University, Fort Collins, CO, 2012.

[4]   Gura, E.; Hückel, M.; Müller, P.J. Specific degradation of hyaluronic acid and its rheological properties. *Polym. Degrad. Stab.* **1998,** 59, 297–302.

[5]   Effect of Shear Stress on Platelet Adhesion to Expanded Polytetrafluoroethylene. http://journals.lww.com/asaiojournal/Fulltext/2000/11000/Effect_of_Shear_Stress_on_Platelet_Adhesion_to.9.aspx. (accessed Mar 28, 2014).

[6]   Dudash, L.A.; Kligman, F.; Sarett, S.M.; Kottke-Marchant, K.; Marchant, R.E. Endothelial cell attachment and shear response on biomimetic polymer-coated vascular grafts. *J. Biomed. Mater. Res. A* **2010,** 100, 2204–2210.

[7]   Sarkar, S.; Sales, K.M.; Hamilton, G.; Seifalian, A.M. Addressing thrombogenicity in vascular graft construction. *J. Biomed. Mater. Res. B Appl. Biomater.* **2007,** 82B, 100–108.

[8]   Chlupác, J.; Filová, E.; Bacáková, L. Blood vessel replacement: 50 years of development and tissue engineering paradigms in vascular surgery. *Physiol. Res. Acad. Sci. Bohemoslov.* **2009,** 58, S119–139.

[9]   Kong, X,; Han, B.; Li, H.; Liang, Y.; Shao, K.; Liu, W. New biodegradable small-diameter artificial vascular prosthesis: A feasibility study. *J. Biomed. Mater. Res. Part A* **2012,** 100A, 1494–1504.

[10] Werner, C.; Maitz, M.F.; Sperling, C. Current strategies towards hemocompatible coatings. *J. Mater. Chem.* **2007,** 17, 3376.

[11] Salacinski, H.J.; Goldner, S.; Giudiceandrea, A.; Hamilton, G.; Seifalian, A.M.; Edwards, A.; Carson, R.J. The Mechanical Behavior of Vascular Grafts: A Review. *J. Biomater. Appl.* **2001,** 15, 241–278.

[12]   Roeder, R.A.; Lantz, G.C.; Geddes, L.A. Mechanical remodeling of small-intestine submucosa small-diameter vascular grafts: A preliminary report. *Biomed. Instrum. Technol.*, 35, 110–120.

5.1 HA-CTA COMPLEXATION

Purpose: Hydrophobic modification of hyaluronan for reaction in anhydrous solvents

Materials and Equipment
- Sodium hyaluronan (NaHA)
- Cetyltrimethylammonium bromide (CTAB)
- Fresh Deionized water (DI H_2O)
- 1000 ml beaker or flask
- 500 ml beaker or flask
- Magnetic stir bars
- Stir plates
- Freezer mill/Cryogrinder
- Liquid nitrogen
- Hyaluronan-cetyl trimethylammonium complex (HA-CTA)
- Vacuum oven
- Vapor trap
- Vacuum pump
- Thermal gloves
- Safety glasses
- Buckner funnel
- Filter paper
- Erlenmeyer flasks

Procedure
1. Prepare a 0.30% w/v solution of sodium hyaluronan in DI H_2O. Minimize large clumps when adding NaHA.
   a. Example: 1.5g NaHA in 500 ml DI H_2O
   b. Stir the reaction at room temperature until the NaHA is completely dissolved. This can take several hours depending on the molecular weight of the NaHA. Stir for 15 hours to 3 days. Parafilm the beaker.
   c. When fully dissolved, the solution is clear.
   d. To get the NaHA into solution, turn the stir bar RPMs high enough to get a vortex on the top part of the stir bar for at least 5 mins. Then, turn the RPMs down to a low setting to form a little vortex.
2. Prepare a 1.00% w/v solution of CTAB in DI H_2O.
   a. Example: 1.69 g CTAB in 169 ml DI H_2O

    b. Stir the reaction at 40°C until the CTAB is completely dissolved. When dissolved, the solution will be clear. This takes 10-15 mins.

3. Slowly add the CTAB solution to the NaHA solution while under magnetic stirring. Parafilm the beaker. The mixture will become increasingly opaque as the CTAB solution is added. When the reaction is complete, a white precipitate forms and the supernatant is clear. Varying the addition rate affects the size of the precipitate (a slower addition rate produces a smaller precipitate). Stir for 15 hours – 36 hours.

4. The precipitate is HA-CTA. Collect and wash the HA-CTA to remove excess CTAB using a Buckner funnel. Use a vapor trap on the oven.
    a. Set up a Buckner funnel to two Erlenmeyer flasks. (pic)
    b. Place filter paper on the funnel and wet it using DI H_2O.
    c. Pour the HA-CTA/DI H_2O solution into the Buckner funnel slowly to prevent HA-CTA from getting under the filter paper.
    d. Rinse the HA-CTA with 500 ml DI H_2O.
    e. Use a spatula to scrape the HA-CTA into an Erlenmeyer flask with 300 ml DI H_2O.
    f. Cover the Erlenmeyer flask with a serum stopper and shake it for 30 seconds.
    g. Pour the contents of the Erlenmeyer flask in the Buckner funnel and vacuum off the water.
    h. A second time, rinse the HA-CTA with 500 ml DI H_2O.
    i. A second time, use a spatula to scrape the HA-CTA into an Erlenmeyer flask with 300 ml DI H_2O.
    j. Cover the Erlenmeyer flask with a serum stopper and shake it for 30 seconds.
    k. Pour the contents of the Erlenmeyer flask in the Buckner funnel and vacuum off the water.
    l. A third time, rinse the HA-CTA with 500 ml DI H_2O.
    m. A third time, use a spatula to scrape the HA-CTA into an Erlenmeyer flask with 300 ml DI H_2O.
    n. Cover the Erlenmeyer flask with a serum stopper and shake it for 30 seconds.
    o. Pour the contents of the Erlenmeyer flask in the Buckner funnel and vacuum off the water.
    p. A fourth time, rinse the HA-CTA with 500 ml DI H_2O.
    q. A fifth time, rinse the HA-CTA with 500 ml DI H_2O.
    r. Move the HA-CTA to the center of the filter paper, and carefully place the filter paper inside a petri dish. Spread the HA-CTA out.
    s. Place the petri dish and filter paper in a vacuum oven to dry at 50°C for 3 days. Occasionally wipe the water off the inside of the oven door. Be sure to watch vapor traps to make sure they don't fill and are functioning correctly. <<note: combine with 5 below>>

5. Dry HA-CTA in a vacuum oven (-25 in Hg, 50°C) for 3 days or until no change in weight is observed. A yield of about 2.5 g HA-CTA is expected for a starting NaHA weight of 1.5 g.

6. Grind the dried HA-CTA to a powder using a freezer mill/cryogrinder.
    a. Wear thermal gloves and safety glasses.
    b. Slowly fill the cryogrinder with liquid nitrogen to the fill line. This typically requires about 5L of liquid nitrogen and will cool the cryogrinder down. Close the top cover and let the cryogrinder sit until vapor stops coming out of the rear vent.
    c. Weigh the HA-CTA and record the weight.

d. Place the bottom cap on a cryogrinder tube, and place half of the HA-CTA into the tube with a magnet.
e. Place the top on the cryogrinder tube, with the slotted end towards the outside so that it can be removed using the "tool".
f. Insert the cryogrinder tube into the cryogrinder so that the cap slot is aligned with the end of the tube chamber.
g. Use a low impact frequency for a total of 3 mins.
h. Collect the HA-CTA powder in a 50 ml centrifuge tube.
i. Repeat the previous steps to cryogrind the remaining half of the HA-CTA.
j. Periodically check the liquid nitrogen level and add more if needed.
k. Clean cryogrinder tubes with 2% Liquinox and DI H_2O. **Do not use solvents, including acetone**. Clean metal caps and magnet with 2% Liquinox, DI H_2O, and acetone.
7. Dry the ground HA-CTA in a vacuum oven (-25 mm Hg, 50°C) for 24 hours or until no change in weight is observed.
8. When dry, HA-CTA should be stored in a dessicator. Save a sample for FTIR analysis.

Special Considerations
- Rinse all stir bars and spatulas with acetone and let air dry prior to use.
- Log lot numbers, etc. in documentation

Revision History

Contributor	Date	Revision Made	Version
N. Lewis	Nov 18, 2013	Major revisions	2.0
H. Dean	Nov 16, 2011	Originator	1.0

REFERENCES

[1] Zhang, M.; James, S.P. Silylation of hyaluronan to improve hydrophobicity and reactivity for improved processing and derivatization. *Polymer* **2005,** 46, 3639–3648.

[2] Zhang, M. Surface Modification of Ultra High Molecular Weight Polyethylene With Hyaluronan For Total Joint Replacement Application. Ph.D. Dissertation, Colorado State University, Fort Collins, CO, 2005.

[3] Dean IV, H. Development of BioPoly(R) Materials for use in Prosthetic Heart Valve Replacements. M.S. Thesis, Colorado State University, Fort Collins, CO, 2012.

5.2 HA-CTA SILYLATION

Purpose: Hydrophobic modification of hyaluronan for reaction in anhydrous solvents

Materials & Equipment
- Hyaluronan-cetyl trimethylammonium complex (HA-CTA)
- Dimethyl sulfoxide ≥ 99.9% reagent grade (DMSO)
- Hexamethyldisilazane ≥ 99.9% reagent grade (HMDS ≥ 99.9% reagent grade)
- Hexamethyldisilazane ≥ 97.0% (HMDS ≥ 97.0%)
- 500 ml Round Bottom Flask (RBF)
- Graduated cylinders
- Serum stoppers
- Copper wire
- Needle nose pliers
- Keck clips
- Condenser
- Dry Nitrogen (N_2) gas
- Magnetic stir bars
- Stir plates
- Vacuum oven
- Vapor trap
- Vacuum pump

Procedure

Glassware preparation
Wash glassware with 2% liquinox, then rinse with DI H_2O, and then rinse with acetone. Place glassware in oven (125°C) for 24 hours. Remove glassware from oven and let cool. When cool, silylate glassware with HMDS ≥ 97.0% for at least 5 mins. Swish the HMDS around, making sure to contact the surface that will contact the silyl HA-CTA, staying below the neck of a RBF or separatory funnel. Pour HMDS ≥ 97.0% into hazardous waste, and rinse the glassware with acetone. Place the glassware back in the oven for 10 mins to dry the acetone. Remove the glassware from the oven and let it cool. The glassware is now ready to use.

Add DMSO
1. Silylate a 50 ml graduated cylinder and a 500 ml RBF.
2. Place a stir bar and the cryoground HA-CTA powder into a 500 ml single neck RBF.
3. Cap the RBF and a graduated cylinder with rubber stoppers and copper wire. The copper wire should be tight and pinch into the rubber.
4. Turn on the dry nitrogen and adjust to a low flow rate.
5. Vent the RBF and graduated cylinder with dry N_2. Depending on the nitrogen flow, venting five times for five seconds each time is recommended.

6. Add 50 ml of DMSO for every 1.5g of starting NaHA to the RBF via a cannula and dry N_2. Maintain positive pressure in the graduated cylinder and RBF.
7. Swell the HA-CTA in the DMSO at room temperature until it is gel-like (about 4-12 hours).
8. Lower the RBF into a 50°C oil bath and continue to stir until the starting material is fully dissolved (4-24 hrs).

Add HMDS
9. Silylate a 25 ml graduated cylinder.
10. Cap a graduated cylinder with a rubber stopper and copper wire. The copper wire should be tight and pinch into the rubber.
11. Vent the graduated cylinder with dry N_2 before adding HMDS. Depending on the nitrogen flow, venting five times for five seconds each time is recommended.
12. Add 25 ml of HMDS ≥ 99.9% reagent grade for every 1.5g of starting NaHA to the RBF via a cannula and dry N_2 while maintaining positive pressure in the graduated cylinder and RBF. Increase the temperature of the oil bath to 75°C for 48 hours. Vigorous stirring is important to mix the HMDS and DMSO layers.
13. Periodically check stirring and hot plate temperature. Stirring is important for mixing the DMSO and HMDS to increase the degree of silylation.

Separating and washing silyl HA-CTA
14. Cool the reaction to room temperature.
15. Silylate a separatory funnel and a crystallizing dish.
16. Pour the reaction mixture into a separatory funnel, and let the two phases separate for 5 mins.
    a. The upper layer contains HMDS and silylated HA-CTA.
    b. The bottom layer is DMSO.
17. Let the DMSO drain into a beaker and dispose of the DMSO into a hazardous waste bottle.
18. Let the upper layer drain into the RBF that was used for silylation. This RBF now contains the silyl HA-CTA.
19. Close the separatory funnel stopper and add 10 ml of xylenes. Cap the funnel and swirl the xylenes to rinse the funnel. Collect the xylenes into the RBF containing the silyl HA-CTA. The purpose of this rinse step is to increase the yield of silyl HA-CTA.
20. Wash the silyl HA-CTA using a rotavap.
    a. Fill the bowl of the rotavap with DI H_2O.
    b. Heat the DI H_2O to 60-70°C. If the water heats to 75°C, cool it down to prevent degradation of the silyl HA-CTA.
    c. Apply vacuum grease to the two stopcocks, to the top surface of the cold finger, and to the inside surface of the RBF condenser as needed (see how to grease a stopcock by Mike).
    d. Place the cold finger inside the outer condensing column.
    e. Place the rubber gasket flat against the rotavap arm.
    f. Screw the grey clamp partially on
    g. Hold the edge of the coldfinger flat against the gasket and screw the grey piece until snug.
    h. Attach the RBF condenser using a keck clip.
    i. Fill the inner cold finger with ice.
    j. Check vacuum tubing connection between the coldfinger and pump.

k. Lower the rotavap arm using the lever so that the RBF containing silyl HA-CTA is partially submerged in water but still able to rotate.
l. Turn the vacuum pump strength to low, and turn the pump on. Wait for the vacuum to pull through the system.
m. Set the rotation speed to 60RPM.
n. Slowly increase the strength of the vacuum until vapor is pulled into the cold finger. Be careful to avoid boiling the solution because this could decrease the yield of silyl HA-CTA by pulling it into the cold finger.
o. When the silyl HA-CTA is mostly dry, turn the rotation off, turn the vacuum pump strength down, and turn the vacuum pump off.
p. Raise the rotavap arm using the lever.
q. Release the vacuum from the system using the upper stopcock, and let air back into the tubing by opening and closing the stopcock a few times.
r. Gently twist and pull the RBF containing silyl HA-CTA off of the rotavap.
s. Add 30 ml of xylenes to the RBF, cover with a serum stopper, and dissolve the silyl HA-CTA by swirling the flask.
t. When dissolved, uncap the RBF and attach it to the rotavap using a keck clip.
u. Wash the xylenes as in the previous steps.
v. Add xylenes 4 more times and wash as described, for a total of 5 washes with xylenes (in addition to the first wash in HMDS).
w. On the last wash, leave a few milliliters (~5 ml) of xylenes in the flask.
x. Pour the silyl HA-CTA/xylenes into a silylated crystallizing dish.
y. Add 5 ml more xylenes to the RBF to dissolve any remaining silyl HA-CTA, and pour it into the same crystallizing dish.

21. Dry the silyl HA-CTA at 50°C using a vapor trap until no weight change is observed. Save a sample for FTIR analysis. A yield of 2.0-2.5 g of silyl HA-CTA is expected when starting with 1.5 g NaHA.

Special Considerations
- Cannula transfers should be performed with at least two people.

Revision History

Contributor	Date	Revisions	Version
Nicole Lewis	Feb 19, 2014	Major revisions	2.0
Justin Gangwish	Feb 21, 2013		1.1
Harold Dean	2012	Originator	1.0

REFERENCES

[1]   Zhang, M.; James, S.P. Silylation of hyaluronan to improve hydrophobicity and reactivity for improved processing and derivatization. *Polymer* **2005,** 46, 3639–3648.

[2]   Zhang, M. Surface Modification of Ultra High Molecular Weight Polyethylene With Hyaluronan For Total Joint Replacement Application. Ph.D. Dissertation, Colorado State University, Fort Collins, CO, 2005.

[3]   Dean IV, H. Development of BioPoly(R) Materials for use in Prosthetic Heart Valve Replacements. M.S. Thesis, Colorado State University, Fort Collins, CO, 2012.

[4]   Kurkowski, R. The chemical crosslinking, compatibilization, and direct molding of ultra high molecular weight polyethylene and hyaluronic acid microcomposites. Colorado State University, Fort Collins, CO, 2007.

5.3 SAMPLE SWELLING

Purpose: Wick silyl HA-CTA and xylenes solution into ePTFE to form a microcomposite

Materials & Equipment
- Silylated Hyaluronan (silyl HA-CTA)
- Xylenes
- Hexamethyldisilazane (HMDS ≥97.0%)
- Poly(hexamethylene diisocyanate) (HMDI)
- ePTFE samples
- 2 single-neck round-bottom flasks (RBF)
- 2 Erlenmeyer flasks
- 2 Crystallizing dishes
- Serum stopper(s)
- Keck clip(s)
- Condenser and tubing
- Oil bath
- Weigh boat(s)
- Analytical scale
- Magnetic stir bar(s)
- Stir plate(s)
- Vortexer
- Vacuum oven

Procedure

Glassware preparation
Wash glassware with 2% liquinox, then rinse with DI H_2O, and then rinse with acetone. Place glassware in oven (125°C) for 24 hours. Remove glassware from oven and let cool. When cool, silylate glassware by adding HMDS ≥97.0% for at least 5 mins. Swish the HMDS around, making sure to contact the surface that will contact the silyl HA-CTA, staying below the neck of a RBF or separatory funnel. Pour HMDS into hazardous waste, and rinse the glassware with acetone. Place the glassware back in the oven for 10 mins to dry the acetone. Remove the glassware from the oven and let it cool. The glassware is now ready to use.

Day 1: Supply preparation
1. Dry silyl HA-CTA in a vacuum oven without heat for a minimum of 24 hours.
2. Weigh samples and then clean by soaking in xylenes for 12-24 hours in an Erlenmeyer flask with serum stopper
3. Dry glassware at >100°C overnight (~125°C)

Day 2: Sample drying, solution preparation
4. Vacuum dry samples for 12-24 hours in a vacuum oven with vapor trap without heat
5. Prepare silyl HA-CTA in xylenes at the desired concentration.
    a. Silylate an Erlenmeyer flask and rinse a stir bar with acetone
    b. Weigh silyl HA-CTA
    c. Place the silyl HA-CTA in the Erlenmeyer flask with the stir bar.
    d. Add xylenes to the Erlenmeyer flask.
        i. ex: for 1.5% silyl HA-CTA swelling solution, add 100mL for every 1.5g silyl HA-CTA
    e. Seal top of flask with a serum stopper and parafilm.
    f. Stir at room temperature until silyl HA-CTA is fully dissolved (12-24 hours).
6. Prepare a crosslinking solution of HMDI in xylenes.
    a. Silylate a single neck RBF and rinse a stir bar with acetone
    b. Measure 200 ml of 2% (v/v) HMDI in xylenes and place in the RBF with the stir bar.
    c. Connect the RBF to a condenser, lower into an oil bath, and stir at 50°C for 12-24 hours.

Day 3: Sample swelling, crosslinking, and acetone rinse
7. Record sample weight and check for a change in weight
8. Transfer the silyl HA-CTA/xylenes solution to a ceramic dish.
9. Allow ePTFE samples to swell in the silyl HA-CTA/xylenes solution at ambient temperature for 15 minutes without stirring. Cover with a glass cover slide.
10. Remove xylenes solution and place ePTFE samples in a 50°C vacuum oven for 3 hours, allowing solvent drying.
11. Let the crosslinking solution cool to ambient temperature and transfer to a crystallizing dish.
12. Record sample weight and check for change in weight
13. Add crosslinking solution to ePTFE samples in the ceramic dish, fully submersed, for 15 minutes. Cover with a glass cover slide or ceramic cover.
14. Remove the crosslinking solution and place samples in a vacuum oven at 50°C for 3 hours to cure the crosslinker.
15. Remove samples from vacuum oven and record sample weight.
16. Wash samples with acetone for 30 seconds using the vortexer to remove excess HMDI and vacuum dry at room temperature until no change in weight is observed.
17. Record the final sample weight when dry.

Revision History

Contributor	Date	Revision Made	Version
N. Lewis	Jan 23, 2014	Originator	1.0

REFERENCES

[1]   Dean IV, H. Development of BioPoly(R) Materials for use in Prosthetic Heart Valve Replacements. M.S. Thesis, Colorado State University, Fort Collins, CO, 2012.

[2]   Kurkowski, R. The chemical crosslinking, compatibilization, and direct molding of ultra high molecular weight polyethylene and hyaluronic acid microcomposites. Colorado State University, Fort Collins, CO, 2007.

[3]   Yonemura, S. Copolymer Washing. Standard operating protocol, Colorado State University Orthopaedic Bioengineering Research Laboratory, Fort Collins, CO, 2007.

[4]   B eauregard, G. Synthesis and characterization of a biomimetic UHMWPE-based interpenetrating polymer network for use as an orthopedic biomaterial. Ph.D. Dissertation, Colorado State University, Fort Collins, CO, 1999.

5.4 INITIAL SAMPLE HYDROLYSIS

Purpose: Remove silyl and CTA groups from silyl HA-CTA after crosslinking

Materials & Equipment
- Beakers
- Stir plate(s)
- Magnetic stir bar(s)
- Ultrasonic bath
- Acetone
- Sodium Chloride (NaCl)
- Deionized water (DI H_2O)
- Ethanol (EtOH)
- Vacuum oven
- Vapor trap
- Vacuum pump

Procedure
1. Prepare a 0.2M NaCl DI H_2O: Ethyl Alcohol (1:1) hydrolyzing solution in a large beaker.
   a. Ex) for 500mL of solution, add 5.844g NaCl to 250mL DI H_2O and 250 mL EtOH
2. Add the hydrolyzing solution to a 500 mL Erlenmeyer flask and sonicate for 60 minutes.
3. Sonicate for 60 minutes in fresh 0.2M NaCl DI H_2O: Ethyl Alcohol (1:1) hydrolyzing solution.
4. Sonicate for 60 minutes once more in fresh 0.2M NaCl DI H_2O: Ethyl Alcohol (1:1) hydrolyzing solution.
5. Sonicate for 60 minutes in a 0.2M NaCl DI H_2O hydrolyzing solution.
   a. Ex) For 100mL of solution, add 1.1688g NaCl to 100 mL DI H_2O
6. Let samples swell in DI H_2O: Ethyl Alcohol (3:2) solution for 2 hours without sonication.
7. Sonicate for 30 minutes in DI H_2O.
8. Partially dry samples by soaking in acetone for 60 minutes.
9. Drain acetone and completely dry in a vacuum oven at 50 °C equipped with a solvent trap at -25 inches Hg until there is negligible change in weight.
10. When the samples are dry, record the weight of the samples.

Revision History

Nicole Lewis	Feb 20, 2014	Clarifications, formatting, references
Harold Dean	2012	Originator

REFERENCES

[1]   Dean IV, H. Development of BioPoly(R) Materials for use in Prosthetic Heart Valve Replacements. M.S. Thesis, Colorado State University, Fort Collins, CO, 2012.

[2]   Kurkowski, R. The chemical crosslinking, compatibilization, and direct molding of ultra high molecular weight polyethylene and hyaluronic acid microcomposites. Colorado State University, Fort Collins, CO, 2007.

[3]   Yonemura, S. Copolymer Washing. Standard operating protocol, Colorado State University Orthopaedic Bioengineering Research Laboratory, Fort Collins, CO, 2007.

[4]   Cranson, C. HA-co-HDPE synthesis methods for DBM carrier. Colorado State University, Fort Collins, CO, 2007.

5.5 REVISED SAMPLE HYDROLYSIS

Purpose: Remove silyl and CTA groups from silyl HA-CTA after crosslinking

Materials & Equipment
- Beakers
- Stir plate(s)
- Magnetic stir bar(s)
- Ultrasonic bath
- Acetone
- Sodium Chloride (NaCl)
- Deionized water (DI H_2O)
- Ethanol (EtOH)
- Vacuum oven
- Vapor trap
- Vacuum pump

Procedure
11. Prepare a 0.2M NaCl DI H_2O: Ethyl Alcohol (1:1) hydrolyzing solution in a large beaker.
    a. Ex) for 500mL of solution, add 5.844g NaCl to 250mL DI H_2O and 250 mL EtOH
12. Add the hydrolyzing solution to a 500 mL Erlenmeyer flask and sonicate for 60 minutes.
13. Replace the 0.2M NaCl DI H_2O: Ethyl Alcohol (1:1) hydrolyzing solution with fresh solution and let samples soak for 11 hours.
14. Sonicate for 60 minutes in a 0.2M NaCl DI H_2O hydrolyzing solution.
    a. Ex) For 100mL of solution, add 1.1688g NaCl to 100 mL DI H_2O
15. Replace the 0.2M NaCl DI H_2O hydrolyzing solution with fresh solution and let samples soak for 11 hours.
16. Let samples swell in DI H_2O: Ethyl Alcohol (3:2) solution for 12 hours without sonication.
17. Sonicate for 30 minutes in DI H_2O.
18. Partially dry samples by soaking in acetone for 60 minutes.
19. Drain acetone and completely dry in a vacuum oven at 50 °C equipped with a solvent trap at -25 inches Hg until there is negligible change in weight.
20. When the samples are dry, record the weight of the samples.

Revision History

Contributor	Date	Revision Made	Version
N. Lewis	Feb 20, 2014	Modified protocol to obtain more complete hydrolysis. Sonicate one time instead of three times in the first solution. Added 11 hour soak times for the first two solutions. Soak for 12 hours in the third solution. Clarifications, references.	2.0
H. Dean	2012	Originator	1.0

REFERENCES

[1]   Dean IV, H. Development of BioPoly(R) Materials for use in Prosthetic Heart Valve
      Replacements. M.S. Thesis, Colorado State University, Fort Collins, CO, 2012.

[2]   Kurkowski, R. The chemical crosslinking, compatibilization, and direct molding of ultra high
      molecular weight polyethylene and hyaluronic acid microcomposites. Colorado State
      University, Fort Collins, CO, 2007.

[3]   Yonemura, S. Copolymer Washing. Standard operating protocol, Colorado State University
      Orthopaedic Bioengineering Research Laboratory, Fort Collins, CO, 2007.

[4]   B Cranson, C. HA-co-HDPE synthesis methods for DBM carrier. Colorado State University,
      Fort Collins, CO, 2007.

5.6 AQUEOUS SURFACE DIP

Purpose: Increase surface composition of HA to create a surface film through crosslinking surface HA to bulk HA

Materials & Equipment
- Sodium Hyaluronan (NaHA)
- Deionized water (DI H_2O)
- Stir plate and stir bar
- Hydrolyzed samples
- Poly(hexamethylene diisocyanate) (HMDI)
- Xylenes
- Round bottom flask (RBF)
- Oil bath
- Cold water condenser setup
- Vacuum oven
- Vapor trap
- Vacuum pump
- Ceramic dishes
- Acetone
- Balance

Procedure
1. Prepare a 1.0% NaHA in DI H_2O solution and dissolve for 12-24 hours at room temperature using a stir plate.
2. Prepare a crosslinking solution of 2% HMDI in xylenes in a RBF connected to a cold water condenser and suspended in an oil bath at 50°C. Dissolve for 12-24 hours.
3. Vacuum dry hydrolyzed samples for 12-24 hours.
4. Measure and record sample weight and size.
5. Submerge samples in the 1.0% aqueous NaHA solution for 15 mins.
6. Place samples in a vacuum oven equipped with a solvent trap for 3 hours at 50°C.
7. Submerge samples in the crosslinking solution for 15 minutes.
8. Place samples in a vacuum oven equipped with a solvent trap for 3 hours at 50°C to cure the crosslinker.
9. Wash samples in acetone using a vortex mixer to remove excess HMDI.
10. Place samples in a vacuum oven equipped with a solvent trap until no change in weight is observed.
11. Measure and record sample weight and size.

Revision History

Contributor	Date	Revision Made	Version
N. Lewis	April 25, 2014	Originator	1.0

REFERENCES

[1] Dean IV, H. Development of BioPoly(R) Materials for use in Prosthetic Heart Valve
     Replacements. M.S. Thesis, Colorado State University, Fort Collins, CO, 2012.

[2]   Kurkowski, R. The chemical crosslinking, compatibilization, and direct molding of ultra high
     molecular weight polyethylene and hyaluronic acid microcomposites. Colorado State
     University, Fort Collins, CO, 2007.

5.7 THERMOGRAVIMETRIC ANALYSIS

Purpose: Quantify weight percent compositions of samples

Materials & Equipment
- Sample for analysis
    - 5-10 mg for dry samples
    - Aluminum pans
    - Forceps
    - TGA platinum loading pan ("basket-like" pan with handle)
    - TA Instruments 2950 Thermogravimetric Analyzer

Procedure

The TGA is programmatically controlled by TA Advantage software. Start the software and set-up control program.
- Typical program settings for bulk compositional analysis and thermal stability testing: temperature range from ambient to 600☐C, 10☐C/min ramp rate.
- *Note: Do not exceed 600☐C when using aluminum pans. Sample should be placed directly on the TGA platinum pan if higher temperatures are required.*
- For hygroscopic samples, temperature may be held isothermally for 15 minutes at 110☐C to evaporate unbound water (will need to adjust for lost water weight during analysis).
- Include external trigger if concurrent mass spectrometry will be used.
- Set the instrument end-of-test condition to air-cool.

Using forceps, place an empty aluminum pan on the TGA loading tray. Tare by pressing the "tare" button on the TGA instrument control panel and allowing the robotic stage to load the pan on the balance.
- If the pan mis-loads, DO NOT attempt to place the loading pan on the balance wire manually (the balance is a precision instrument, and "dropping" a sample on the balance wire can damage the instrument).
- Wait for the robotic stage to return to its start position, then rotate the TGA loading pan to reposition its "basket" handle.
- Push the tare button again and observe the position of the handle relative to the balance wire. If it looks like the pan will mis-load again, gently guide the balance wire by pushing and holding it in proximity to the pan handle with forceps. Allow the instrument to load pan on to the balance wire.
- The pan will be loaded into the furnace, then the instrument will automatically tare the pan. Wait for the instrument to return the pan to the start position.
- Prepare samples for analysis. Generally, for dry samples the most consistent results will be obtained from samples with high surface area, e.g. powders.
    - Pack powder into tared aluminum pan and place on TGA loading pan with forceps. Load the sample by pushing the "load" button on the TGA control panel.

Observe the same precautions as described for taring the pan if the sample mis-loads

  o   Observe the sample weight measured by the instrument – powdered samples should be in the 5-10 mg range. If sample weight is not in the right range, unload the sample by pushing "unload" on the instrument panel. Adjust sample and repeat load process.

Note: the sample will not be loaded into the TGA furnace until the TGA program is started

- Click "run" in the TA Advantage software to load the sample and run the control program.

Analyze collected data using TA Universal Analysis software. Plot the weight% and derivative weight% as a function of temperature. Typical analysis parameters to identify include start and end temperatures for degradation steps, peak degradation rate temperatures, % mass loss over a degradation step, and sample residues.

Revision History

Contributor	Date	Revision Made	Version
H. Dean	June 28, 2011	Originator	1.0

REFERENCES

[1]   Dean IV, H. Development of BioPoly(R) Materials for use in Prosthetic Heart Valve Replacements. M.S. Thesis, Colorado State University, Fort Collins, CO, 2012.

[2]   Kurkowski ASTM E1131-08, *Standard Test Method for Compositional Analysis by Thermogravimetry*. West Conshohocken, PA: ASTM International.

5.8 ENZYME DEGRADATION

Purpose: Qualitative determination of relative amounts of surface HA

Materials & Equipment
- 8mm biopsy punches
- ePTFE samples
- Hyaluronan
- Hyaluronidase
- Toluidine Blue
- Urea
- Deionized water (DI H_2O)
- Phosphate buffered saline (PBS)
- Sterile centrifuge tubes
- Balance
- Water bath
- Viscometer

Procedure

Day 1
1. Obtain 8mm biopsy punches of samples
2. Sterilize samples by soaking in 70% ethanol for 10 mins and exposure to UV light for 30 mins
3. Rinse samples 2x with PBS
4. Soak samples in fresh PBS for at least 12 hours

Day 2
5. Prepare 10 ml of a 0.1% HA solution in DI H_2O in a sterile centrifuge tube. Invert and vortex to dissolve.
6. Prepare 125 ml of a 150 units/ml hyaluronidase in PBS solution in an autoclaved glass bottle. Dissolve.
7. Mix 5 ml of the HA solution with 5 ml of the hyaluronidase solution in a sterile centrifuge tube. Invert and vortex to dissolve.
8. Equilibrate in a 37°C water bath for 30mins.
9. Measure the viscosity of the combined HA/hyaluronidase solution and the HA solution.
   a. A decrease in viscosity from the HA solution to the HA/hyaluronidase solution indicates a decrease in molecular weight of the HA, indicating that the enzyme is active.
10. If the enzyme is active, place samples in individual sterile 15ml centrifuge tubes.
11. Add 5 ml of enzyme solution to each centrifuge tube.
12. Tightly cap tubes and place in a 37°C water bath for 1 and 7 days.

13. Place the remaining hyaluronidase solution and HA solution into a 37°C water bath until day 8.

<u>Day 3</u>
14. Prepare a 0.1% TBO solution (in 8M urea)
    a. Add 96.08864 g urea to 200 mL H2O and mix at room temperature for 30 minutes.
    b. Add 0.2 g of TBO to the aqueous urea solution allowing it to dissolve completely.
15. Remove Day 1 samples from the hyaluronidase solution
16. Rinse samples 1x with water
17. Rinse samples 1x with ethanol
18. Dye samples with 0.1% TBO solution (in 8M urea) for 10 minutes, rinse with distilled water, and dry at room temperature.
19. Rinse off excess TBO using distilled H2O, leaving behind bound TBO.
20. Dip stained sample in fresh distilled H2O and agitate. Rinse the stained sample with distilled H2O until no more dye is leached out.
21. Obtain pictures of samples
22. Save TBO solution for day 7

<u>Day 9</u>
23. Prepare 10 ml of a fresh 0.1% HA solution in DI H_2O in a sterile centrifuge tube. Invert and vortex to dissolve.
24. Mix 5 ml of the aqueous HA solution with 5 ml of the hyaluronidase solution from Day 2 in a sterile centrifuge tube. Invert and vortex to dissolve.
25. Equilibrate the HA/hyaluronidase solution in a 37°C water bath for 30mins
26. Measure the viscosity of the combined HA/hyaluronidase solution and the HA solution.
    a. A decrease in viscosity from the HA solution to the HA/hyaluronidase solution indicates a decrease in molecular weight of the HA, indicating that the enzyme is active.
27. Remove Day 7 samples from the hyaluronidase solution
28. Rinse samples 1x with water
29. Rinse samples 1x with ethanol
30. Dye samples with 0.1% TBO solution (in 8M urea) for 10 minutes, rinse with distilled water, and dry at room temperature.
31. Rinse off excess TBO using distilled H2O, leaving behind bound TBO.
32. Dip stained sample in fresh distilled H2O and agitate. Rinse the stained sample with distilled H2O until no more dye is leached out.
33. Obtain pictures of samples

Protocol Revision History

Contributor	Date	Revision Made	Version
Nicole Lewis	March 28, 2014	Originator	1.0

REFERENCES

[1]   Dean IV, H. Development of BioPoly(R) Materials for use in Prosthetic Heart Valve
       Replacements. M.S. Thesis, Colorado State University, Fort Collins, CO, 2012.

[2]   Kurkowski, R. The chemical crosslinking, compatibilization, and direct molding of ultra high
       molecular weight polyethylene and hyaluronic acid microcomposites. Colorado State
       University, Fort Collins, CO, 2007.

[3]   Zhang, M. Surface Modification of Ultra High Molecular Weight Polyethylene With
       Hyaluronan For Total Joint Replacement Application. Colorado State University, Fort
       Collins, CO, 2005.

5.9 TOLUIDINE BLUE O

Purpose: Use the nucleic acid and polysaccharide stain, Toluidine Blue O, to evaluate presence of HA

Materials & Equipment
- Toluidine Blue O (TBO) (Dye content 84%) (Aldrich; 19804BA)
  ◦ Store at room temperature
- Urea (99+%, A.C.S. reagent) (Sigma-Aldrich; U2709)
  ◦ Store at room temperature
- Distilled H20
  ◦ Store at room temperature
- 250 mL glass beaker
- Glass Petri dish

Procedure
1. Prepare a 0.1% TBO solution (in 8M urea)
   a. Add 96.08864 g urea to 200 mL H2O and mix at room temperature for 30 minutes.
   b. Add 0.2 g of TBO to the aqueous urea solution allowing it to dissolve completely.
2. Submerge sample in TBO solution for 10 minutes at room temperature
3. Rinse off excess TBO using distilled H2O, leaving behind bound TBO.
4. Dip stained sample in fresh distilled H2O and agitate. Rinse the stained sample with distilled H2O until no more dye is leached out.
5. Take a picture of samples from each treatment group.

Revision History

Contributor	Date	Revision Made	Version
R. Kurkowski	2007	Originator	1.0

REFERENCES

[1] Dean IV, H. Development of BioPoly(R) Materials for use in Prosthetic Heart Valve Replacements. M.S. Thesis, Colorado State University, Fort Collins, CO, 2012.

[2] Kurkowski, R. The chemical crosslinking, compatibilization, and direct molding of ultra high molecular weight polyethylene and hyaluronic acid microcomposites. Colorado State University, Fort Collins, CO, 2007.

5.10 TUBULAR EPTFE SAMPLE PREPARATION FOR STATIC TESTING

Purpose: Mount ePTFE samples for blood studies to prevent floating and minimize residual sample curvature

Materials & Equipment
- Sterile 8mm biopsy bunches
- PTFE white disc liners with 0.050" thickness and 8mm diameter (Berlin Packaging, LLC)
- Ethanol
- 48 well plate(s)
- Double sided carbon conductive tape (Ted Pella)
- Glass slide
- Phosphate buffered saline (PBS)

Procedure
1. Place 8mm PTFE pucks and ePTFE samples in a 48 well plate.
2. Sterilize pucks and ePTFE samples by adding 500µl of 70% ethanol to each well for 10-30mins.
3. Aspirate ethanol.
4. Move samples to a new well plate and let samples air dry.
5. When dry, place PTFE pucks on 8mm double sided carbon tape.
6. Press PTFE pucks uniformly on the tape using a glass slide.
7. Use an 8mm biopsy punch to obtain a PTFE puck with attached carbon tape.
8. Remove the adhesive backing on the carbon tape.
9. UV the carbon tape for 10-30mins.
10. Place ePTFE samples on the carbon tape/PTFE puck and press sample flat using a glass slide.
11. Place samples in a new 48 well-plate.
12. Rinse samples 2x with 1ml of PBS, pipetting against the wall of the well.
13. Let samples air dry.
14. UV samples for 10-30mins.
15. Hydrate samples in PBS for at least overnight prior to incubation with plasma.

Revision History

Contributor	Date	Revision Made	Version
N. Lewis	December 2, 2013	Originator	1.0

5.11 PLASMA ISOLATION FROM WHOLE BLOOD AND SAMPLE INCUBATION

Purpose: Isolate plasma from whole blood and incubate on sample surfaces

Materials & Equipment
- Vacuum tubes coated eith EDTA
- Centrifuge
- Sterile centrifuge tube
- Ethanol (70%)
- Phosphate buffered saline (PBS)
- 48 well plate(s)
- Horizontal shaker plate
- Incubator

Procedure

Plasma Isolation from whole blood
1. Collect whole blood by venopuncture
2. Collect into 10mL vacuum tubes coated with EDTA (an anti-coagulant)
3. Discard the first tube to account for the skin plug and locally activated platelets from the needle insertion
4. Centrifuge vials at 300g for 15mins to separate plasma from red blood cells
5. Pool plasma into a fresh sterile centrifuge tube
6. Use plasma within 2 hours of removal from the body

Plasma incubation on samples
1. Clean and sterilize samples
   a. Soak in 70% ethanol for 10 mins
   b. Wash 2x in PBS
   c. UV for 30 mins
   d. Hydrate ePTFE samples in PBS overnight to hydrate the HA
2. Incubate in 48 well-plate with 500 uL of pooled plasma at 37°C and 5% CO_2 in a horizontal shaker plate (100rpm) for 2 hours.
   a. Clean the horizontal shaker plate very well using 70% ethanol before placing in an incubator

Special Considerations
- The author typically estimated that 30% of the whole blood volume would be plasma, but this depends on the person, their hydration level, etc.
- Invert vacuum tubes during transport to prevent clotting.

Revision History

Contributor	Date	Revision Made	Version
N. Lewis	August 8, 2013	Originator	1.0

REFERENCES

[1]   Smith, B.S.; Popat, K.C. Titania nanotube arrays as interfaces for blood-contacting implantable devices: a study evaluating the nanotopography-associated activation and expression of blood plasma components. *J. Biomed. Nanotechnol.* **2012,** 8, 642–658.

[2]   Leszczak, V.; Smith, B.S.; Popat, K.C. Hemocompatibility of polymeric nanostructured surfaces. *J. Biomater. Sci. Polym. Ed.* **2013,** 24, 1529–1548.

5.12 CALCEIN-AM

Purpose: Measure whole blood clotting kinetics to assess surface thrombogenic potential

Materials & Equipment

- Calcein-AM
- Dimethyl sulfoxide (DMSO)
- Vortex mixer
- Phosphate buffered saline (PBS)
- Sterile centrifuge tubes
- 48 well plate(s)
- Fluorescence microscope
- ImageJ software

Procedure

1. Remove calcein-AM from the -20 freezer
2. Reconstitute calcein-AM lysate in 50 µl of DMSO
3. Cap mixture and mix thoroughly via vortex machine
4. Solution is now ready to be used
5. Make a stock solution with the amount of mixture that you will be needing for all of the samples
   a. For 10 samples: 10 µl calcein-AM in5 ml PBS (for a 2 µM concentration)
6. Vortex or invert tube to mix
7. Remove samples from the incubator
8. Aspirate cell rich media
9. Wash 2x in PBS
10. Move samples to new well plates
11. Add 500 µl of stock solution to each well
12. Incubate for 30 mins at room temp
13. Aspirate staining solution from wells
14. Wash 1x in PBS
15. Image by fluorescence microscope imaging (62 HE BP 474/28 (green))
16. Save images as .tiff files.
17. Determine cell coverage using Image J software

Special Considerations

- Calcein-AM concentration should be determined by material type and cell type. A lower concentration may be sufficient if photobleaching is not present.

Revision History

Contributor	Date	Revision Made	Version
N. Lewis	March 5, 2013	Originator	1.0

REFERENCES

[1]   Smith, B.S.; Popat, K.C. Titania nanotube arrays as interfaces for blood-contacting implantable devices: a study evaluating the nanotopography-associated activation and expression of blood plasma components. *J. Biomed. Nanotechnol.* **2012,** 8, 642–658.

[2]   Leszczak, V.; Smith, B.S.; Popat, K.C. Hemocompatibility of polymeric nanostructured surfaces. *J. Biomater. Sci. Polym. Ed.* **2013,** 24, 1529–1548.

5.13 SEM FIXATION

Purpose: SEM fixation for samples exposed to cells

Materials & Equipment
- Ethanol
- DI H_2O
- Hexamethyldisilazane (HMDS)
- Gluteraldehyde
- Sucrose
- Sodium cacodylate
- Phosphate buffered saline (PBS)
- Petri dishes
- Tweezers
- Beaker
- Stir bar
- Stir plate
- Spatula

Procedure
1. Aspirate cell rich media
2. Rinse (2x) with PBS
3. Move samples to new container and place into the following solutions for the designated times:
   a. 45 min ~ Primary fixative
   b. 10 min ~ Buffer solution
   c. 10 min ~ 35% ethanol
   d. 10 min ~ 50% ethanol
   e. 10 min ~ 70% ethanol
   f. 10 min ~ 100% ethanol
   g. 10 min ~ HMDS (Hexamethyl disilisone)

Preparation: Buffer and Fixative
~ Fixative: 3% Gluteraldehyde in 0.1 M sodium cacodylate & 0.1 M Sucrose

To make 10 ml buffer and 10 ml fixative ~ Mix:
- 19.4 ml di-H2O
- 0.68 g sucrose
- 0.43 g sodium cacodylate

~ Separate 10 ml of soln. and place into a petri-dish = **buffer**

Add to the other 10 ml of solution:
- 0.3ml gluderaldehyde = **fixative**

Revision History

Contributor	Date	Revision Made	Version
N. Lewis	April 23, 2014	Formatting	1.1
K. Popat	Unknown	Originator	1.0

5.14 PROTEIN ADSORPTION

Purpose: Measure amount of adsorbed protein on substrate surfaces

Materials & Equipment
- Stock protein solutions (100μg/ml)
- Horizontal shaker plate
- 1% Sodium dodecyl sulfate (SDS)
- 48 well plate(s)
- Incubator (37°C)
- Phosphate buffered saline (PBS)
- microBCA kit (Thermo Scientific)
- 96 well plate
- Plate reader

Procedure
1. Create stock protein solution (100 μg/ml)
2. Seed over samples
3. Incubate for 2 hours on a horizontal shaker plate at 100 rpm at 37°C (in incubator)
4. While samples are incubating, create SDS solution (1%)
5. Move samples to a fresh well plate, rinse 3X w/ PBS (keep original protein solution)
6. Seed SDS solution onto samples
7. Incubate for 1 hour at room temp on shaker plate at 100 rpm
8. Collect SDS into a fresh well plate
9. Seed fresh SDS onto samples
10. Incubate for 1 hour at room temp on shaker plate at 100 rpm
11. Collect SDS into well plate from step 8
12. Seed fresh SDS onto samples
13. Incubate for 1 hour at room temp on shaker plate at 100 rpm
14. While samples are incubating, create working reagent and standards (see micro BCA protocol)
15. Collect SDS into well plate from steps 8 & 11
16. Prep the 96 well plates with 150 μL of each standard and sample - use both the original protein solution and the pooled SDS solutions for comparison
17. Add 150 μL of working reagent to each well
18. Mix on shaker plate for 30 seconds
19. Incubate for 2 hours at 37°C
20. Read with plate reader at 562 nm

Revision History

Contributor	Date	Revision Made	Version
N. Lewis	Jan 29, 2014	Originator	1.0

REFERENCES

[1]   "Micro BCA (TM) Protein Assay Kit." Thermo Scientific.

[2]   Leszczak, V.; Smith, B.S.; Popat, K.C. Hemocompatibility of polymeric nanostructured surfaces. *J. Biomater. Sci. Polym. Ed.* **2013,** 24, 1529–1548.

5.15 DAPI AND RHODAMINE

Purpose: Assess platelet and leukocyte adhesion on surfaces, as well as cytoskeletal structure

Materials & Equipment
- Blood plasma incubated on sample surfaces for two hours
- Phosphate buffered saline (PBS)
- Fixing solution (3.7 wt% formaldehyde in PBS)
- Tweezers
- Rhodamine-conjugated phalloidin (dilution 1:40) in PBS
- DAPI stain (0.2ug/mL)
- Triton-X (1.0% in PBS)
- Fluorescence microscope

Procedure
1. Aspirate plasma to remove unadherent cells
2. Gently rinse 2x with PBS
3. Transfer samples to a new 48 well plate
4. Add fixing solution to samples for 15mins at room temperature
5. Wash 3x with PBS, 5mins per wash. After the first wash, move samples to a new 48 well plate.
6. Add 1%Triton-X in PBS for 3mins at room temperature to permeabilize membranes
7. Wash 3x with PBS, 5mins per wash. After the first wash, move samples to a new 48 well plate.
8. Incubate in rhodamine-conjugated phalloidin (dilution 1:40) in PBS for 25mins at room temperature (stains F-actin on cell membranes)
9. Add DAPI stain (0.2ug/mL) directly to the wells containing rhodamine-conjugated phalloidin
10. Rinse once with PBS for 5mins and let samples sit in PBS while imaging
11. Image with a fluorescence microscope using a 49 DAPI BP 445/50 blue filter and filter set 62 HE BP 585/35 (red)
12. Determine the number of adherent cells using ImageJ software

Special Considerations
- DAPI nucleus stain identifies adherent leukocytes (platelets don't have a nucleus)
- F-actin cytoskeletal stain identifies adherent platelets and leukocytes
- Have fixing solution prepared (3.7 wt% formaldehyde in PBS)

Revision History

Contributor	Date	Revision Made	Version
N. Lewis	March 19, 2014	Originator	1.0

REFERENCES

[1]   Smith, B.S.; Popat, K.C. Titania nanotube arrays as interfaces for blood-contacting implantable devices: a study evaluating the nanotopography-associated activation and expression of blood plasma components. *J. Biomed. Nanotechnol.* **2012,** 8, 642–658.

[2]   Leszczak, V.; Smith, B.S.; Popat, K.C. Hemocompatibility of polymeric nanostructured surfaces. *J. Biomater. Sci. Polym. Ed.* **2013,** 24, 1529–1548.

5.16 MTT CELL PROLIFERATION ASSAY

Purpose: Measure metabolic activity of adhered platelets and leukocytes on sample surfaces

Materials & Equipment
- Vybrant MTT Cell Proliferation Assay Kit (Invitrogen/Molecular Probes)
- Phosphate buffered saline (PBS)
- Vortex mixer
- 48 well plate(s)
- Incubator
- 96 well plate(s)
- Plate reader

Procedure
1. After plasma incubation for 2 hours on a horizontal shaker plate (100rpm) at 37°C and 5% CO_2, aspirate plasma
2. Rinse 1x with 500µl of PBS, move samples to a new well plate, and rinse 1x more with 500µl of PBS
3. Reconstitute 50mg of MTT in 1mL PBS, vortex and pipette to dissolve the MTT powder
4. Dilute the MTT solution to desired volume (50µl per 500µl PBS)
5. Add 500µL of the diluted MTT solution to each well
6. Incubate 4 hours at 37°C and 5% CO_2. At high densities incubation time can be shortened to 2 hours.
7. Prepare the MTT solvent by adding 10 ml DI H_2O and 8.27µl of 12.1M HCl to 1g of SDS. Dissolve.
8. Add 500µl of MTT solvent to each well. Do not aspirate the MTT solution.
9. Incubate for 4 hours at 37°C and 5% CO_2.
10. Mix each well and transfer 100µl of solution from each sample to a 96 well-plate
11. Measure absorbance at 570 nm. Change the solution volume for the path length on the plate reader.

Revision History

Contributor	Date	Revision Made	Version
N. Lewis	March 21, 2014	Originator	1.0

REFERENCES

[1]   Smith, B.S.; Popat, K.C. Titania nanotube arrays as interfaces for blood-contacting implantable devices: a study evaluating the nanotopography-associated activation and expression of blood plasma components. *J. Biomed. Nanotechnol.* **2012,** 8, 642–658.

[2]   Leszczak, V.; Smith, B.S.; Popat, K.C. Hemocompatibility of polymeric nanostructured surfaces. *J. Biomater. Sci. Polym. Ed.* **2013,** 24, 1529–1548.

5.17 WHOLE BLOOD CLOTTING

Purpose: Measure whole blood clotting kinetics to assess surface thrombogenic potential

Materials & Equipment
- 48 well plate(s)
- 96 well plate(s)
- Plate Reader
- Prepared test samples (15 of each sample)
- Venopuncture tubes
- DI H_2O
- ~10 mL whole blood
- Micropipettes and tips
- Tweezers
- Timer

Procedure
12. Place samples in 48 well plates.
13. Sterilize samples in the biohood under UV light for 30 minutes.
14. Prepare 48 well plates containing 1ml DI H_2O (or enough volume to cover the sample surface) per well for each sample and for five control wells.
15. Obtain blood collected through venopuncture
16. Place 5 µL of whole blood onto each sample immediately.
    a. Use a new pipette tip for each sample to prevent blood clotting.
    b. Also place 5 µL of whole blood into positive control wells containing DI H_2O.
17. At indicated time points,
    a. Place samples in DI H_2O without disturbing the blood droplet.
    b. Gently shake the well plate for 30 seconds and let it sit for a total of 5 minutes.
    c. Transfer samples from DI H_2O to a third well plate for SEM.
18. Repeat Step 6 until all samples have been rinsed.
19. Transfer 200 µL of the water/blood mixture from each well to a 96 well plate
20. Run plate reader using a designated absorbance program and save results.
21. Place SEM samples in a desiccator until ready to image. Gold coat with a thin (3µm) layer of gold.

Special Considerations
- Use blood immediately to prevent clotting.
- Change pipette tip for each sample.

Revision History

Contributor	Date	Revision Made	Version
N. Lewis	April 23, 2014	Updated special considerations	2.0
H. Dean	June 28, 2011	Originator	1.0

REFERENCES

[1]   Dean, H. *Development of Biopoly® Materials for Use in Prosthetic Heart Valve Replacements.* M.S. thesis, Colorado State University Department of Mechanical Engineering, Fort Collins, CO (2012).

[2]   Leszczak, V.; Smith, B.S.; Popat, K.C. Hemocompatibility of polymeric nanostructured surfaces. *J. Biomater. Sci. Polym. Ed.* **2013,** 24, 1529–1548.